TEICHMÜLLER THEORY AND HANDLE ADDITION FOR MINIMAL SURFACES

Matthias Weber
Universität Bonn
Beringstraße 1
Bonn, Germany

Michael Wolf*
Dept. of Mathematics
Rice University
Houston, TX 77251 USA

1. Introduction
   1.1 The Surfaces
   1.2 The Proof
2. Background, Notation and a Sketch of the Argument
   2.1 Minimal Surfaces
   2.2 Teichmüller Theory
   2.3 A Brief Outline of the Proof
3. The Geometry of Orthodisks
   3.1 Orthodisks
   3.2 From orthodisks to Riemann surfaces
   3.3 From orthodisks to Weierstraß data
   3.4 Geometric significance of the formal Weierstraß data
   3.5 Examples of simple orthodisks
   3.6 Orthodisks for the Costa Towers
   3.7 More orthodisks by drilling holes
4. The Space of Orthodisks
   4.1 Introduction
   4.2 Geometric coordinates for the $DH_{1,1}$-surface
   4.3 Height Function for the $DH_{1,1}$-surface
   4.4 Geometric coordinates for the $DH_{m,n}$-surfaces
   4.5 Height Functions for the $DH_{m,n}$-surfaces
   4.6 Properness of the height functions for the $DH_{m,n}$-surfaces
   4.7 A Monodromy Argument

*Partially supported by NSF grant number DMS 9626565 and the SFB

5. The Gradient Flow
   5.1 Overall Strategy
   5.2 Deformations of $DH_{1,1}$
   5.3 Infinitesimal Pushes
6. Regeneration
7. Non-Existence of the $DH_{m,n}$-surfaces with $n < m$
8. Extensions and Generalizations
   8.1 Higher symmetry
   8.2 Deformations with more catenoidal ends
   8.3 Embeddedness Aspects of $DH_{m,n}$
9. References

§1. Introduction.

In this paper, we develop Teichmüller theoretical methods to construct new minimal surfaces in $\mathbb{E}^3$ by adding handles and planar ends to existing minimal surfaces in $\mathbb{E}^3$. We exhibit this method on an interesting class of minimal surfaces which are likely to be embedded, and have a low degree Gaußmap for their genus. In particular, we exhibit a two-parameter family of complete minimal surfaces in the Euclidean three-space $\mathbb{E}^3$; these surfaces are embedded (at least) outside a compact set and are indexed (roughly) by the number of ends they have and their genus. They have at most eight self-symmetries despite being of arbitrarily large genus, and are interesting for a number of reasons. Moreover, our methods also extend to prove that some natural candidate classes of surfaces cannot be realized as minimal surfaces in $\mathbb{E}^3$. As a result of both aspects of this work, we obtain a classification of a family of surfaces as either realizable or unrealizable as minimal surfaces.

This paper is a continuation of the study we initiated in [WW]; in a strong sense it is an extension of that paper, as the essential organization of the proof, together with many details, have been retained. Indeed, part of our goal in writing this paper was a demonstration of the robustness of the methods of [WW], in that here we produce minimal surfaces of a very different character than those produced in [WW], yet the proof changes only in a few quite technical ways. (In particular, the present proof handles the previous case of Chen-Gackstatter surfaces of high genus as an elementary case.) Indeed in the intervening years between our initial preparation of this manuscript and its final revision for publication, this method has been applied to produce other families surfaces of substantively different characteristics or to prove their non-existence ([WW2], [MW]).

1.1 **The Surfaces**. Hoffman and Meeks (see [Ho-Ka]) have conjectured that any complete embedded minimal surface in space has genus at least $r - 2$, where r denotes the number of ends of the surface. In this paper, we provide significant evidence for this conjecture in the situation where the surfaces have eight symmetries. This is an important case for two reasons: first, it is presently unknown whether there are any complete embedded minimal surfaces which have no symmetries, and second, there are very few families of examples known where there are more than four ends. (Indeed, the only such constructions available are from the recent work of Kapouleas [Kap], where the genus is both high and inestimable.)

In particular, we consider two families of surfaces, with the first included in the second. The first case consists of surfaces CT_g which generalize Costa's example [Cos]. We prove

Theorem A. *For all odd genera g, there is a complete minimal surface $CT_g \subset \mathbb{E}^3$ which is embedded outside a compact surface with boundary of genus g, with g parallel (horizontal) planar ends and two catenoid ends. The symmetry group of CT_g is generated by reflective symmetries about a pair of orthogonal vertical planes and a rotational symmetry about a horizontal line.*

These surfaces represent the borderline case for the conjecture. (The even genus cases have substantially different combinatorics, and require a different treatment.) Consider the Riemann surface underlying such an example: it is a fundamental theorem of Osserman [Oss1] that such a surface is conformally a compact surface of genus g, punctured at points corresponding to the ends. Let Z denote the vertical coordinate of such a minimal surface: clearly, Z is critical at the g points corresponding to the planar ends, the two points corresponding to the catenoid ends, and g interior points where the two reflective planes meet the surface.

We generalize these surfaces as follows, imagining **D**rilling additional **H**oles to obtain surfaces $DH_{m,n}$ (see §3.7).

Theorem B. (i) *For every pair of integers $n \geq m \geq 1$, there exists a complete minimal surface $DH_{m,n} \subset \mathbb{E}^3$ of genus $m+n+1$ which is embedded outside a compact set with the following properties: it has $2n+1$ vertical normals, $2m+1$ planar ends, and two catenoid ends. The symmetry group is as in Theorem A.* (ii) *For $n < m$, there is no complete minimal surface with those symmetries of the type $DH_{m,n}$ (and $2n+1$ vertical normals, $2m+1$ planar ends, and two catenoid ends).*

In the second statement, the surfaces for which we prove non-existence are in precise analogy with the surfaces for which we prove existence. There are many configurations of surfaces which have the given eight symmetries and $2n+1$ vertical normals, $2m+1$ planar ends, and two catenoid ends, and we will indicate the range of possible choices in §3: in the non-existence section, we concentrate *only* on the candidates which the rest of the paper indicates are most likely to exist. In particular, we do not prove a more general statement ruling out all surfaces of the rough description of having $2n+1$ vertical normals, $2m+1$ planar ends, and two catenoid ends (although many of the possible configurations we do not treat would also have no minimal representatives, with the proofs of non-existence being precisely analogous to the proof we give in §7). We give a precise formulation of the statement of Theorem B(ii) at the outset of §7.

Theorem A follows from Theorem B (i) by setting $n = m = \frac{1}{2}(g-1)$. The weak embeddedness statement in Theorem B is strengthened somewhat in §9; we conjecture (supported by some numerical evidence) that these surfaces are, in fact, embedded. The restriction to planar ends is unnecessary: in §8 we show that these surfaces are deformable to having catenoid ends. Theorem B is displayed in tabular form at the end of §3. (In that table, we also add some information about the case $m = 0$, which was excluded from the statement of the Theorem B.))

In summary, for the case of "essentially embedded" surfaces (i.e. those surfaces which are embedded outside of a compact set) with eight symmetries and odd ends, the conjecture is robustly true: no counterexamples (of the type $DH_{m,n}$) may exist for $g < r - 2$, and any pair (r, g) describes an example when $g \geq r - 2$.

Below are two pictures of the surface $DH_{1,2}$, one showing it completely, the other exhibiting only the central planar end:

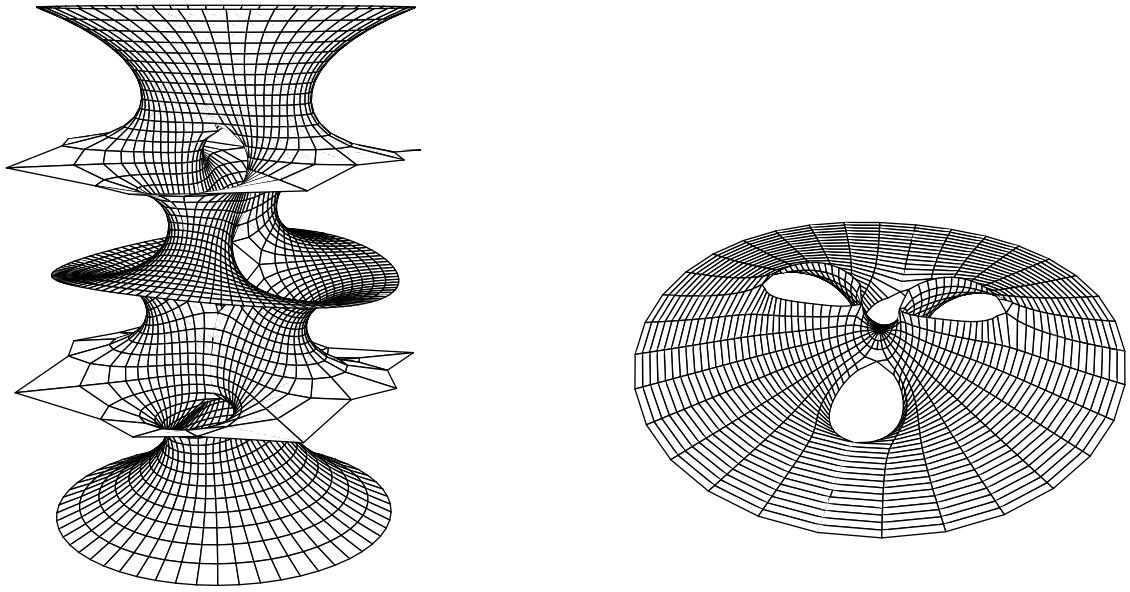

$DH_{1,2}$ surface and middle end

1.2 **The Proof**. As one of our principal goals is the description of this method, we now give an overview; in §2.3, we give a fairly detailed sketch. In particular, our discussion in that subsection is quite general, as we aim to outline an approach to proving existence results for wide classes of minimal surfaces, even if we only carry out that plan for the specific classes described above.

Minimal surfaces in space can be defined in terms of their Weierstrass data: a pair of meromorphic forms on the underlying Riemann surface. Conversely, a pair of meromorphic forms on a simply connected domain naturally determines a (local) minimal surface, up to some mild compatibility requirement on the divisors. Defining a minimal surface with some homology is substantially more difficult however, as this requires a compatibility of periods of three one-forms (say $(\alpha_1, \alpha_2, \alpha_3)$) defined via the data. A common approach to this global "period problem" is to prescribe sufficient symmetry of the minimal surface so that the conformal structure of the minimal surface is apparent; one then searches for appropriate meromorphic one-forms α_1, α_2, α_3 on that Riemann surface. As our minimal surfaces will have only a few symmetries, we are unable to determine the conformal structure of the surface a priori, or even to restrict it sufficiently well so that we might adapt that common approach; we develop a different approach. We handle this "period

problem" by instead studying the (developed) flat structures associated to the α_i: in this formulation, the periods are identifiable as vectors in $\mathbb{C}$, and the period problem is soluble when those vectors are compatible (see sections 3.2, 3.3 for the precise relationships). In fact, for many surfaces with interesting shapes, there are large moduli spaces of triples of flat structures whose geometries are compatible in the sense that if the underlying Riemann surfaces were conformally identical, the flat structures would correspond to Weierstrass data with a "solved" period problem.

Thus, we have translated the problem of producing a minimal surface in $\mathbb{E}^3$ with prescribed shape into a problem in Teichmüller theory: in a moduli space $\mathcal{M}$ of compatible triples of flat structures, find a triple whose underlying Riemann surfaces coincide. This we solve non-constructively by introducing a non-negative height function $\mathcal{H} : \mathcal{M} \to \mathbb{R}^+$ on $\mathcal{M}$, which has the features of being proper, and whose only critical point is at a solution to our problem. The bulk of the paper is a description of this height function (§4.3), a proof of its properness (§4.6), and a proof that its only critical points are at solutions (§5, §6). An interesting feature of this proof is that it is inductive: the triples of flat structures for a slightly less complicated minimal surface lie on a boundary face of the compactified moduli space $\overline{\mathcal{M}}$ of compatible triples of flat structures for more complicated surfaces. We consider this solution (on $\overline{\mathcal{M}}$) to the less complicated problem as the point-at-infinity of a particularly good locus in the moduli space $\mathcal{M}$ on which to restrict the height and look for a solution. This bootstrapping from slightly less complicated solutions to solutions is the 'handle addition' referred to in the title of the paper.

Along the way, we learn quite a bit about moduli spaces of pairs of flat structures. The bulk of §4 is devoted to describing asymptotic relationships between the underlying conformal structures of flat disks with alternating horizontal and vertical sides of corresponding lengths. Most of §5 concerns estimates on infinitesimal changes in the conformal structure of a flat structure given a prescribed infinitesimal change in its Euclidean geometry; section six concerns the effects on a flat structure of the opening of a node in a Riemann surface.

Our pace in this exposition is occasionally casual, as we have tried to include a number of motivating examples along the way. Indeed, we feel these illustrate the power of our approach. For instance, it is occasionally immediately clear (and even a straightforward calculation) that the moduli space $\mathcal{M}$ for a shape is empty — we then conclude that there is no minimal surface with that shape (see §3.5.2, §7). There are also instances when the moduli space is an identifiable singleton, from which we may conclude immediately that such a shape is realizable minimally; in §3.5.1, we find that this is true for Costa's surface, obviating the need for the analysis of elliptic functions in the proof of the existence of this particular surface, and yielding a conceptually new proof of the existence of this surface.

Here is a detailed discussion of the contents of this paper: we begin in §2 with some background in Teichmüller theory and minimal surfaces, the two subjects which we relate in this paper. The proof of Theorem B occupies the bulk of the paper (sections §3 through §7, §9). While the details are occasionally quite technical and the arguments require some space to present completely, the basic plan and ideas are rather straightforward; we give a step-by-step summary in §2.3. Our objects of study are minimal surfaces which have

sufficient symmetries so that the fundamental domain for the action is a disk. An equivariant form on that surface induces a flat structure on the disk with straight boundaries, and we study such domains ("orthodisks") and their moduli spaces in §3. Also in §3, we meet our main new technical obstacle: we allow our domains to develop into $\mathbb{E}^2$ as branched covers of the plane. This introduces many complications into the analysis in terms of allowing many different types of geometrically defined motions and degenerations within the moduli spaces, as well as some difficulties in defining the frontiers of the moduli space. We deal with these difficulties in §4, where we introduce our height function and prove its properness. In §6 we find a good locus within moduli space on which to flow to a solution, and in §5 we prove that we may flow along that locus to a solution. In §7, we prove the non-existence portion of the classification Theorem B, and we conclude in §8 by extending some of our results: we extend to cases of higher dihedral symmetry in §8.1, and to non-planar ends in §8.2. Finally, in §8.3, we end by offering evidence that our surfaces are embedded; in particular, we state that the surfaces are regularly homotopic to an embedding, by a compactly supported regular homotopy. (Space considerations force us to defer the proofs of the statements in §8.2 and §8.3 to the book [WW2].)

Acknowledgments. It is once again a pleasure to acknowledge our indebtedness to Hermann Karcher for many conversations related to this work, and for a very careful reading which led to a much improved exposition. We also appreciate the helpful comments of the referee.

§2. Background, Notation, and a Sketch of the Argument.

2.1. Minimal Surfaces.

2.1.1 The Weierstraß Representation. Any complete minimal surface M of finite total curvature in $\mathbb{E}^3$ can be defined by

$$z \mapsto \mathrm{Re} \int_{\cdot}^{z} (\omega_1, \omega_2, \omega_3)$$

where ω_i are 3 meromorphic 1-forms on a compact Riemann surface $\mathcal{R}$ such that

$$\omega_1^2 + \omega_2^2 + \omega_3^2 \equiv 0$$

This last condition is usually eliminated by writing

$$\omega_1 = \frac{1}{2}(G - G^{-1})dh, \omega_2 = \frac{i}{2}(G + G^{-1})dh, \omega_3 = dh$$

where G is the Gauß map and dh the height differential. Here dh is a closed (but not necessarily exact) differential on the underlying Riemann surface $\mathcal{R}$.

The pair G and dh are called the Weierstraß data for the minimal surface M.

Significant geometric data attached to such a surface are the total absolute curvature

$$\mathcal{K} := \int_R |K| dA = 4\pi \cdot \text{degree of the Gauß map}$$

and its Riemannian metric

$$ds = \left(|G| + \frac{1}{|G|} \right) |dh|$$

At an end, the value of the Gauß map gives the normal to the asymptotic plane. The metric becomes infinite by completeness, and the order of decay or degeneration describes the type of end: The only possible embedded ends are Catenoid ends and planar ends for which

$$ds \sim \infty^2$$

They are distinguished by the Gauß map: for a catenoid end, it is single-valued and for a flat end, the Gauß map has higher multiplicity. *For the planar ends we will construct, we will assume that the Gauß map at a flat end has local degree three.*

Given a Riemann surface $\mathcal{R}$, a meromorphic function G on $\mathcal{R}$ and a meromorphic form dh on $\mathcal{R}$ for which the metric ds above is regular except at an acceptable collection of distinguished points on $\mathcal{R}$, we can attempt to use the constructed forms ω_i and the formula (called the Weierstraß representation)

$$z \mapsto \text{Re} \int_{\cdot}^{z} \frac{1}{2}(G - G^{-1})dh, \frac{i}{2}(G + G^{-1})dh, dh)$$

to define a minimal surface in space. This procedure works locally, but the surface is only well-defined globally if the periods

$$\text{Re} \int_{\gamma} \frac{1}{2}(G - G^{-1})dh, \frac{i}{2}(G + G^{-1})dh, dh)$$

vanish for every cycle $\gamma \subset \mathcal{R}$. The problem of finding compatible meromorphic data (G, dh) which satisfies the above conditions on the periods of ω_i is known as 'the period problem for the Weierstraß representation'.

We will find it convenient to use the following psychologically different well-known version of the above period conditions and Weierstraß data: we will attempt to specify compatible forms Gdh and $G^{-1}dh$ so that the periods satisfy

$$\text{Re} \int_{\gamma} dh = 0 \tag{2.1a}$$

and

$$\int_{\gamma} Gdh = \overline{\int_{\gamma} G^{-1}dh}. \tag{2.1b}$$

The equivalency to the original period problem is elementary.

The forms $\alpha_1 = Gdh, \alpha_2 = G^{-1}dh$, and $\alpha_3 = dh$ lead to singular flat structures on the underlying Riemann surfaces, defined via the line elements $ds_{\alpha_i} = |\alpha_i|$. These singular metrics are flat away from the support of the divisor of α_i; on elements p of that divisor, the metrics have cone points with angles equal to $2\pi(ord_{\alpha_i}(p)+1)$. More importantly, the periods of the forms are given by the Euclidean geometry of the developed image of the metric ds_{α_i} – a period of a cycle γ is the distance in $\mathbb{C}$ between consecutive images of a distinguished point in γ. We reverse this procedure in section 3: we use putative developed images of the one-forms Gdh, $G^{-1}dh$, and dh to solve formally the period problem for some formal Weierstraß data.

2.2. Teichmüller Theory. For M a smooth surface, let Teich (M) denote the Teichmüller space of all conformal structures on M under the equivalence relation given by pullback by diffeomorphisms isotopic to the identity map id: $M \longrightarrow M$. Then it is well-known that Teich (M) is a smooth finite dimensional manifold if M is a closed surface.

There are two spaces of tensors on a Riemann surface $\mathcal{R}$ that are important for the Teichmüller theory. The first is the space $\mathrm{QD}(\mathcal{R})$ of holomorphic quadratic differentials, i.e., tensors which have the local form $\Phi = \varphi(z)dz^2$ where $\varphi(z)$ is holomorphic. The second is the space of Beltrami differentials $\mathrm{Belt}(\mathcal{R})$, i.e., tensors which have the local form $\mu = \mu(z)d\bar{z}/dz$.

The cotangent space $T^*_{[\mathcal{R}]}(\text{Teich } (M))$ is canonically isomorphic to $\mathrm{QD}(\mathcal{R})$, and the tangent space is given by equivalence classes of (infinitesimal) Beltrami differentials, where μ_1 is equivalent to μ_2 if

$$\int_{\mathcal{R}} \Phi(\mu_1 - \mu_2) = 0 \qquad \text{for every } \ \Phi \in \mathrm{QD}(\mathcal{R}).$$

If $f : \mathbb{C} \to \mathbb{C}$ is a diffeomorphism, then the Beltrami differential associated to the pullback conformal structure is $\nu = \frac{f_{\bar{z}}}{f_z}\frac{d\bar{z}}{dz}$. If f_ϵ is a family of such diffeomorphisms with $f_0 = id$, then the infinitesimal Beltrami differential is given by $\frac{d}{d\epsilon}\big|_{\epsilon=0} \nu_{f_\epsilon} = \left(\frac{d}{d\epsilon}\big|_{\epsilon=0} f_\epsilon\right)_{\bar{z}}$. We will carry out an example of this computation in §5.2.

A holomorphic quadratic differential comes with a picture that is a useful aid to one's intuition about them. The picture is that of a pair of transverse measured foliations, whose properties we sketch briefly (see [FLP] for more details).

A C^k measured foliation on $\mathcal{R}$ with singularities $z_1, \ldots, z_l$ of order $k_1, \ldots, k_l$ (respectively) is given by an open covering $\{U_i\}$ of $\mathcal{R} - \{z_1, \ldots, z_l\}$ and open sets $V_1, \ldots, V_l$ around $z_1, \ldots, z_l$ (respectively) along with real valued C^k functions v_i defined on U_i s.t.

(i) $|dv_i| = |dv_j|$ on $U_i \cap U_j$

(ii) $|dv_i| = |\operatorname{Im}(z - z_j)^{k_j/2}dz|$ on $U_i \cap V_j$

Evidently, the kernels $\ker dv_i$ define a C^{k-1} line field on $\mathcal{R}$ which integrates to give a foliation $\mathcal{F}$ on $\mathcal{R} - \{z_1, \ldots, z_l\}$, with a $k_j + 2$-pronged singularity at z_j. Moreover, given an arc $A \subset \mathcal{R}$, we have a well-defined measure $\mu(A)$ given by

$$\mu(A) = \int_A |dv|$$

where $|dv|$ is defined by $|dv|_{U_i} = |dv_i|$. An important feature that we require of this measure is its "translation invariance". That is, suppose $A_0 \subset \mathcal{R}$ is an arc transverse to the foliation $\mathcal{F}$, with ∂A_0 a pair of points, one on the leaf l and one on the leaf l'; then, if we deform A_0 to A_1 via an isotopy through arcs A_t that maintains the transversality of the image of A_0 at every time, and also keeps the endpoints of the arcs A_t fixed on the leaves l and l', respectively, then we require that $\mu(A_0) = \mu(A_1)$.

Now a holomorphic quadratic differential Φ defines a measured foliation in the following way. The zeros $\Phi^{-1}(0)$ of Φ are well-defined; away from these zeros, we can choose a canonical conformal coordinate $\zeta(z) = \int^z \sqrt{\Phi}$ so that $\Phi = d\zeta^2$. The local measured foliations $(\{\operatorname{Re}\zeta = \text{const}\}, |d\operatorname{Re}\zeta|)$ then piece together to form a measured foliation known as the vertical measured foliation of Φ, with the translation invariance of this measured foliation of Φ following from Cauchy's theorem.

Work of Hubbard and Masur ([HM]) (see also alternate proofs in [K], [Gar] and [Wo]), following Jenkins ([J]) and Strebel ([Str]), showed that given a measured foliation $(\mathcal{F}, \mu)$ and a Riemann surface $\mathcal{R}$, there is a unique holomorphic quadratic differential Φ_μ on $\mathcal{R}$ so that the horizontal measured foliation of Φ_μ is equivalent to $(\mathcal{F}, \mu)$.

Extremal length. The extremal length $\operatorname{Ext}_{\mathcal{R}}([\gamma])$ of a class of arcs Γ on a Riemann surface $\mathcal{R}$ is defined to be the conformal invariant

$$\operatorname{Ext}_{\mathcal{R}}([\gamma]) = \sup_{\rho} \frac{\ell_\rho^2(\Gamma)}{\operatorname{Area}(\rho)}$$

where ρ ranges over all conformal metrics on $\mathcal{R}$ with areas $0 < \operatorname{Area}(\rho) < \infty$ and $\ell_\rho(\Gamma)$ denotes the infimum of ρ-lengths of curves $\gamma \in \Gamma$. Here Γ may consist of all curves freely homotopic to a given curve, a union of free homotopy classes, a family of arcs with endpoints in a pair of given boundaries, or even a more general class. Kerckhoff ([Ke]) showed that this definition of extremal lengths of curves extended naturally to a definition of extremal lengths of measured foliations.

For a class Γ consisting of all curves freely homotopic to a single curve $\gamma \subset M$, (or more generally, a measured foliation $(\mathcal{F}, \mu)$) we see that $\operatorname{Ext}_{(\cdot)}(\Gamma)$ (or $\operatorname{Ext}_{(\cdot)}(\mu)$) can be constructed as a real-valued function $\operatorname{Ext}_{(\cdot)}(\Gamma)$: $\operatorname{Teich}(M) \longrightarrow \mathbb{R}$. Gardiner ([Gar]) showed that $\operatorname{Ext}_{(\cdot)}(\mu)$ is differentiable and Gardiner and Masur ([GM]) showed that $\operatorname{Ext}_{(\cdot)}(\mu) \in C^1(\operatorname{Teich}(M))$. [In our particular applications, the extremal length functions on our moduli spaces will be real analytic: this will be explained in §4.5.] Moreover Gardiner computed that

$$d\operatorname{Ext}_{(\cdot)}(\mu)\,\big|_{[\mathcal{R}]} = 2\Phi_\mu$$

so that

$$\left(d\operatorname{Ext}_{(\cdot)}(\mu)\,\big|_{[\mathcal{R}]}\right)[\nu] = 4\operatorname{Re}\int_{\mathcal{R}} \Phi_\mu \nu. \tag{2.2}$$

This formula will be crucial to our discussion in §5.3.

2.3 A Brief Sketch of the Proof.

While the details of the arguments are sometimes quite involved, the basic logic of the approach and the ideas of the proofs are quite simple. Moreover, it is quite likely that they extend to large classes of other minimal surfaces (see [MW], [WW2]), so in this subsection, we sketch the approach, as a step-by-step recipe.

Step 1. Draw the Surface. The first step in proving the existence of a minimal surface is to work out a detailed proposal. This can either be done numerically, as in the work of Thayer ([Th]) for the Chen-Gackstatter surfaces and Boix and Wohlgemuth ([Bo], [Woh2]) for the low genus surfaces we treat here, or it can be schematic, showing how various portions of the surface might fit together. We follow the latter approach here, which requires quite a bit of terminology – there are many ways to orient and order the handles and ends in a surface of genus five with five planar ends and two catenoid ends, even under an additional restriction on symmetry. To narrow the list of possibilities, one applies either some numerical work, or some intuition, or one attempts to continue with the outline of the proof. We develop the terminology for this process and define the models for some of our candidates in §3.6, and for the rest of them in §3.7.

Step 2. Compute the Divisors for the Forms Gdh and $G^{-1}dh$. From the model that we drew in Step 1, we can compute the divisors for the Weierstraß data, which we just defined to be the Gauss map G and the 'height' form dh. (Note here how important it is that the Weierstraß representation be given in terms of geometrically defined quantities – for us, this gives the passage between the extrinsic geometry of the minimal surface as defined in Step 1 and the conformal geometry and Teichmüller theory of the later steps.) Thus we can also compute the divisors for the meromorphic forms Gdh and $G^{-1}dh$ on the Riemann surface (so far undetermined, but assumed to exist) underlying the minimal surface. Of course the divisors for a form determine the form up to a constant, so the divisor information nearly determines the Weierstraß data for our surface. This Weierstraß data is computed in §3.6 (and §3.7, for an extended class) as well.

Step 3. Compute the Flat Structures for the Forms Gdh and $G^{-1}dh$ required by the period conditions. A meromorphic form on a Riemann surface defines a flat singular (conformal) metric on that surface: for example, from the form Gdh on our putative Riemann surface, we determine a line element $ds_{Gdh} = |Gdh|$. This metric is locally Euclidean away from the support of the divisor of the form and has a complete Euclidean cone structure in a neighborhood of a zero or pole of the form. Thus we can develop the universal cover of the surface into the Euclidean plane.

The flat structures for the forms Gdh and $G^{-1}dh$ are not completely arbitrary: because the periods for the pair of forms must be conjugate (formula 2.1b), the flat structures must develop into domains which have a particular Euclidean geometric relationship to one another. This relationship is crucial to our approach, so we will dwell on it somewhat. If the map $D : \Omega \longrightarrow \mathbb{E}^2$ is the map which develops the flat structure of a form, say α, on a domain Ω into $\mathbb{E}^2$, then the map D pulls back the canonical form dz on $\mathbb{C} \cong \mathbb{E}^2$ to the form α on Ω. Thus the periods of α on the Riemann surface are given by integrals of dz along the developed image of paths in $\mathbb{C}$, i.e. by differences of the complex numbers representing endpoints of those paths in $\mathbb{C}$.

We construe all of this as requiring that the flat structures develop into domains that are "conjugate": if we collect all of the differences in positions of parallel sides for the developed image of the form Gdh into a large complex-valued n-tuple V_{Gdh}, and we collect all of the differences in positions of corresponding parallel sides for the developed image of the form $G^{-1}dh$ into a large complex-valued n-tuple $V_{G^{-1}dh}$, then these two complex-valued vectors V_{Gdh} and $V_{G^{-1}dh}$ should be conjugate. This is the flat structure implication of the period condition formula (2.1b), here using that our situation allows that the periods of all cycles can be found from differences of positions of parallel sides in a flat structure. Thus, we translate the "period problem" into a statement about the Euclidean geometry of the developed flat structures. This is done at the end of section §3.6 (and again in §3.7, for the extended class of surfaces).

The period problem (2.1a) for the form dh will be trivially solved for the surfaces we treat here.

Step 4. Define the moduli space of pairs of conjugate flat domains. Now we work backwards. We know the general form of the developed images (called Ω_{Gdh} and $\Omega_{G^{-1}dh}$, respectively) of flat structures associated to the forms Gdh and $G^{-1}dh$, but in general, there are quite a few parameters of the flat structures left undetermined, even after we have assumed symmetries, determined the Weierstraß divisor data for the models and used the period conditions (2.1b) to restrict the relative Euclidean geometries of the pair Ω_{Gdh} and $\Omega_{G^{-1}dh}$. Thus, there is a moduli space Δ of possible candidates of pairs Ω_{Gdh} and $\Omega_{G^{-1}dh}$: our period problem (condition 2.1b) is now a conformal problem of finding such a pair which are conformally equivalent by a map which preserves the corresponding cone points. (Solving this problem means that there is a well-defined Riemann surface which can be developed into $\mathbb{E}^2$ in two ways, so that the pair of pullbacks of the form dz give forms Gdh and $G^{-1}dh$ with conjugate periods.)

The condition of conjugacy of the domains Ω_{Gdh} and $\Omega_{G^{-1}dh}$ often dictates some restrictions on the moduli space, and even a collection of geometrically defined coordinates. We work these out in the sections §4.2 and §4.4.

When these moduli spaces are empty, then we have a proof of non-existence: this is the case for the surfaces studied in part (ii) of Theorem B – see §7.

Step 5. Solve the Conformal Problem using Teichmüller theory. At this juncture, our minimal surface problem has become a problem in finding a special point in a product of moduli spaces of complex domains: we will have no further references to minimal surface theory. The plan is straightforward: we will define a height function $\mathcal{H} : \Delta \longrightarrow \mathbb{R}$ with the properties:

1. (Reflexivity) The height $\mathcal{H}$ equals 0 only at a solution to the conformal problem
2. (Properness) The height $\mathcal{H}$ is proper on Δ. This ensures the existence of a critical point.
3. (Non-critical Flow) If the height $\mathcal{H}$ at a pair $(\Omega_{Gdh}, \Omega_{G^{-1}dh})$ does not vanish, then the height $\mathcal{H}$ is not critical at that pair $(\Omega_{Gdh}, \Omega_{G^{-1}dh})$.

This is clearly enough to solve the problem: we now sketch the proofs of these steps.

Step 5a. Reflexivity. We need conformal invariants of a domain that provide a complete set of invariants (for Reflexivity), have estimable asymptotics (for Properness),

and computable first derivatives in moduli space (for the Non-critical Flow property). One obvious choice is a set of functions of extremal lengths for a good choice of curve systems, say $\Gamma = \{\gamma_1, \ldots, \gamma_K\}$ on the domains; it is sufficient for Reflexivity that the extremal lengths of these curves provide coordinates for Δ. Suitable curve systems are defined for our examples in sections §4.2 and §4.4. We then define a height function $\mathcal{H}$ which vanishes only when there is agreement between all of the extremal lengths $Ext_{\Omega_{Gdh}}(\gamma_i) = Ext_{\Omega_{G^{-1}dh}}(\gamma_i)$ and which blows up when $Ext_{\Omega_{Gdh}}(\gamma_i)$ and $Ext_{\Omega_{G^{-1}dh}}(\gamma_i)$ either decay or blow up at different rates. See for example Definition 4.3.1 and Lemma 4.5.5.

Step 5b Properness. Our height function will measure differences in the extremal lengths $Ext_{\Omega_{Gdh}}(\gamma_i)$ and $Ext_{\Omega_{G^{-1}dh}}(\gamma_i)$. Often, but not always, a geometric degeneration of the flat structure of either Ω_{Gdh} or $\Omega_{G^{-1}dh}$ will force one of the extremal lengths $Ext.(\gamma_i)$ to tend to zero or infinity, while the other extremal length stays finite and bounded away from zero. This is a straightforward situation where it will be obvious that the height function will blow up. A more subtle case arises when a geometric degeneration of the flat structure forces *both* of the extremal lengths $Ext_{\Omega_{Gdh}}(\gamma_i)$ and $Ext_{\Omega_{G^{-1}dh}}(\gamma_i)$ to *simultaneously* decay (or explode). In that case, we begin by observing that there is a natural map between the vector $< Ext_{\Omega_{Gdh}}(\gamma_i) >$ and the vector $< Ext_{\Omega_{G^{-1}dh}}(\gamma_i) >$. This pair of vectors is reminiscent of pairs of solutions to a hypergeometric differential equation, and we show, by a monodromy argument analogous to that used in the study of those equations, that it is not possible for corresponding components of that vector to vanish or blow up at identical rates. In particular, we show that the logarithmic terms in the asymptotic expansion of the extremal lengths near zero have a different sign, and this sign difference forces a difference in the rates of decay that is detected by the height function, forcing it to blow up in this case. The monodromy argument is given in §4.7, and the properness discussion consumes §4.

Step 5c. Non-critical Flow. The domains Ω_{Gdh} and $\Omega_{G^{-1}dh}$ have a remarkable property: if $Ext_{\Omega_{Gdh}}(\gamma_i) > Ext_{\Omega_{G^{-1}dh}}(\gamma_i)$, then when we deform Ω_{Gdh} so as to decrease $Ext_{\Omega_{Gdh}}(\gamma_i)$, the conjugacy condition forces us to deform $\Omega_{G^{-1}dh}$ so as to increase $Ext_{\Omega_{G^{-1}dh}}(\gamma_i)$. We can thus always deform Ω_{Gdh} and $\Omega_{G^{-1}dh}$ so as to reduce one term of the height function $\mathcal{H}$. We develop this step in §5.

Step 5d. Regeneration. In the process described in the previous step, an issue arises: we might be able to reduce one term of the height function via a deformation, but this might affect the other terms, so as to not provide an overall decrease in height. We thus seek a locus $\mathcal{Y}$ in our moduli space where the height function has but a single non-vanishing term, and all the other terms vanish to at least second order. If we can find such a locus $\mathcal{Y}$, we can flow along that locus to a solution. To begin our search for such a locus, we observe which flat domains arise as limits of our domains Ω_{Gdh} and $\Omega_{G^{-1}dh}$: commonly, the degenerate domains are the flat domains for a similar minimal surface problem, maybe of slightly lower genus or a few fewer ends.

We find our desired locus by considering the boundary $\partial\overline{\Delta}$ of the closure $\overline{\Delta}$ of the moduli space Δ: this boundary has strata of moduli spaces Δ' for minimal surface problems of lower complexity. By induction, there is a solution X' of those problems represented on such a boundary strata Δ' (with all of the corresponding extremal lengths in agreement),

and we prove that there is a locus $\mathcal{Y} \subset \Delta$ inside the larger moduli space Δ (with $\mathcal{Y}$ limiting on X') which has the analogues of those same extremal lengths in agreement. As a corollary of that condition, the height function on $\mathcal{Y}$ has the desired simple properties. This is developed in §6.

The proof then summarizes as follows: we restrict to a locus $\mathcal{Y}$ on which we have the Non-critical Flow Property. By step 5b, the height function $\mathcal{H}$ is proper on $\mathcal{Y}$; thus there is a critical point X on $\mathcal{Y}$ for $\mathcal{H}$. The Non-critical Flow then forces $\mathcal{H}(X) = 0$, so by Reflexivity, the surface represented by X is a solution to our conformal problem, and hence also defines a solution to the minimal surface problem.

§3. The Geometry of Orthodisks.

In this section we introduce the notion of orthodisks.

3.1. Orthodisks.

Consider the upper half plane and $n \geq 3$ distinguished points t_i on the real line. The point $t_\infty = \infty$ will also be a distinguished point. We will refer to the upper half plane together with these data as a *conformal polygon* and to the distinguished points as *vertices*. Two conformal polygons are *conformally equivalent* if there is a biholomorphic map between the disks carrying vertices to vertices, and fixing ∞.

Let a_i be some odd integers such that

$$a_\infty = -4 - \sum_i a_i \tag{3.1}$$

By a Schwarz-Christoffel map we mean the map

$$F : z \mapsto \int_i^z (t - t_1)^{a_1/2} \cdot \ldots \cdot (t - t_n)^{a_n/2} dt \tag{3.2}$$

A point t_i with $a_i > -2$ is called *finite*, otherwise *infinite*. By (3.1), there is at least one finite vertex (possibly at t_∞).

Definition 3.1.1. Let a_i be odd integers. The pull-back of the flat metric on $\mathbb{C}$ by F defines a complete flat metric with boundary on $\mathbb{H} \cup \mathbb{R}$ without the infinite vertices. We call such a metric an *orthodisk*. The a_i are called the *vertex data* of the orthodisk. The *edges* of an orthodisk are the boundary segments between vertices; they come in a natural order. Consecutive edges meet orthogonally at the finite vertices. Every other edge is parallel under the parallelism induced by the flat metric of the orthodisk. Oriented distances between parallel edges are called *periods*. The periods can have 4 different signs: $+1, -1, +i, -i$.

Remark. The integer a_i corresponds to an angle $(a_i + 2)\pi/2$ of the orthodisk. Negative angles are meaningful because a vertex (with a negative angle $-\theta$) lies at infinity and is the intersection of a pair of lines which also intersect at a finite point, where they make a *positive* angle of $+\theta$.

In all the drawings of the orthodisks to follow, we mean the domain to be to the left of the boundary.

Example 3.1.2. Conceivably the simplest orthodisk, bounding the second quadrant in $\mathbb{R}^2$:

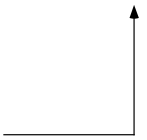

Simple orthodisk

Example 3.1.3. Here is an orthodisk with a branch point which is drawn fat. The disk consists of the region northwest of the larger 5-vertex boundary *and* the region northwest of the fat vertex boundary.

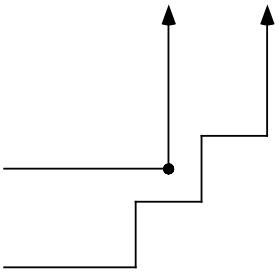

Branched Orthodisk ...

To get a clear picture of this orthodisk, we can glue the following two domains together along the fat diagonal boundary line, in exactly the way that a Riemann surface is assembled from several sheets and a branch cut.

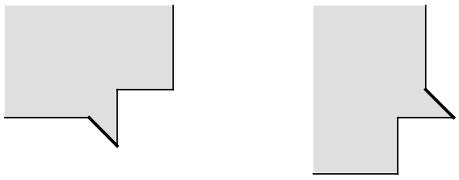

... decomposed into two pieces

Denote by γ_i an oriented curve connecting edge $t_i t_{i+1}$ with edge $t_{i+2} t_{i+3}$. There are $n-1$ such curves. We will denote by the same name also their homotopy classes. It is well-known that the extremal lengths $\mathrm{Ext}(\gamma_i)$ determine the conformal structure of the conformal polygon. This follows because the extremal lengths of a conformal quadrilateral determine the cross-ratios of the vertices of the quadrilateral, and the cross-ratios then determine the vertices of the polygon, where we view the vertices as distinguished points on the boundary of, say, the disk.

Each orthodisk has a natural conformal structure and hence determines a conformal polygon. Vice versa, given a conformal polygon and applying the Schwarz-Christoffel map

to it, one obtains an orthodisk with certain periods. By scaling one can arrange for one period to be (say) 1. We then call this map a normalized period map.

Applying the Schwarz-Christoffel discussion above, and then using the implicit function theorem, one can prove the following proposition (which we will never use, so we omit a detailed proof):

Lemma 3.1.4. *The normalized map from the space of conformal polygons to periods of orthodisks of given vertex data is locally injective.*

We will restrict our attention to a subclass of orthodisks which have a real symmetry.

Definition 3.1.5. An orthodisk is called *symmetric* if it has a reflectional symmetry which fixes two vertices.

All of the orthodisks that will enter our discussion have angles which are odd multiples of $\pi/2$, and, with but two exceptional cases of the vertices representing the catenoid ends, the angles alternate between being congruent to $\pi/2$ and congruent to $3\pi/2$ modulo 2π; the result of this combinatorics of angles is that any symmetric orthodisk must fix a pair of vertices that are on 'opposite' sides of the orthodisks, each halfway between the vertices representing the catenoid ends.

The above examples 3.1.2 and 3.1.3 are symmetric. As a convention we will draw all orthodisks such that the symmetry line is the diagonal $y = -x$.

3.2 From orthodisks to Riemann surfaces.

We begin with an orthodisk X and we describe in this section a method to canonically construct a hyperelliptic Riemann surface Z with a meromorphic 1-form ω_X from X.

Let X be a conformal polygon. First double X along its boundary; i.e. take X and a copy $\overline{X}$ (with the opposite orientation) and glue X and $\overline{X}$ together along their commonly labelled edges. The resulting complex space Y is then topologically a sphere with distinguished points which we also call t_i; moreover, the sphere Y (punctured at the infinite vertices) inherits a complete singular flat structure from X and $\overline{X}$. To see this last statement, begin by observing that the flat structure on $(intX) \cup int(\overline{X})$ extends across the interior of the boundary segments of ∂X and $\partial\overline{X}$ because those segments are straight. At the finite vertices, the flat structure has cone-like singularities, while the infinite vertices are at infinite distance from any point in a neighborhood of them. More precisely, we compute that at the finite vertices, the cone angle at the vertex of the sphere Y corresponding to t_i will be $\alpha_i = 2\pi(a_i/2 + 1)$. We use formally the same formula to attach (negative) cone angles to the vertices at infinity. In fact the end corresponding to an vertex t_i at infinity in $\mathbb{C}$ is conformally the same as the infinite end of a cone with cone angle $-\alpha_i$.

Next, construct simple closed curves $c_i = \gamma_i \cup \overline{\gamma_i}$ on Y by connecting γ_i on X with the oppositely oriented arc $\overline{\gamma_i}$ on $\overline{X}$. Now, as Y is a double of X, the extremal lengths of the c_i determine the conformal structure of the punctured sphere Y. Finally, construct the hyperelliptic double cover Z over Y branched over the vertices t_i. The conformal structure of this covering is independent of the choice of branching slits. However, this is not true for its Teichmüller class: the choice of slits affects the marking of the surface, i.e. the choice of a basis for $\pi_1 Z$. Because we soon want to measure distances in Teichmüller space between

points constructed this way, we need to choose the slits consistently: we take as branch slits the odd numbered edges. It is then easy to check that c_i has two lifts to Z whose sum is null homologous. To pick a specific lift, we make, once and for all, a choice: choose, for each i, a lift $\tilde{c}_i$ of c_i. Subsequent constructions will depend on that choice, so we will have to ensure that the final statements are independent of this choice.

Metrically, on the double cover Z we obtain a lifted flat cone metric with cone angles $\tilde{\alpha}_i = 2\pi(a_i+2)$ at the lifts of t_i: this angle is an odd multiple of 2π. Furthermore, because only parallel edges of X and $\overline{X}$ are glued together in the whole construction, the cone metric on Z has no linear holonomy. Hence the exterior derivative of the (locally defined) developing map of the flat structure defines a global holomorphic 1-form ω_X on Z. (In slightly different language: we develop the flat structure on Z into the Euclidean plane $\mathbb{E}^2$, on which there is defined the one form dz, in the usual coordinates. Because the flat structures on the orthodisks X and $\overline{X}$ are bounded by horizontal and vertical lines, and our identifications take horizontal edges to horizontal edges and vertical edges to vertical edges, the transition maps between the distinct developed images of, say, X, are given by translations. Thus the form dz pulls back to a well-defined one-form ω_X on Z.) This form ω_X has zeroes at the lifts of t_i of order $a_i + 1$; here, negative orders correspond to poles. Because the developing map is only defined up to a complex linear transformation, the 1-form ω_X will only be defined up to homothety.

Lemma 3.2.1. *Up to a factor independent of i, the period of ω_X along $\tilde{c}_i$ is the period of γ_i.*

Proof. Note that the developing map of a flat metric is (locally) only well-defined up to post-composition with a complex linear transformation, so that the 1-form ω is well-defined up to multiplication by some non-vanishing complex number. After having made that choice, a period of ω along $\tilde{c}_i$ is by construction the difference between the image (under the developing map defining this choice of ω) of the endpoint of c_i and the image of its initial point: this is because integrals of ω_X along paths in Z push down via the developing map to integrals of dz along pushed-forward paths in $\mathbb{E}^2 \cong \mathbb{C}$. □

3.3. From orthodisks to Weierstraß data.

We describe how pairs of orthodisks can be used to write down *formal* Weierstraß data for minimal surfaces. This procedure reverses the construction of section 2.1.1 where we find the flat structures associated to a minimal surface; here we will begin to solve the period problem for a minimal surface by first specifying pairs of relevant flat structures (formally Ω_{Gdh} and $\Omega_{G^{-1}dh}$) whose geometry represents compatible periods, in the sense of section 2.1.1.

Definition 3.3.1. Two orthodisks X_1 and X_2 on the same underlying conformal polygon but with different angles (exponents) are called *conformal*. By the construction above, they give rise to two distinct meromorphic 1-forms ω_1, ω_2 on the same Riemann surface Z.

Definition 3.3.2. Two orthodisks X_1 and X_2 with different vertex data are called *conjugate* if there is a line $l \subset \mathbb{C}$ so that corresponding periods are symmetric with respect to that line.

Definition 3.3.3. Two orthodisks X_1 and X_2 are called *reflexive* if they are conformal and conjugate.

Now suppose that the pair of orthodisks X_1 and X_2 are defined on the same conformal polygon. Let the corresponding 1-forms on Z be denoted ω_1 and ω_2. We want to find a meromorphic function G (the Gauß map) and a meromorphic 1-form dh (the height differential) such that

$$\omega_1 = G dh$$
$$\omega_2 = G^{-1} dh$$

and such that G and dh are Weierstraß data of a minimal surface on Z.

To solve the above equations, denote the vertex data of X_1 by a_i and the vertex data of X_2 by b_i (recall that these are odd numbers). Then at a point t_i on the putative underlying Riemann surface, the meromorphic quadratic differential $\omega_1\omega_2$ has a zero of order $a_i + b_i + 2$ which is an even number; thus, we first ask for dh with zero of order $\frac{1}{2}(a_i + b_i) + 1$.

Here is a simply defined but quite general case where one can find such a dh:

Lemma 3.3.4. *Suppose that, for each index i, the sum $a_i + b_i \equiv 0 \pmod 2$. Then there is a meromorphic 1-form dh on Z as above with all periods purely imaginary.*

Proof. Consider on the sphere Y the meromorphic 1-form

$$\omega = \prod_{i=1}^{n} (t - t_i)^{(a_i+b_i)/2} dt.$$

Lift it via the hyperelliptic covering projection to Z and call the lift dh. Clearly, this meromorphic 1-form has the required zeroes (and poles) at the preimages of the t_i.

The periods of dh are all computable as periods of the form ω on Y which are all computable as $2\pi i$ multiples of purely real residues.

This lemma will apply to all cases we need. We deduce:

Theorem 3.3.5. *Let X_1 and X_2 be reflexive orthodisks with exponents a_i and b_i. Suppose that $a_i + b_i \equiv 0 \pmod 2$. Then the above Weierstraß data define a minimal surface.*

Proof. It remains to show that the thus found Weierstraß data have purely imaginary periods, or equivalently (see formula (2.2)) that the forms Gdh and $G^{-1}dh$ have conjugate periods. Yet the forms Gdh and $G^{-1}dh$ on the Riemann surface Z are lifted from the canonical forms on the orthodisks X_1 and X_2, respectively: the conjugacy of the orthodisks X_1 and X_2 then forces the periods of Gdh and $G^{-1}dh$ on the Riemann surface Z to be conjugate.

□

Definition 3.3.6. We call the pair of vertex data a_i, b_i of a pair of orthodisks of the same genus *formal Weierstraß data*.

3.4 Geometric significance of the formal Weierstraß data.

In this section we assume that we have a pair of reflexive orthodisks (i.e. conjugate orthodisks defined over the same underlying conformal ploygon) and we then determine the geometric data of the resulting minimal surface. These data will be given in terms of the formal Weierstraß divisor data a_j and b_j.

First, by construction, the Riemann surface resulting from a pair of conformal orthodisks with $n = 2g + 1$ vertices will have genus g.

Recall (section 2.2) that the Riemannian metric of the associated minimal surface with Weierstraß data G and dh is given by

$$ds = (|G| + \frac{1}{|G|})|dh|$$

Singularities of this metric can only occur at the $2g+2$ vertices of the conformal polygon, where the branching (of the surface Z over the double Y) occurs. By the divisor discussion, the one-form dh will have a zero of order $1 + \frac{a_i+b_i}{2}$ and G a zero of order $\frac{a_i-b_i}{2}$ Hence $|G|+\frac{1}{|G|}$ will have a pole of order $\frac{|a_i-b_i|}{2}$ and thus to have a complete metric it is necessary and sufficient that

$$2 + a_i + b_i \leq |a_i - b_i|$$

for all i (including the vertex at infinity!).

It is also easy to compute the total curvature or equivalently the degree of the Gauß map as

$$\deg G = \frac{1}{2} \sum_{a_i > b_i} a_i - b_i$$

where the index $i = \infty$ is possibly included.

In the following table we compile a list of typical special points on minimal surfaces and the resulting vertex data. Formal Weierstraß data are then given as ordered lists of points of these types, and these types only. In particular, these special points appear as vertices on the conformal polygons, with vertex data given as fractions of cone angles for the flat structures of the forms $(Gdh, G^{-1}dh, dh)$. The fractions arise because a neighborhood of a special point on the Riemann surface may n-fold cover a neighborhood of its image on the conformal polygon, so the cone angle on the conformal polygon will be $\frac{1}{n}$ of the cone angle on the Riemann surface. Formal Weierstraß data are conformal polygons labelled with vertex data chosen from this table.

Denote by H finite non-branch points of the minimal surface where the symmetry curves intersect, by C a catenoid end, by P a planar end with degree of Gauß map equal to 3, and R is a point which lies on just one symmetry arc. An uparrow ($\uparrow$) means that the Gauß map takes the value ∞, a downarrow ($\downarrow$) that the Gauß map takes the value 0. Then the

divisors at the respective points are given by

	G	dh	Gdh	$G^{-1}dh$	$\angle Gdh$	$\angle G^{-1}dh$	$ex(Gdh)$	$ex(G^{-1}dh)$
$H\uparrow$	-1	1	0	2	$\pi/2$	$3\pi/2$	-1	1
$H\downarrow$	1	1	2	0	$3\pi/2$	$\pi/2$	1	-1
$C\uparrow$	-1	-1	-2	0	$-\pi/2$	$\pi/2$	-3	-1
$C\downarrow$	1	-1	0	-2	$\pi/2$	$-\pi/2$	-1	-3
$P\uparrow$	-3	1	-2	4	$-\pi/2$	$5\pi/2$	-3	3
$P\downarrow$	3	1	4	-2	$5\pi/2$	$-\pi/2$	3	-3
$R\uparrow$	-1	1	0	2	π	3π	0	2
$R\downarrow$	1	1	2	0	3π	π	2	0

The last two columns just contain the vertex data a_i and b_i of the formal Weierstraß data for Gdh and $G^{-1}dh$. The last two rows record angles that are not quite in the same pattern as the previous rows; the points R have a surrounding neighborhood with but a two-fold symmetry while the points H, C, and P all have neighborhoods with a four-fold symmetry. These points will only be important in section 8.2 when we indicate how one might deform the surfaces with planar ends into those with catenoid ends. (Full details will be given in [WW2].)

3.5 Examples of simple orthodisks.

In this section we give some motivating examples of minimal surfaces and their corresponding orthodisks. We begin first with some discussion about moduli spaces of orthodisks, which we shall later formalize at the outset of section 4. We then organize our examples into families, depending upon whether the associated moduli spaces are empty, singletons, or non-trivial.

To begin then, observe that from some formal Weierstraß data, we may draw orthodisk systems consisting of conjugate orthodisks Ω_{Gdh} and $\Omega_{G^{-1}dh}$ for the forms Gdh and $G^{-1}dh$, respectively. We often have some freedom in deciding the lengths of the edges of the orthodisks, even up to equivalence of conformal polygons. Thus, the formal Weierstraß data determines a moduli space of conjugate orthodisk systems $\{\Omega_{Gdh}, \Omega_{G^{-1}dh}\}$. While the function theory of this moduli space is the principal subject of this paper, here we shall content ourselves with a few examples for which the moduli space is either trivial or small. (See [WW2] for more examples.)

3.5.1. A singleton moduli space

Example 3.5.1. The Costa surface $DH_{0,0}$ $(= CT_0)$

This surface is the starting point for the investigations in this paper. We seek a torus with two catenoid ends (C_1 and C_2), one planar end P_1 and one finite point H_1 with vertical normal. We also assume our standard eight symmetries: reflections about two orthogonal vertical planes and a rotation about a horizontal line. (Previous existence and uniqueness proofs may be found in [Cos] and [Ho-Me]) ¿From the table in section 3.4, we can write formal Weierstraß data for this surface, assuming that the points occur on the real line in the order $C_1 - P_1 - C_2 - H_1$. We will justify this assumption in section 3.6; however, below we reproduce a computer image of a fundamental domain of Costa's

surface for the group generated by reflections in vertical planes. This makes apparent the conformal polygon, and the order of the special points on its boundary.

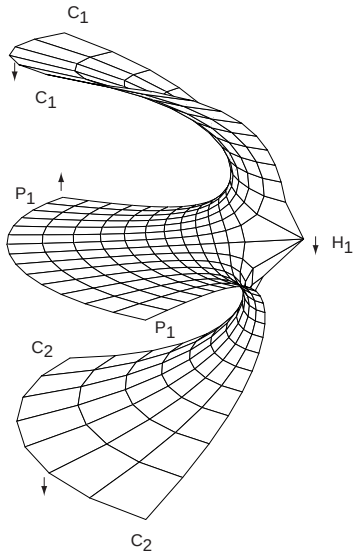

A quarter of Costa's surface — a conformal image of the orthodisks

A table corresponding to the one in §3.4 is given below; it computes the cone angles for the forms Gdh and $G^{-1}dh$ on the putative conformal polygon for Costa's surface. These flat structures are drawn below, assuming an additional symmetry about the line $\{y = -x\}$.

	G	dh	Gdh	$G^{-1}dh$	$\angle Gdh$	$\angle G^{-1}dh$	$ex(Gdh)$	$ex(G^{-1}dh)$
$C_1 \downarrow$	1	-1	0	-2	$\pi/2$	$-\pi/2$	-1	-3
$P_1 \uparrow$	-3	1	-2	4	$-\pi/2$	$5\pi/2$	-3	3
$C_2 \downarrow$	1	-1	0	-2	$\pi/2$	$-\pi/2$	-1	-3
$H_1 \downarrow$	1	1	2	0	$3\pi/2$	$\pi/2$	1	-1

Yet recall that any conformal quadrilateral with a symmetry across a diagonal is conformally equivalent to a square.

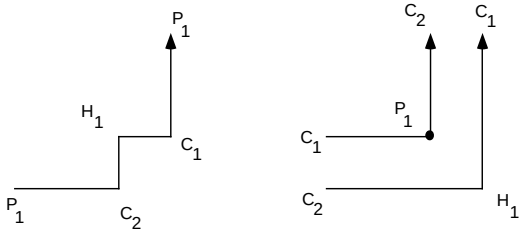

Costa orthodisks

Thus we then note that (as in example 3.5.1), the moduli space of possible examples

consists only of the singleton of a pair of square tori, so the only element in the moduli space is a reflexive pair. This establishes the existence of this surface, by a proof that is somewhat distinct from the other proofs of existence of this surface ([Cos], [Ho-Ka]).

3.5.2. Empty moduli spaces

Non-Example 3.5.2(i). Catenoid with one handle

In this example, we try to construct a minimal surface with two catenoid ends and one handle. Now, a theorem of Schoen [Sch] implies that any minimal surface of genus $g \geq 1$ with but two embedded catenoid ends cannot exist; here we will require in addition the eightfold symmetry present in all of our examples. Yet, it is clear from an analysis of the orthodisks pictured below that such a surface cannot exist with 4-fold symmetry, because there is no symmetric and conjugate pair: the periods from $\overline{C_1C_2}$ to $\overline{H_1H_2}$ are conjugate about the line $\{y = -x\}$, while the periods from $\overline{C_2H_2}$ to $\overline{H_1C_1}$ are conjugate across the line $\{y = -x\}$.

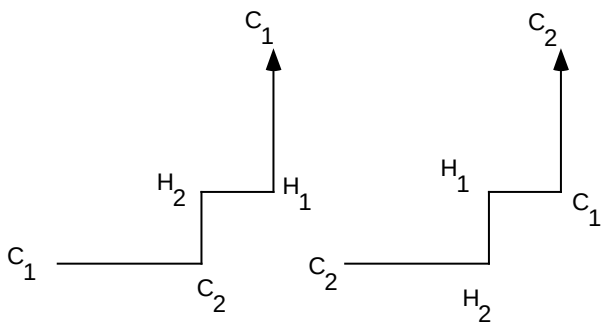

Catenoid with one handle

We will use this technique of showing non-existence extensively when we prove the non-existence parts of the main theorem.

Non-Example 3.5.2(ii). The Horgan surface $DH_{0,1}$

The second example is called the Horgan surface (see [Ho-Ka]): To visualize it, start with one plane and two handles growing upwards and downwards and perpendicular to each other. Both handles connect to catenoid ends. This looks almost as shown in the following figure:

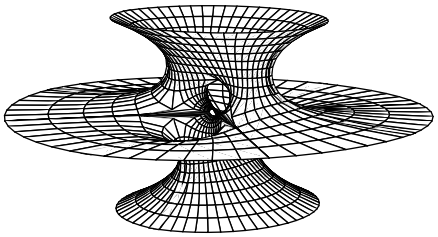

The Horgan surface?

This pattern leads to a sequence

$$C_1 - P - C_2 - H_2 - M - H_1 - C_1$$

(see section 3.6) where M denotes a previously unencountered regular point where the symmetry lines cross. The orthodisks are as follows:

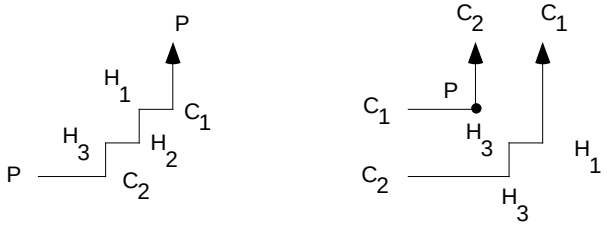

Horgan orthodisk

Recently, one of us [W] showed that this surface cannot exist by a method that is different from that used in Example 3.5.2(ii). Therefore, this moduli space is empty. We find it remarkable that our general existence proof fails at precisely one point for the case of this surface: see §4, after Definition 4.1.1.

3.6 Orthodisks for the Costa Towers.

This section is intended to give a heuristical picture for the Costa towers and to derive the orthodisk pairs from this picture.

As a first series of new examples, we introduce the orthodisks for generalized Costa surfaces which we call *Costa towers*:

Definition 3.6.1. A *Costa tower* of genus g is a complete minimal surface CT_g of genus g with two parallel catenoid ends and g planar ends which are all embedded. These surfaces have total curvature $4\pi(g+2)$.

Remark 3.6.2. The existence of generalized Costa surfaces is known for $g \leq 2$ and numerical evidence has been provided for $g = 3$, see [Cos, Bo, Ho-Me, Woh1, Woh2]. All these examples have (at least) a twofold reflectional symmetry at two perpendicular planes intersecting in the z-axis. In their construction, this assumption makes the period problem

low dimensional. The genus 1 Costa surface has the square torus as underlying Riemann surface and is known to admit a deformation to all rectangular tori such that the planar end becomes catenoidal.

We will briefly discuss these deformations from our point of view in section 8.2.

To get an impression of how these surfaces might appear, imagine cutting a catenoid by g horizontal planes. For each plane, we have to resolve a singularity which looks topologically like a horizontal plane cut by a vertical cylinder. We replace a neighborhood of the singular locus in the complex of cylinder and plane by one of the two shapes below, i.e. we replace the upper part of the cylinder by a Y-piece whose lower two boundary components are glued to two holes in the plane and glue the boundary component of the lower part of the cylinder to another hole in the plane in between the two first holes, and finally glue the boundary of the flat planar piece to the planar boundary of the excised neighborhood.

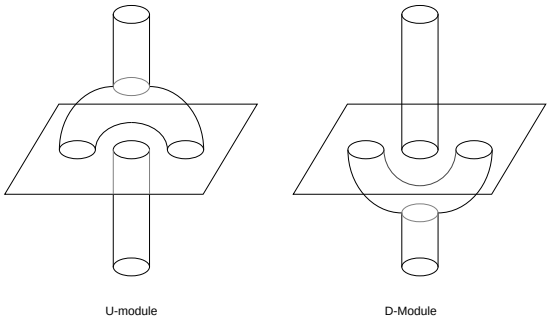

Building blocks for informal surface models

We will call the left gadget an U-module (for *up*) and the right one a D-module (for *down*). It is convenient to regard the planar portions of the figures as extending indefinitely.

Stacking g copies of these modules over each other and finishing with catenoidal ends yields a rough informal model of candidates for a Costa tower of genus g. These models are not very realistic, but they will suffice to write down candidate formal Weierstraß data for the surfaces.

Remark 3.6.3. At first glance there are two more possible constructions of this type, which are obtained by rotating the above pieces by 90° around the z-axis, but it turns out that these give no new Weierstraß data, so we will neglect them from the beginning.

Despite this, there are still many possible ways to attach these modules to each other, and we will not attempt to discuss all of them. Only for a very distinctive construction will our proof establish the existence of minimal surfaces corresponding to these models, and we have presently no contribution to make regarding the others. For these other models, no complete existence or non-existence proofs are known, but numerical experiments make it doubtful that other module towers will produce more minimal surfaces.

Now we proceed to derive the Weierstraß candidate data defined by a module tower. Cutting a generalized Costa surface composed of these modules by its two vertical symmetry planes decomposes it into four congruent simply connected domains which we want

to describe using orthodisks. The first step is to recover the formal Weierstraß data from the putative geometry:

Lemma 3.6.4. *Let X be a generalized Costa surface consisting of g modules X_i of type U. Denote by P_i the point on X corresponding to the planar end of module i and by H_i the saddle point of that module X_i. Denote by G the Gauß map and by dh the height differential of X. Then the divisors of G and dh are given by*

$$\begin{aligned}(G) &= C_1^1 P_1^{-1} H_1^1 P_2^1 H_2^{-1} \cdots P_g^{(-1)^g} H_g^{-(-1)^g} C_2^{-(-1)^g} \\ (dh) &= C_1^{-1} P_1^1 H_1^1 P_2^1 H_2^1 \cdots P_g^1 H_g^1 C_2^{-1} \\ (Gdh) &= H_1^2 P_2^2 \cdots \\ (G^{-1}dh) &= C_1^{-2} P_1^2 H_2^2 \cdots\end{aligned}$$

Proof. First we determine the direction of the normal vector at all of the vertical points of G. We can assume that the outer normal vector at the upper catenoid end C_1 is pointing downward. As can be read off from the above figure, the normal will switch between up and down from planar end to planar end. Hence all odd labeled planar ends will have an upward pointing normal, all even planar ends a downward pointing normal, and the bottom catenoid end has normal pointing up if and only if g is even. Again by the figure above, the normal at the saddle point of a module point is always in the opposite direction as the normal at the planar end. Using the information from the table at the end of section 3.4, we get the claimed divisors. □

Definition 3.6.5. Let T be a sequence of length g consisting of symbols U and D. A surface of type T is a generalized Costa surface consisting of modules X_i where the handle of module i grows upwards (resp. downwards) if the symbol i is U (resp. D).

Lemma 3.6.6. *Let X be a surface of type T. Then the formal Weierstraß data are explicitly determined by the type T.*

Proof. To see this, we first consider a surface where all modules are U-modules. We follow the symmetry line given by the intersection with the $y = 0$-plane, beginning at the top catenoid end on the left. This line goes down to the first planar end to the left. There the total angle is divided into 4 equal pieces by the two symmetry lines meeting there. We continue now on the symmetry line defined by the $x = 0$-plane which goes down into the second planar end. Continuing this process and switching to another symmetry line at each vertex, we descend through all planar ends until we reach the bottom catenoid end. From there, we ascend through all handles back to the top catenoid end. We denote this closed path by

$$C_1 \to P_1 \to P_2 \to \ldots \to P_g \to C_2 \to H_g \to \ldots \to H_2 \to H_1 \to C_1$$

Now exchange the k^{th} module by a D-module. As can be seen from the figure above, this affects only the entries P_k and H_k in the path list: they are just exchanged. Hence for an arbitrary surface X of type D we get a path sequence

$$C_1 \to A_1 \to A_2 \to \ldots \to A_g \to C_2 \to B_g \to \ldots \to B_2 \to B_1 \to C_1$$

where $A_k = P_k$ and $B_k = H_k$ if the module X_k is of type U and $A_k = H_k$ and $B_k = P_k$ otherwise.

We now give some low genus examples to illustrate the domains. The images are developed images of the flat structures Ω_{Gdh} and $\Omega_{G^{-1}dh}$ for Gdh and $G^{-1}dh$ (respectively) on the Riemann surfaces: the domain is locally always to the left of the curve. We indicate the corners with angle $5\pi/2$ by a fat dot.

The genus 1 example using just one handle is the Costa surface, see example 3.5.1.

For genus 3, there are essentially two distinct possible symmetric module sequences with types (UUU) and (UDU): i.e. there are only these two up to replacing a 'U' by a 'D' and vice versa.

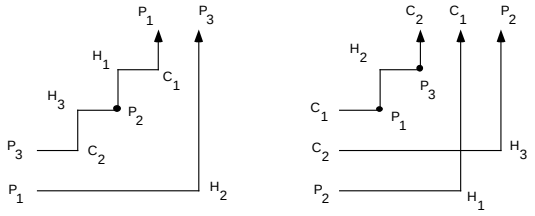

Orthodisks for the UUU candidate surface

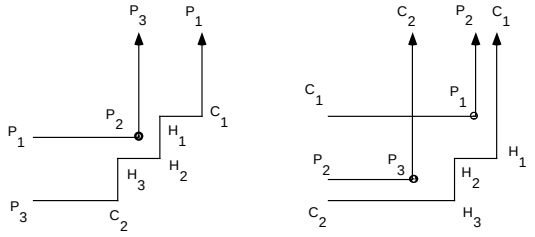

Orthodisks for the UDU candidate surface

We will only be able to prove the existence of the second one. Numerical investigations give little hope that the first one also exists. Starting with the second surface, we will inductively construct all our other examples.

To see how the surface of type $T = (UD)^n U$ evolves as n increases, here are the orthodisks for $UDUDU$:

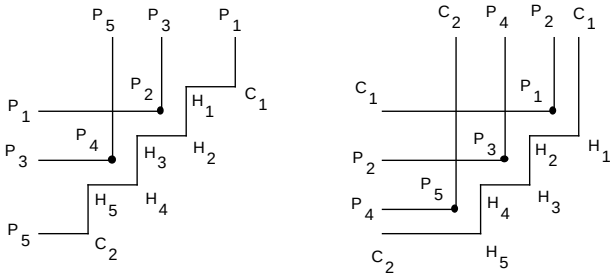

The $UDUDU$ candidate orthodisks for a genus 5 surface

Geometrically, our choice of candidate surfaces can be characterized by the property that the intersection of the surface with the symmetry planes contains one arc componenet which connects all the finite points with vertical normal (on the z-axes) while all other arc components connect the ends.

The pair of orthodisks for the general surface of type $CT_n = (UD)^n U$-surface of genus $g = 2n + 1$ are indicated below. These surfaces have 2 catenoid ends denoted by C_1, C_2; g planar ends denoted by $\{P_k\}$; and g finite points with vertical normals at the handles denoted by $\{H_k\}$. There are $4n + 4$ vertices in each orthodisk, of which n are branch points.

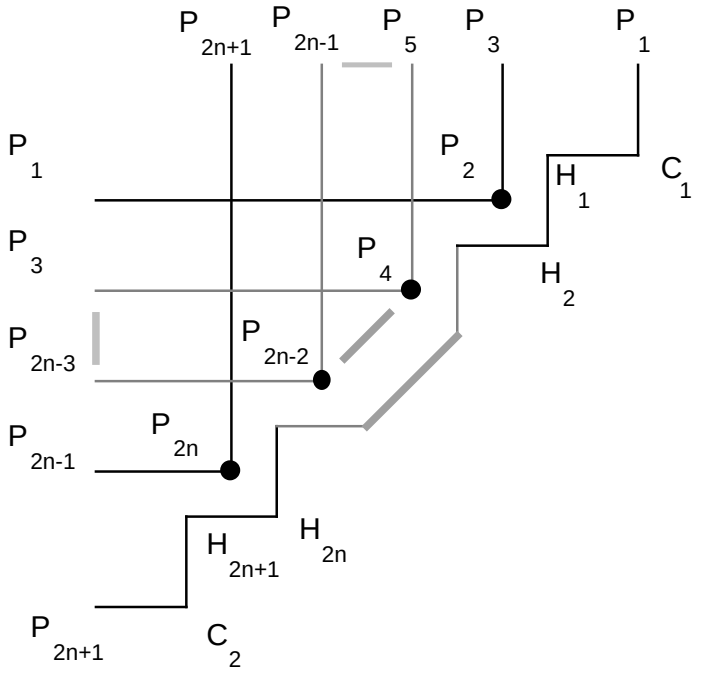

The Ω_{Gdh} orthodisk for CT_n

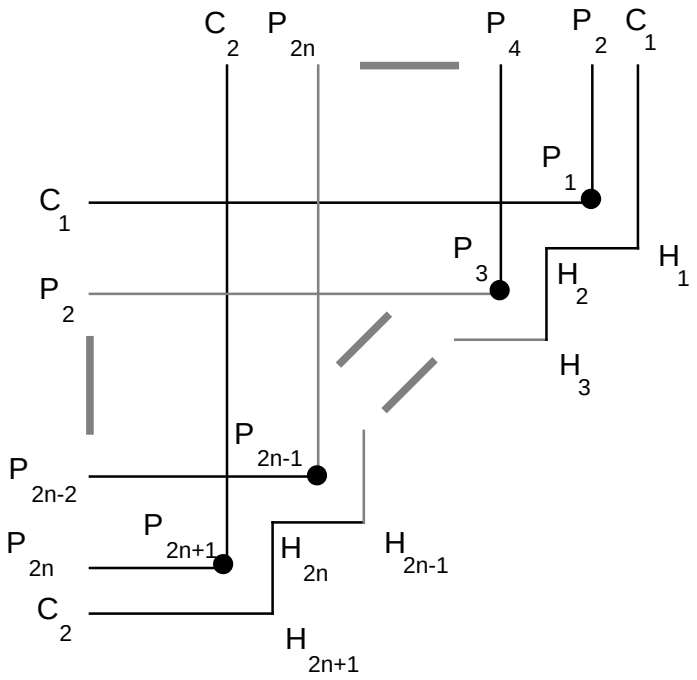

The $\Omega_{G^{-1}dh}$ orthodisk for CT_n

3.7 More orthodisks by drilling holes.

In the previous section, we have described the candidate formal Weierstraß data of a family of minimal surfaces generalizing Costa's surface for every odd genus greater than 1. Now we are going to add handles (without enlarging the symmetry group) to all these surfaces in a symmetric fashion. We call this process *hole drilling*, and we will designate the resulting surfaces as $DH_{m,n}$ surfaces.

We start with an informal description.

For each odd integer $n \geq 3$ we describe a process of handle addition which inductively adds to the surface of type $(UD)^n U$ an arbitrary number of handles without adding ends. Recall that our Costa-tower surfaces are composed of a stack of modules called U- and D-module.

Now we allow two other kind of modules, called F- and S-module (for front and side) which are vertical cylinders with handles drilled through them from the front or the side, as indicated:

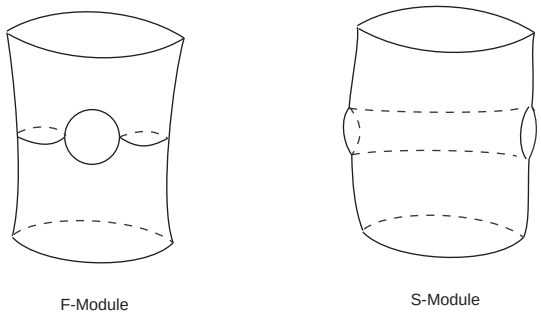

Modules for drilling holes

As in the case of the U- and D- modules, we are not able to prove existence for surfaces made of arbitrary module sequences.

As for the Costa Towers, our choice of candidate surfaces is be characterized by the property that the intersection of the surface with the symmetry planes contains one arc component which connects all the finite points with vertical normal (on the z-axes) while all other arc components connect the ends.

To be more specific, we will now add one handle to the UDU-surface.

There are apparently two possibilities according to the above rule, namely $USDU$ and $UDFU$. But it is easy to see that the module sequences SD and DL generate equivalent formal Weierstraß data: If one follows the intersection curves of these module sequences with the vertical symmetry planes, one obtains the same pattern of special points at the z-axes, hence the same formal Weierstraß data. So the topological significance of these modules does not impose much restriction on the possible geometry of the surfaces.

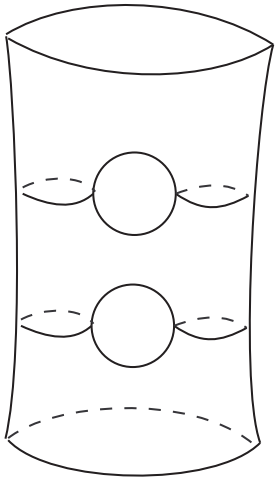

Iterated hole drilling

Remark 3.7.1. This process does work formally for $n = 1$, but the candidate surface would be Costa's surface with one handle added; this is known as the Horgan surface. See Non-Example 3.5.2(ii).

We now describe the orthodisks arising from the handle addition process. A module sequence of type UF or DU results in two consecutive finite corners of angle $\pi/2$ and $3\pi/2$ (or vice versa) of the orthodisks. Inserting a handle according to the above rules results in adding two new finite corners in between the old corners in a zigzag fashion. We illustrate this for $USDU$ (compare with example 3.5.1).

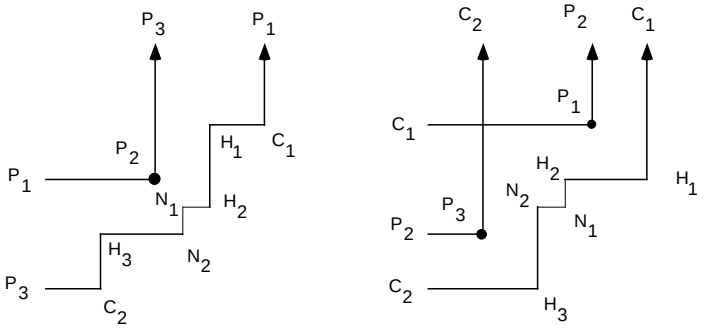

Growing a handle by adding the two new corners N_1 and N_2

Now that we have introduced these new module sequences, we can extend our original one-parameter sequence of Costa towers to a two-parameter sequence of orthodisks. We introduce a new two-parameter family of orthodisks and give geometric coordinates. To set notation, we consider a pair of orthodisks with $2n+1$ vertical normals at the z-axis and $2m+1$ planar ends. Together with the two catenoid ends we have $2m+2n+4$ Weierstraß points so that the Riemann surface will have genus $m+n+1$. In the case $m = n$ we are in the situation of the Costa tower surfaces of type $(UD)^nU$. We are aiming now for $n > m \geq 0$, the cases in which we will establish existence in the next three sections.

Here is a table depicting these surfaces and giving their historical context:

$m\backslash n$	0	1	2	3	4	5	6	7
0	Costa	Horgan	?	?	?	?	?	?
1	−	B-W	+	+	+	+	+	+
2	−	−	+	+	+	+	+	+
3	−	−	−	+	+	+	+	+
4	−	−	−	−	+	+	+	+
5	−	−	−	−	−	+	+	+

Meaning of the symbols:

(1) ?: We have not been able to construct these surfaces. Constructing one would imply the existence of the others with higher genus. We conjecture that these do not exist.

(2) $-$: We will see that these do not exist. This is a very special case of the Hoffman-Meeks conjecture, and is the second portion of the Main Theorem B.
(3) $+$: Dealt with in the following sections, this is the first portion of the main theorem.
(4) $B - W$: This surface was found numerically by Boix and Wohlgemuth, see [Bo].

§4. The Space of Orthodisks.

4.1 Introduction.

In this chapter, we will parameterize the space of pairs of conjugate orthodisks by geometric data, set up a height function on this space which measures the conformal distance between the two orthodisks and prove its properness. The main point in choosing the geometric coordinates lies in what we call the *completeness condition:* We require that whenever we have a sequence of points leaving every compact set of the coordinate space (that is, when a *geometric degeneration* occurs), at least one of the two orthodisks Ω_{Gdh} and $\Omega_{G^{-1}dh}$ degenerates conformally. After introducing complete geometric coordinates, the height function is set up to measure differences in the extremal lengths of cycles in a way which detects precisely the degenerations coming from a geometric degeneration. Because it can easily happen that a geometric degeneration forces the simultaneous conformal degeneration of both orthodisks, we also need to measure the rates of extremal lengths. This is done by a technical monodromy argument which is postponed to the final section 4.7. For the sake of clarity, we will now describe the height function and formulate the monodromy theorem.

The height is constructed as a sum of terms each of which measures the possible conformal degeneration of the extremal length of one cycle:

Definition 4.1.1. Fix formal Weierstraß data and consider a cycle c in a conformal disk. Given a pair of conjugate orthodisks Ω_{Gdh} and $\Omega_{G^{-1}dh}$ with the chosen formal Weierstraß data, define the height of a cycle c by

$$\mathcal{H}(c) = \left| e^{1/\operatorname{Ext}_{\Omega_{Gdh}}(c)} - e^{1/\operatorname{Ext}_{\Omega_{G^{-1}dh}}(c)} \right|^2 + \left| e^{\operatorname{Ext}_{\Omega_{Gdh}}(c)} - e^{\operatorname{Ext}_{\Omega_{G^{-1}dh}}(c)} \right|^2$$

Then the definition of the height requires a choice of cycles c_i and will then be defined as

$$\mathcal{H} = \sum_i \mathcal{H}(c_i)$$

This choice is restricted by a couple of different requirements:

(1) Asymptotic computability: To prove properness, we need a precise asymptotic formula in the case of geometric degenerations. Such formulas are available only in special situations. For us, this means that we have to choose simple cycles or double cycles which are symmetric with respect to the diagonal. Such cycles will be called *admissible* cycles.
(2) Avoidance of certain edges: In the next chapter, we need to compute the derivative of the height with respect to changes in the coordinates which can be described as

'pushing edges'. There, more cycles ending at the pushed edge yield more terms of the height function that we will need to control, so we aim not to have too many cycles meeting a given edge.

These restrictions have the curious effect that it becomes easier to choose the right cycles for surfaces of higher genus and with more topology; it is the lowest genus case which causes most problems. And in fact, the reason that our present proof does not extend to prove the existence of the non-existing Horgan surface (see [W]) is our inability to choose sufficiently many good cycles.

¿From the above form of the height function it is clear that we can prove properness when we can ensure that the extremal length of a chosen cycle tends to 0 or ∞ for one domain but remains bounded and bounded away from 0 for the other one. However, we will encounter situations where the extremal length of a cycle degenerates to zero (or infinity) simlutaneously in *both* domains. Here we will need to invoke the following theorem, proven in section 4.7 as lemmas 4.7.1 and 4.7.2 by a monodromy argument:

Monodromy Theorem 4.1.2. *Fix formal Weierstraß data and an admissible cycle c (see above). Consider a sequence of pairs of conjugate orthodisks Ω_{Gdh} and $\Omega_{G^{-1}dh}$ such that either c encircles a single edge in Ω_{Gdh} shrinking geometrically to zero and both $\mathrm{Ext}_{X_1(n)}(\gamma) \to 0$ and $\mathrm{Ext}_{X_2(n)}(\gamma) \to 0$ or c foots on an edge in Ω_{Gdh} shrinking geometrically to zero and both $\mathrm{Ext}_{X_1(n)}(\gamma) \to \infty$ and $\mathrm{Ext}_{X_2(n)}(\gamma) \to \infty$. Then $\mathcal{H}(c) \to \infty$ as $n \to \infty$.*

For the sake of a clear exposition, we have treated in detail the special but most fundamental case $CT_3 = DH_{1,1}$ in §4.2 and §4.3, postponing the general case to the two subsequent sections §4.4 and §4.4. Historically, this surface was first discovered numerically by Boix and Wohlgemuth ([Bo]).

4.2 Geometric coordinates for the $DH_{1,1}$ surface.

In this section, we describe geometric coordinates for our basic surface $DH_{1,1}$.

Denote by

$$\Delta = \{(y, b, g) \in \mathbb{R}^3 : 0 < y, b, g < 1, y + b + g = 1\}$$

and by $\bar{\Delta}$ its closure. For each point in Δ, we will associate a pair of orthodisks. We introduce three cycles, called yellow , green , and blue :

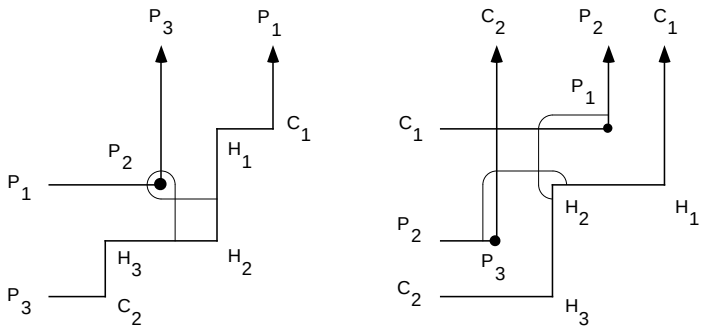

yellow cycle

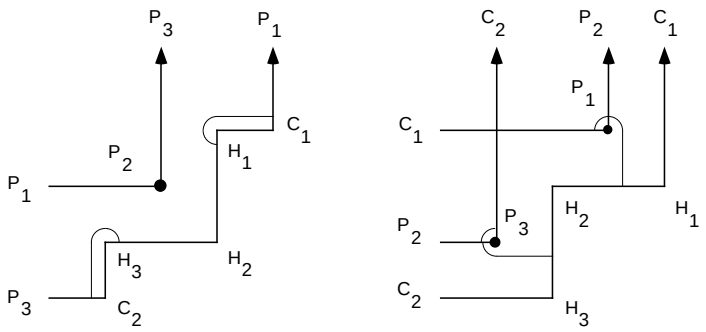

blue cycle

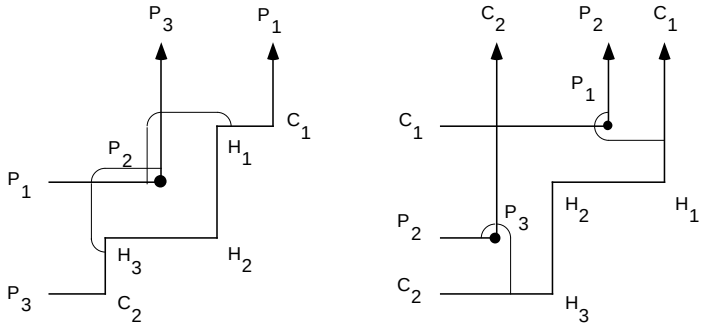

green cycle

Formally,

(1) yellow consists of (undirected) arcs connecting H_3H_2 with P_1P_2 and symmetrically H_2H_1 with P_2P_3.
(2) blue consists of (undirected) arcs connecting P_3C_2 with H_3H_2 and symmetrically C_1P_1 with H_2H_1.
(3) green consists of (undirected) arcs connecting P_1P_2 with H_1C_1 and symmetrically P_2P_3 with C_2H_3.

Why should we choose these particular curves? At this stage, the choice has little to do with the eventual geometry of the minimal surface, and much to do with the conformal and combinatorial geometry of the orthodisk: our goal is to meet criteria (1) and (2) of the last subsection.

Now each orthodisk is determined up to scaling by the lengths of the periods of these cycles which we denote by y, b, g subject to the condition $y + b + g = 1$. Hence for any triple $(y, b, g) \in \Delta$ we can form a pair of orthodisks with these normalized period lengths. It is clear that these orthodisks will be conjugate.

We call Δ a geometric coordinate system for the formal Weierstraß data of type $DH_{1,1}$. By this we mean the following:

Definition 4.2.1. Let formal symmetric Weierstraß data be given. A geometric coordinate system is an open subset Δ of a Euclidean space such that for each point in Δ, there

is a pair of normalized symmetric conjugate orthodisks with the given Weierstraß data such that the periods of the orthodisk are linear functions in the coordinates of the point in Δ.

Here a pair of symmetric orthodisks is *normalized* if the outer sheet boundary of the orthodisk Ω_{Gdh} consists of finite edges with total length equal to 1.

We will from now on only consider normalized orthodisks.

Here our geometric coordinate system Δ records the periods for a set of cycles that span the homology of the (covering) surface, hence provides sufficient information for determining all of the periods via linear functions of the given ones.

In the rest of this section we will show that our coordinate geometric system is *complete* in the following sense:

Definition 4.2.2. A geometric coordinate system Δ is called *complete* if for any sequence of points in Δ leaving any compact set, the conformal structure of at least one of the orthodisks degenerates.

This condition will ensure that our height function satisfies the minimal necessary requirements for being proper.

Lemma 4.2.3. *The above geometric coordinate system Δ for $DH_{1,1}$ is complete.*

Proof. Consider a sequence $p_n \in \Delta$ with $p_n \to \partial\Delta$. After choosing a subsequence, we can assume that $p_n \to p_0 \in \partial\Delta$ Now we want to detect conformal degenerations of the orthodisk domains. For this it will be convenient to use the extremal lengths of the cycle blue and another cycle mauve introduced below:

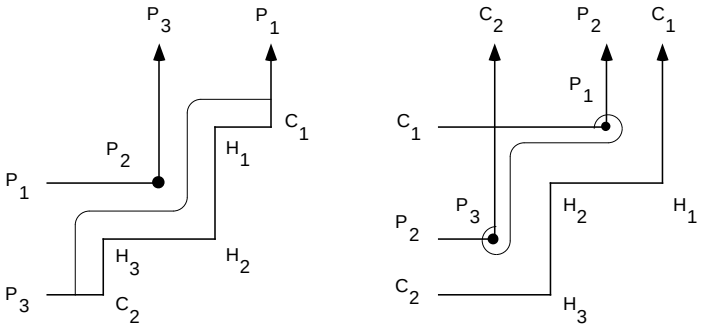

mauve cycle

Mauve consists of curve connecting P_3C_2 with C_1P_1.

Denote the extremal length of a cycle (say blue) in (say) the orthodisk Ω_{Gdh} as usual by $\mathrm{Ext}_{\Omega_{Gdh}}(\text{blue})$.

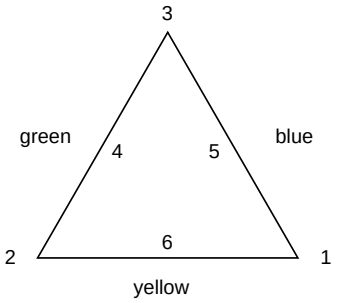

Geometric coordinate simplex

We need to distinguish six cases (which are indicated in the above figure), depending on the location of p_0 in $\partial\Delta$:

(1) $p_0 = (0,0,1)$: $\mathrm{Ext}_{\Omega_{Gdh}}(\text{blue}) = 0$
(2) $p_0 = (0,1,0)$: $\mathrm{Ext}_{\Omega_{G^{-1}dh}}(\text{blue}) = \infty$
(3) $p_0 = (1,0,0)$: $\mathrm{Ext}_{\Omega_{Gdh}}(\text{blue}) = 0$
(4) $p_0 \in (>0, >0, 0)$: $\mathrm{Ext}_{\Omega_{G^{-1}dh}}(\text{mauve}) = \infty$
(5) $p_0 \in (>0, 0, >0)$: $\mathrm{Ext}_{\Omega_{Gdh}}(\text{blue}) = 0$
(6) $p_0 \in (0, >0, >0)$: $\mathrm{Ext}_{\Omega_{Gdh}}(\text{mauve}) = \infty$

Since the degeneration of an extremal length clearly signals the degeneration of the conformal structure, we are done.

4.3 The height function for $DH_{1,1}$.

Our aim is to define a proper function on Δ which is zero iff the two domains Ω_{Gdh} and $\Omega_{G^{-1}dh}$ given by the geometric coordinates of the point are conformal. The conformal difference between the two domains is naturally measured by expressions in the extremal length like the Teichmüller distance, which however is not proper.

To obtain properness, we need to measure rather subtle growth differences of extremal lengths.

Another important point for the choice of the height function is that we need to be able to decrease the height at noncritical points. This requires that we control the first derivative of the height, and this means heuristically that we should use as few curve families as possible in the definition of the height.

Definition 4.3.1. Consider on Δ the height function

$$\begin{aligned}\mathcal{H}_{1,1} = &\left| e^{1/\,\mathrm{Ext}_{\Omega_{Gdh}}(\text{blue})} - e^{1/\,\mathrm{Ext}_{\Omega_{G^{-1}dh}}(\text{blue})} \right|^2 + \\ &\left| e^{1/\,\mathrm{Ext}_{\Omega_{Gdh}}(\text{mauve})} - e^{1/\,\mathrm{Ext}_{\Omega_{G^{-1}dh}}(\text{mauve})} \right|^2 + \\ &\left| e^{\mathrm{Ext}_{\Omega_{Gdh}}(\text{blue})} - e^{\mathrm{Ext}_{\Omega_{G^{-1}dh}}(\text{blue})} \right|^2 + \\ &\left| e^{\mathrm{Ext}_{\Omega_{Gdh}}(\text{mauve})} - e^{\mathrm{Ext}_{\Omega_{G^{-1}dh}}(\text{mauve})} \right|^2\end{aligned}$$

Clearly the conformal structure of a domain Ω_{Gdh} or $\Omega_{G^{-1}dh}$ is determined by the extremal lengths of blue and mauve, so the height function is zero iff the two domains are conformal.

It is also clear that the height function admits at least the possibility of being proper, because at a boundary point, at least one of the extremal lengths used is either 0 or ∞ by lemma 4.2.3. The main difficulty arises when the extremal lengths for the same cycle degenerate for both orthodisks. This requires that we measure extremal length growth rates and is responsible for the complicated shape of the height function.

We can now prove, up to the crucial monodromy Theorem 4.1.2, the:

Theorem 4.3.2. *The above height function $\mathcal{H}_{1,1}$ is proper.*

Proof. Consider a sequence $p_n \in \Delta$ with $p_n \to \partial\Delta$.

After choosing a subsequence, we can assume that $p_n \to p_0 \in \partial\Delta$ and that all extremal lengths of blue and mauve converge to some numbers in $\mathbb{R} \cup \{0, \infty\}$.

By lemma 4.2.3, at least one of the extremal lengths in the definition of the height function is 0 or ∞. Now observe that in the cases (3), (4) and (5) of lemma 4.2.3, $\mathrm{Ext}_{\Omega_{G^{-1}dh}}(\text{mauve}) \to \infty$ while $\mathrm{Ext}_{\Omega_{Gdh}}(\text{mauve})$ remains bounded. Similarly in case (6) $\mathrm{Ext}_{\Omega_{Gdh}}(\text{mauve}) \to \infty$ while $\mathrm{Ext}_{\Omega_{G^{-1}dh}}(\text{mauve})$ remains bounded. This leaves us with the cases (1) and (2). Here both mauve extremal lengths go to ∞.

The point now is that we are able to control the growth rates of the extremal length of blue. It then follows from Theorem 4.1.2 that, independently of the paths of approach to $\partial\Delta$, in case (1)

$$|e^{1/\mathrm{Ext}_{\Omega_{Gdh}}(\text{blue})} - e^{1/\mathrm{Ext}_{\Omega_{G^{-1}dh}}(\text{blue})}|^2 \to \infty$$

while in case (2)

$$|e^{\mathrm{Ext}_{\Omega_{Gdh}}(\text{blue})} - e^{\mathrm{Ext}_{\Omega_{G^{-1}dh}}(\text{blue})}|^2 \to \infty$$

□

4.4 Geometric coordinates for the $DH_{m,n}$ surfaces.

The goal of this section is to introduce a set of coordinates for the moduli space of pairs of symmetric orthodisks with formal Weierstraß data of type $DH_{m,n}$ and to prove that they are complete.

Fix formal Weierstraß data a_i of a symmetric orthodisk of type $DH_{m,n}$ for the rest of this section.

The corresponding pairs of orthodisks have the following geometry: The orthodisk Ω_{Gdh} has an outer sheet bounded by a polygonal arc with finite vertices

$$C_2 - H_{2n+1} - H_{2n} - \ldots - H_1 - C_1$$

and m interior sheets, each having one finite vertex, the branch point P_{2k}.

The orthodisk $\Omega_{G^{-1}dh}$ has an outer sheet bounded by a polygonal arc with finite vertices

$$H_{2n+1} - H_{2n} - \ldots - H_1$$

and $m+1$ interior sheets containing each one finite branched vertex P_{2k+1}.

A picture of such a pair of orthodisks is shown below for $DH_{5,8}$. In the following figures, the orthodisk Ω_{Gdh} will always be the left one. We discard the labeling of the vertices.

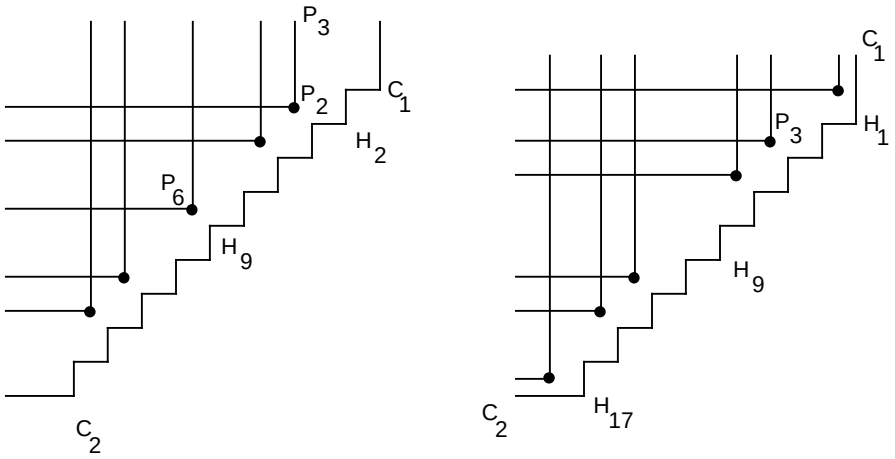

The $DH_{5,8}$ orthodisks

The first step is to set up a space of complete geometric coordinates as we did for the $DH_{1,1}$ surface. We face here a new difficulty: it is not the case that for every orthodisk Ω_{Gdh} there is necessarily a conjugate orthodisk $\Omega_{G^{-1}dh}$, and vice versa. Thus, the geometric coordinate space has to be an appropriate subset of the natural parameter spaces of both orthodisks, and in addition we have to ensure that the coordinates are complete. We begin by an informal description with examples and then give a formal definition. After we give the formal definitions, we prove the setup suffices for our purposes in Lemmas 4.4.4 and 4.4.5.

The idea is to require that each branch point lie in a box which is bounded by (extensions of) suitable orthodisk edges. Not only will this allow for the existence of well-behaved moduli spaces, but it will also provide for important degenerations of the domain at the boundary.

In the following figures, these boxes are shaded in gray, and when necessary, separated by additional (suggestive) edges. When boxes overlap, they are shaded more darkly. We also discard from now on the fat dots marking the interior branch point — all interior vertices are branch points.

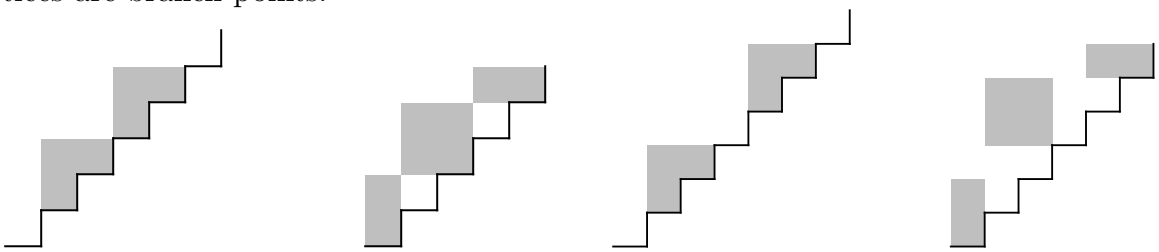

Bounding boxes for $DH_{2,4}$ and $DH_{2,5}$

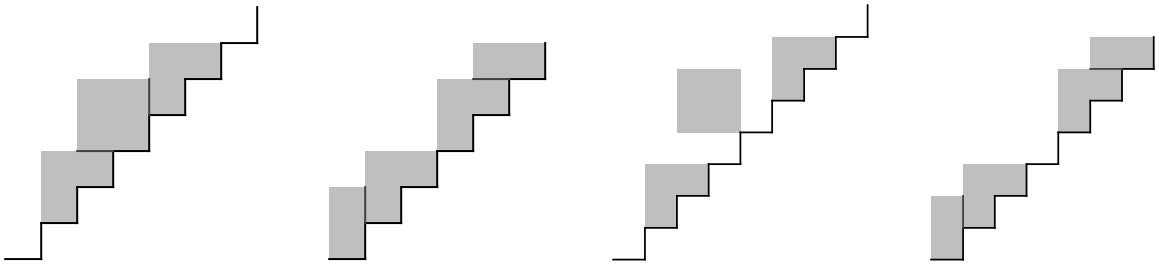

Bounding boxes for $DH_{3,5}$ and $DH_{3,6}$

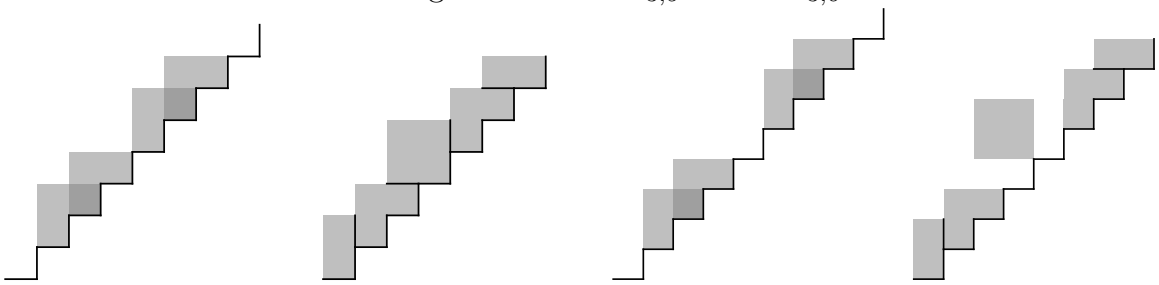

Bounding boxes for $DH_{4,6}$ and $DH_{4,7}$

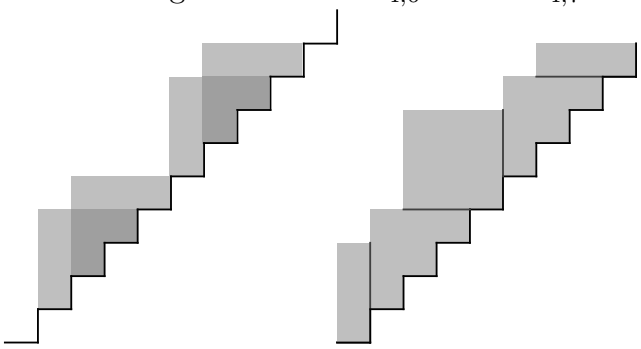

Bounding boxes for $DH_{4,8}$

As a general rule, there are m boxes for Ω_{Gdh} (one for each branch point) which are intersections of finite rectangles with the orthodisks. For $\Omega_{G^{-1}dh}$, there are $m+1$ boxes, the two outermost of them being intersections of half-infinite rectangular strips with the orthodisks.

As an illustration, we explain in detail how the boxes can be deduced from the geometry for the $DH_{2,4}$ surface:

In $\Omega_{G^{-1}dh}$, the edge P_4P_5 clearly has to lie above the edge C_2H_9. The conjugacy requirement for Ω_{Gdh} forces that the edge P_4P_5 lie to the right of the edge C_2H_9. This forces, in Ω_{Gdh}, the edge P_3P_4 to lie above the edge H_8H_9. Observe that this is an inductive process to get border lines of the bounding boxes. In this most simple case, the induction immediately terminates: by symmetry, the branch point P_3 has to lie on the diagonal in $\Omega_{G^{-1}dh}$, hence the edge P_3P_4 lies left of H_4H_5, which causes, by conjugacy, the corresponding edges to lie below each other in Ω_{Gdh}. This way we get a backward induction in the general case, providing us with left and upper border lines for bounding boxes for all branch points on and below the diagonal, up to the outermost branch point in $\Omega_{G^{-1}dh}$ for which we do not get a left border line. By symmetry, we also obtain such borders for the branch points above the diagonal. Finally, the branch point on the diagonal

is also bounded because the edge P_2P_3 lies left of H_1H_2 in Ω_{Gdh} which gives a bound for P_3 in $\Omega_{G^{-1}dh}$.

The idea now is to specify the set of geometric coordinates as follows: First, record the edge lengths of the boundary of the outer sheet of the orthodisk Ω_{Gdh}. Then adjoin to those the positions of the branch points within the bounding boxes, measured as horizontal and vertical distances to the boundary.

In this $DH_{2,4}$ example, the space of geometric coordinates can be described as the space of Ω_{Gdh} (left) orthodisks with the requirement that the branch points lie inside the bounding boxes. Each such orthodisk is given by the data for its outer sheet boundary zigzag and the position of one point in the L-shaped box which itself is defined by the boundary zigzag. Using these data, it is possible to construct a unique conjugate orthodisk $\Omega_{G^{-1}dh}$ such that its branch points lie in the shaded bounding boxes. Furthermore, these coordinates are complete: any degeneration of the coordinates which does not come from an edge degeneration in Ω_{Gdh} stems from one branch point coming close to the inner boundary of its shaded box. But this forces a branch point in $\Omega_{G^{-1}dh}$ to come close to the outer boundary, forcing a conformal degeneration. This concludes the discussion of the case $DH_{2,4}$; the completeness of the coordinates for the general case of $DH_{m,n}$ is proven in Lemma 4.4.5.

As a first step towards formally describing these boxes in the general case, we introduce families of cycles which will be useful both for specifying the coordinates and for defining the height function. In principle, there are four cases to distinguish depending on the parities of m and n, but our notation will hide most of the differences.

Denote by

$$k = [m/2] \qquad \text{and} \qquad d = [\frac{n-m}{2}] + 1$$

We first introduce cycles related to the outer sheet:

$$\begin{aligned}
\alpha_1 : P_1C_1 &\to H_1H_2 \\
\alpha_2 : C_1H_1 &\to H_2H_3 \\
\alpha_3 : H_1H_2 &\to H_3H_4 \\
\cdots : \cdots &\to \cdots \\
\alpha_{2n} : H_{2n-2}H_{2n-1} &\to H_{2n}H_{2n+1} \\
\alpha_{2n+1} : H_{2n-1}H_{2n} &\to H_{2n+1}C_2 \\
\alpha_{2n+2} : H_{2n}H_{2n+1} &\to P_{2m+1}C_2
\end{aligned}$$

These cycles connect consecutive parallel edges of the outer sheet boundary. Their periods are realized as the finite edges. The symmetry condition on the orthodisk implies for these cycles

$$|\operatorname{Per}\alpha_k| = |\operatorname{Per}\alpha_{2n+3-k}|$$

Next we introduce four families of cycles called $\lambda_k, \rho_k, \upsilon_k$ and δ_k (for left, right, up, and down) connecting the horizontal and vertical edges of the inner sheets to certain carefully

chosen horizontal and vertical edges of the outer sheet. The periods of these cycles will be used to define the bounding boxes:

$$\begin{aligned}
\rho_1 : P_2P_3 &\to H_1H_2\\
\rho_2 : P_4P_5 &\to H_3H_4\\
\cdots : \cdots &\to \cdots\\
\rho_k : P_{2k}P_{2k+1} &\to H_{2k-1}H_{2k}\\
\upsilon_1 : P_1P_2 &\to H_1C_1\\
\upsilon_2 : P_3P_4 &\to H_3H_2\\
\cdots : \cdots &\to \cdots\\
\upsilon_k : P_{2k-1}P_{2k} &\to H_{2k-1}H_{2k-2}\\
\delta_1 : P_1P_2 &\to H_{d+3}H_{d+2}\\
\cdots : \cdots &\to \cdots\\
\delta_k : P_{2k-1}P_{2k} &\to H_{2k+d+1}H_{2k+d}\\
\lambda_1 : P_2P_3 &\to H_{d+3}H_{d+4}\\
\cdots : \cdots &\to \cdots\\
\lambda_k : P_{2k}P_{2k+1} &\to H_{2k+d+1}H_{2k+d+2}
\end{aligned}$$

In the case that m is odd, we introduce in addition cycles for the box at P_{k+1}. For odd n we set

$$\begin{aligned}
\rho_{k+1} : P_{m+1}P_{m+2} &\to H_{n+1}H_{n+2}\\
\delta_{k+1} : P_mP_{m+1} &\to H_nH_{n+1}\\
\upsilon_{k+1} : P_mP_{m+1} &\to H_{n-d-2}H_{n-d-1}\\
\lambda_{k+1} : P_{m+1}P_{m+2} &\to H_{n+d+3}H_{n+d+4}
\end{aligned}$$

and for even n:

$$\begin{aligned}
\rho_{k+1} : P_{m+1}P_{m+2} &\to H_nH_{n+1}\\
\delta_{k+1} : P_mP_{m+1} &\to H_{n+1}H_{n+2}\\
\upsilon_{k+1} : P_mP_{m+1} &\to H_{n-d-1}H_{n-d}\\
\lambda_{k+1} : P_{m+1}P_{m+2} &\to H_{n+d+2}H_{n+d+3}
\end{aligned}$$

This defines cycles emanating from the inner Ω_{Gdh} sheet edges for the sheets containing the branch points $P_2, \ldots, P_k$, that is, for all sheets above the diagonal. For the sheets below the diagonal, we employ symmetry: Denote by α' the image of a cycle α under reflection at the diagonal $y = -x$. We then define

$$\begin{aligned}
\lambda_j &= \upsilon'_{m+1-j}\\
\rho_j &= \delta'_{m+1-j}\\
\upsilon_j &= \lambda'_{m+1-j}\\
\delta_j &= \rho'_{m+1-j}
\end{aligned}$$

This way all cycles are defined for $j = 1, \ldots, m$.

The next two figures show all the cycles for $DH_{5,8}$. For visibility, we have omitted the names of the vertices, the fat dots indicating the branch points, and shortened the edges of the inner sheets.

The first figure shows the υ-cycles and the δ-cycles (dotted), the second the ρ-cycles and the λ-cycles (dotted). Informally, for each inner sheet of the orthodisk Ω_{Gdh} there is a cycle of each type $(\upsilon, \delta, \rho, \lambda)$. The υ-cycles have periods which point upward in Ω_{Gdh} for the first half of the cycles in the upper right part of the orthodisk, and similarly the periods of ρ, λ, δ point right, left and down.

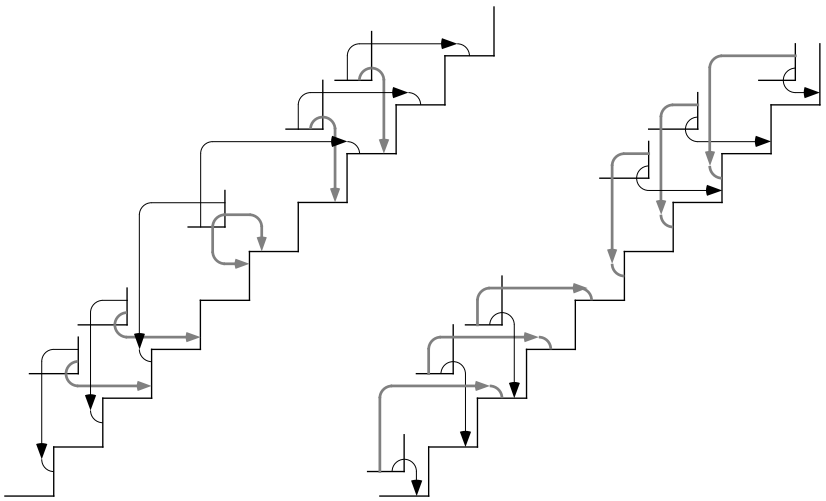

υ-cycles and the δ-cycles for $DH_{5,8}$

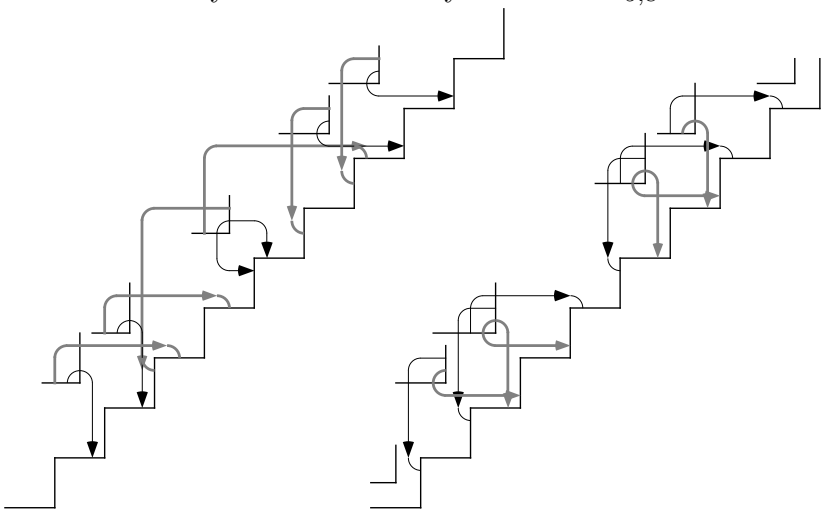

ρ-cycles and the λ-cycles for $DH_{5,8}$

Now we are able to define the bounding boxes for the branch points:

Definition 4.4.1. Denote by B_{2j} the rectangle defined by

$$\operatorname{Per} \upsilon_j > 0, \operatorname{Per} \delta_j > 0, \operatorname{Per} \lambda_j > 0 \operatorname{Per} \rho_j > 0$$

and by B_{2j-1} the rectangle defined by

$$\operatorname{Per}\rho_{j-1} > 0, \operatorname{Per}\delta_{j-1} > 0, \operatorname{Per}\lambda_j > 0, \operatorname{Per}\upsilon_j > 0$$

Note that the boxes B_1 and B_{2m+1} require the additional cycle $\lambda_0 := \alpha_0$ whereas ρ_0 is undefined so that the rectangle is open at one side.

To define the geometric coordinates, we impose two restrictions on the branch points:

(1) $P_j \in B_j$

(2) P_j must lie within the outer sheet.

While the second requirement is obviously necessary to impose, the first will imply that the geometric coordinates are complete.

Definition 4.4.2. An orthodisk Ω_{Gdh} or $\Omega_{G^{-1}dh}$ is called *admissible* if they satisfy the above condition for their respective branch points. A pair of orthodisks is called admissible if the orthodisks are conjugate and both admissible.

Definition 4.4.3. The *geometric coordinates* of Ω_{Gdh} are given by the periods of the cycles $\alpha_j, \rho_j, \lambda_j, \upsilon_j, \delta_j$ subject to the above condition. Similarly, the geometric coordinates of $\Omega_{G^{-1}dh}$ are given by the periods of these cycles subject to the above condition. This clearly defines two open subsets of a Euclidean space of dimension $g + 1 = m + n$. Each subset parameterizes the configuration space of admissible orthodisks Ω_{Gdh} or $\Omega_{G^{-1}dh}$. Denote by Δ the intersection of these subsets; this set parameterizes admissible pairs of orthodisks and is called *geometric coordinate space* for $DH_{m,n}$.

Lemma 4.4.4. *Δ is an open cell of dimension $g - 1$.*

Proof. To prove openness we just observe that all imposed conditions are open in a certain linear space. To compute its dimension, we can get easily rid of the redundant equations of the definition of geometric coordinates for (say) Ω_{Gdh}: The cycles $\delta_j - \upsilon_j$ and $\lambda_i - \rho_i$ are a certain sum of cycles α_j. So to specify a symmetric orthodisk, we need just $m + n$ cycles. To prove that it is a non-empty cell, we construct a retraction to an interior point as follows: First, by using convex combinations of the outer sheet edge lengths, we can easily deform a given pair of admissible orthodisks to an admissible pair of orthodisks with the outer sheet periods being of length 1. Now we move the edge $P_{2m}P_{2m+1}$ in $\Omega_{G^{-1}dh}$ down, this is unobstructed in $\Omega_{G^{-1}dh}$ but has to be accommodated by a movement of $P_{2m}P_{2m+1}$ to the left in Ω_{Gdh}. We move so far to the left here, that we are left of the edge $H_{2n-1}H_{2n-2}$. This allows us to move the edge $H_{2m-1}H_{2m}$ down in Ω_{Gdh}. We move so far down that we are, in $\Omega_{G^{-1}dh}$, left of the edge $H_{2n-2}H_{2n-3}$, which enables us again to move $H_{2m-2}H_{2m-1}$ down. We continue this process, doing the same with the symmetric edges simultaneously. If we agree to move always to a position 0.5 apart from the left or lower boundary sheet, we will reach, in this way, a canonical point in the space Δ. This defines the retraction. □

Lemma 4.4.5. *Δ provides complete geometric coordinates.*

Proof. We first have to show that each point in Δ gives a pair of well-defined symmetric (normalized) orthodisks. Using the coordinates of such a point, it is immediate that

one can reconstruct the outer sheets for the Ω_{Gdh} and the $\Omega_{G^{-1}dh}$ domains. Also, the positions of the branch points are specified so that they lie within the outer sheets and their respective bounding boxes. To obtain a correct pair of orthodisks, we have to make sure that these branch points do not coincide as one might expect for instance in the $DH_{5,8}$ case where the bounding boxes overlap. However, this can be excluded as follows: If two branch points come close to each other, the periods of the two cycles connecting the parallel edges of their respective sheets vanish. This causes in the other domain a vanishing period between two inner sheets closer to the diagonal, and inductively we produce such a period degeneration on the diagonal, switching between the two domains. But on the diagonal, this cannot happen, because the branch point there is confined to the diagonal.

Finally, we have to show that when we have a sequence of admissible orthodisks leaving the space of geometric coordinates, at least one of the conformal structures of the Ω_{Gdh} or $\Omega_{G^{-1}dh}$ orthodisks degenerates. The geometric degeneration means by definition that for at least one of the orthodisks, either an edge of the outer sheet boundary degenerates or a branch point hits the boundary of its bounding box (The exceptional case of the half-infinite bounding rectangle in the domain $\Omega_{G^{-1}dh}$ domain does not actually allow the branch point to drift to infinity, because the corresponding period in the Ω_{Gdh} domain is represented by a finite edge of the outer sheet, which is bounded by normalization). In the first case, we get a node and are obviously done. In the second case, the branch point can either converge to some point on the outer boundary (in which case we pinch a cycle and are also done), or it can converge to a point on one of the virtual border lines of the bounding box. Then we clearly have no conformal degeneration for *this* orthodisk sequence, so we must prove that we get such a degeneration for the other family. (The next figure shows two conjugate orthodisks with bounding boxes. Equally labeled arrows indicate equal distances from orthodisk edges to the virtual border lines of bounding boxes. As long as these distances are equal, the branched point can move freely within their bounding boxes.)

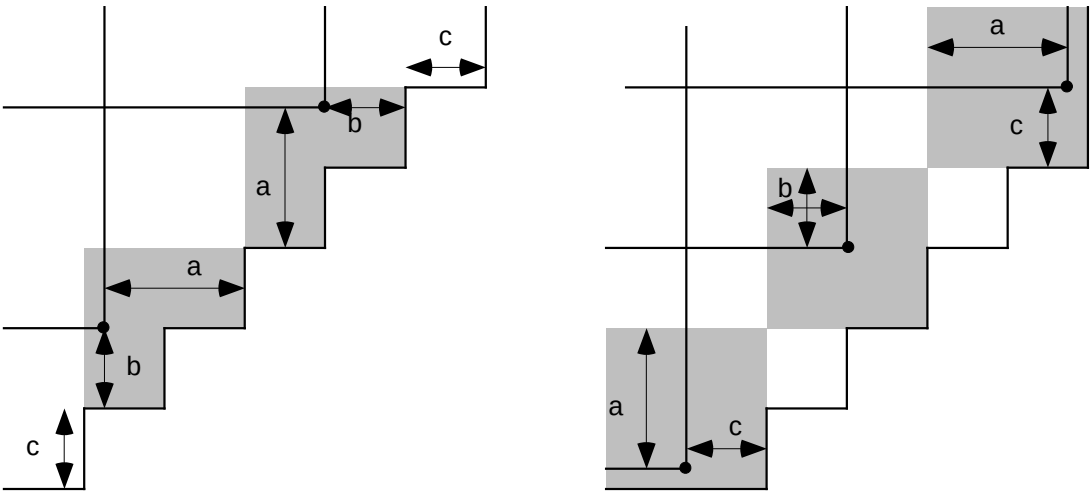

Conjugate orthodisks with coupled branch points

Suppose, for concreteness, that we have a sequence of orthodisks $\Omega_{Gdh}(n)$ where a branch point converges to an upper virtual border line of its bounding box. This branch point P_k belongs to an edge $E = P_kP_{k-1}$ which comes close to this virtual line from below. By conjugacy, in the corresponding $\Omega_{G^{-1}dh}$ orthodisks, the corresponding edge $E^* = P_kP_{k-1}$ comes close to a bounding border line to the right. The other endpoint P_{k-1} of this edge is a branch point for $\Omega_{G^{-1}dh}$ which hence comes arbitrarily close to the outer sheet boundary. So we pinch a curve in $\Omega_{G^{-1}dh}$ and get a conformal degeneration. The other cases are treated similarly.

□

4.5 Height Functions for $DH_{m,n}$.

In this section, we will provide a proper height function defined on the geometric coordinate space Δ of the previous section for the $DH_{m,n}$ surfaces with $m + n > 2$.

We begin by stating the basic requirements on a height function which we require for the steps of the proof of Theorem B(i) in sections §4-§6.

To estimate the rate of growth/decay of extremal lengths in terms of geometric degenerations, we need an asymptotic expression for the extremal lengths of the cycles we use in the height function. Such an expression (see [Oht]) is only known to us in the case that the cycle is a lift of an arc in the upper half-plane connecting two disjoint edges. This is the case of a conformal quadrilateral. Informally, an *admissible* cycle in an orthodisk is one which can be reduced to such a cycle as just described. More precisely:

Definition 4.5.1. A cycle in an orthodisk is called *admissible* if it is either simple and connects a pair of symmetric edges or has two symmetric components which do not cross the diagonal.

Using admissible cycles, the height will be composed as a sum of the following terms:

Definition 4.5.2. Let c be an admissible cycle. Define

$$\mathcal{H}(c) = |e^{1/\operatorname{Ext}_{\Omega_{Gdh}}(c)} - e^{1/\operatorname{Ext}_{\Omega_{G^{-1}dh}}(c)}|^2 + |e^{\operatorname{Ext}_{\Omega_{Gdh}}(c)} - e^{\operatorname{Ext}_{\Omega_{G^{-1}dh}}(c)}|^2$$

Recall that the conformal polygon of a $DH_{m,n}$-surface is (two-fold) symmetric and has $2m + 2n + 4$ vertices; there are thus $m + n$ conformal moduli of such a shape. We will use the cycles of the previous section to select $m + n$ admissible cycles. In addition to the requirement that the cycles detect conformal degenerations, we will also need some more properties which we will state here but only explain and use in section 6. (There, we take a low genus reflexive orthodisk, and append some thrice punctured spheres to it along nodes; we then open the nodes to obtain high genus surfaces in a stratum $\mathcal{Y} \subset \Delta$ along which we flow in section 5 to a reflexive orthodisk solution to our problem). This 'regeneration' in §6 requires a set of $m + n$ cycles for the height which provide conformal coordinates for the points in Δ; moreover, the set of curve systems that we specify for the higher genus surface which do not degenerate as we pinch the surface to a noded surface (i.e are either not pinched into the node or do not cross the node) should also provide local coordinates for the boundary stratum of lower genus surfaces. In particular, there should

be exactly two 'bad' curves (which degenerate as $DH_{n+1,n+1}$ degenerates to $DH_{n,n}$ — i.e. with extremal lengths which go to 0 or ∞ as P_1 and H_1 converge) in the $n = m$ case, and one bad curve in the $n \neq m$ case (i.e. which degenerates as $m + 1 \to m$ in $DH_{m+1,n}$) with an extremal length that goes to ∞ as the finite vertex nearest the central vertex approaches it.)

The subset of of the cycles that is principally used in the properness argument is defined by

$$\gamma_i = \alpha_i + \alpha_i'$$

for $i = 1, \ldots, n$. These cycles measure degenerations of the outer sheet boundary. Note that we haven't included the cycles α_{n+1} and α_{n+2} because they cross the diagonal, and hence are not admissible.

The only other cycle that is needed for the properness proof is chosen in such a way that its extremal length detects degenerations which occur when inner sheets tend to the border of their bounding boxes. Now essentially all these bounding boxes are bounded by two good sides and two bad sides, in sense of goodness and badness we will now explain. A good side lies to the right or below a branch point, and when the branch point comes close to one of them, we get a conformal degeneration which we can hope to detect. On the other hand, the bad sides lie above and to the left, and a branch point coming close to them leads to no conformal degeneration, so the extremal lengths of the chosen curve systems on that orthodisk are of no help here in proving the properness of the height $\mathcal{H}$. However, by completeness of the the geometric coordinates, in the case of a geometric degeneration, at least one branch point of *one* of the orthodisks comes close to a good outer edge. This is critical in the sense that the height has to detect conformal degenerations only in the case that the central branch point degenerates towards the central vertex of the outer sheet, where no α-cycle is pinched. Therefore we choose the next cycle γ in such a way that this branch point is separated from the outer sheet boundary by γ. This is achieved concretely by including, for all but one cases, the admissible cycle

$$\gamma : H_1 H_2 \to H_{n-1} H_n, (m, n) \neq (1, 2)$$

into the list of cycles whose heights will contribute to the height function $\mathcal{H}$. There is a slight difference in the combinatorics for the cases $m = n$ and $m < n$ which complicates this definition; the argument we give in §6 requires γ to avoid certain loci of degeneration, so for the case of $(m, n) = (1, 2)$ we will define

$$\gamma : C_1 H_1 \to H_n C_2, (m, n) = (1, 2).$$

Surprisingly, this set of $n + 1$ cycles $\{\gamma_i, \gamma\}$ is sufficient by itself to prove that a height function built just with these is proper.

We add some additional cycles to our list with but two final requirements: 1) the extremal lengths of the full list should provide conformal coordinates for the Riemann surfaces parametrized geometrically by Δ, and 2) all of the new curves should avoid the locus where a node will develop. It is easy to see that there are many such choices available.

In particular, we may select these additional cycles such that in fact from each inner sheet (up to the exceptional outermost sheets in the $\Omega_{G^{-1}dh}$ domain and the central sheet on the diagonal) we have two admissible cycles emanating. From the central sheet and the outermost sheets, we have just one cycle emanating.

Definition 4.5.3. The height for the $DH_{m,n}$ surface is defined as

$$\mathcal{H} = \sum_{i=1}^{n} \mathcal{H}(\gamma_i) + \mathcal{H}(\gamma)$$

For the induction step for $DH_{m,m}$, we need to have no curves footing on H_1C_1 and just one curve encircling it.

Also, for $m < n$, we need that the only curve that foots on the innermost finite edge should also foot on an infinite edge.

So we need to change our definition of the height function accordingly.

Note that our height function for $DH_{1,1}$ is slightly different: The cycle γ would be of no use here, so we have replaced it by mauve. This cycle does not satisfy the requirements above which are needed in section 6 for regeneration, but we do not need this section for the construction of $DH_{1,1}$.

rethink this remark above

Example 4.5.4. As an example, we show the cycles for the height of the $DH_{2,4}$ surface which are relevant for the properness proof:

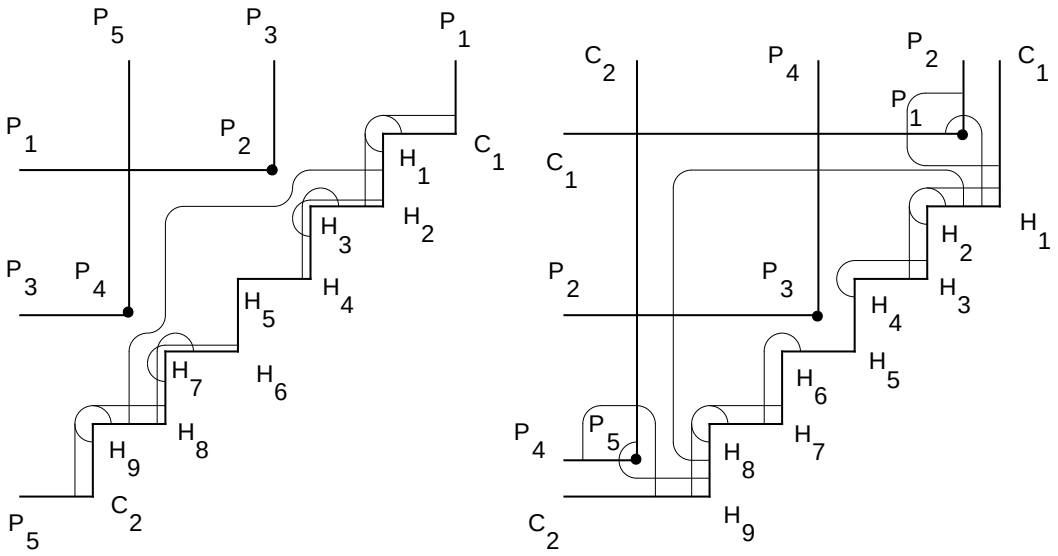

The essential cycles for the height function for $DH_{2,4}$

on right hand o-disk, omit the cycle P4P5-C2H9 or add to LH o-disk

We record for later reference the following trivial consequence of our using curves in the height function whose extremal lengths are conformal coordinates for the domains defined by the geometric coordinates.

Lemma 4.5.5. *Let $X = \{\Omega_{Gdh}, \Omega_{G^{-1}dh}\}$ be an orthodisk system in Δ. Then X is reflexive if and only if $\mathcal{H}(X) = 0$.*

4.6 Properness of the height functions for $DH_{m,n}$.

In this section, we prove, modulo the postponed monodromy argument,

Theorem 4.6.1. *The height functions $\mathcal{H}$ from section 4.5 are proper.*

Proof. To show that the height functions from 4.5 are proper, we need to prove that for any sequence of points in Δ converging to some boundary point, the height goes to infinity. The idea is as follows. First, by Lemma 4.2.3, at least one of the two orthodisks degenerates conformally. We will now analyze the possible geometric degenerations. Recall that we have normalized the geometric coordinates such that the outer sheet of Ω_{Gdh} has fixed 'total length' 1. If the geometric degeneration occurs in this outer boundary sheet of Ω_{Gdh}, then one of the cycles α_j either encircles or ends on an edge which shrinks to zero. Furthermore, because not all of the edges can shrink to zero by normalization, there must be an α_j whose extremal length goes either to zero or infinity. By the monodromy theorem 4.1.2, the corresponding term of the height function goes to infinity, and we are done.

Next we assume that there is no geometric degeneration on the outer sheet of Ω_{Gdh}. This means that a geometric degeneration must come from an inner branch point of Ω_{Gdh} or $\Omega_{G^{-1}dh}$ tending to the outer sheet boundary, by the proof of lemma 4.4.5. Note that we might have multiple degenerations of branch points in this case. Because we cannot necessarily rely on the monodromy theorem in this case, we need to find a cycle which is pinched in only one of the domains. Consider then the outermost sheets with a branch point degenerating to the outer sheet boundary. This geometric degeneration is measured by the period of some cycle θ connecting an inner sheet edge with an outer sheet edge. We first discuss two exceptional cases in the $\Omega_{G^{-1}dh}$ sheet: The cycle θ cannot be the cycle $C_1P_1 \to H_1H_2$ (and its symmetric companion) as this cycle represents a finite edge of Ω_{Gdh} whose possible degeneration is excluded. If, on the other hand, θ is the cycle $P_1P_2 \to H_1C_1$ (and its symmetric companion), then the cycle $C_1P_1 \to H_1H_2$ is pinched on the domain $\Omega_{G^{-1}dh}$, but not on the domain Ω_{Gdh} because it is a finite outer edge there.

Hence the cycle θ connects to an edge of the outer sheet boundary which is either represented by an α-cycle or is central. In the first case, the degeneration causes a node to develop along the α-cycle by the degenerating branch point. But in the other domain, this same cycle has no node developing, because otherwise we would have a degeneration of a branch point belonging to sheet further down in that domain. In the second case, this central degeneration is the only degeneration occurring because otherwise we again would have a degenerating sheet further down. So in this case, the cycle γ is pinched in that domain but not in the other.

This treats all possible cases, and the theorem is proven. $\square$

4.7 A monodromy argument.

In this section, we prove that the periods of orthodisks have incompatible logarithmic singularities in suitable coordinates and apply this to prove the monodromy theorem 4.1.2. The main idea has already been used in [WW]: to study the dependence of extremal lengths of the geometric coordinates, it is necessary to understand the asymptotic dependence of extremal lengths of the degenerating conformal polygons (which is classical and well-known, see [Oht]), and the asymptotic dependence of the geometric coordinates of the degenerating conformal polygons. This dependence is given by Schwarz-Christoffel maps which are well-studied in many special cases. Especially, it is known that these maps possess an asymptotic expansions in logarithmic terms. Instead of computing this expansion explicitly for the two maps we need (which is possible but tedious), we use a monodromy argument to show that the crucial logarithmic terms have a different sign for the two expansions.

Let Δ be a domain of dimension at least 2 defining geometric coordinates for a pair of orthodisks X_1 and X_2 corresponding to given formal Weierstraß data as usual. Suppose γ is a cycle in the underlying conformal polygon which joins edges P_1P_2 and Q_1Q_2 which are parallel (and hence non-adjacent) in the orthodisks. In our applications, γ will be one of the α-cycles used in the height function. Denote by R_1 the vertex before Q_1 and by R_2 the vertex after Q_2 and observe that by assumption, $R_2 \neq P_1$ and $P_2 \neq R_1$. Introduce a second cycle β which connects R_1Q_1 with Q_2R_2.

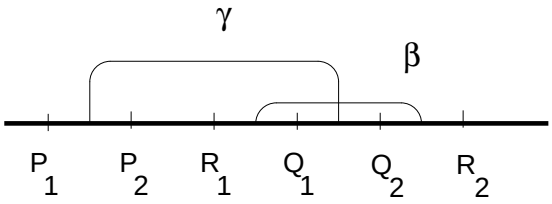

Monodromy argument

We formulate the claim of Theorem 4.1.2 more precisely in the following two lemmas:

Lemma 4.7.1. *Suppose that for a sequence $p_n \in \Delta$ with $p_n \to p_0 \in \partial\Delta$ we have that $\mathrm{Ext}_{X_1(p_n)}(\gamma) \to 0$ and $\mathrm{Ext}_{X_2(p_n)}(\gamma) \to 0$. Suppose furthermore that γ is a cycle encircling a single edge which degenerates geometrically to 0 as $n \to \infty$ in $X_1(p_n)$. Then*

$$|e^{1/\mathrm{Ext}_{X_1(p_n)}(\gamma)} - e^{1/\mathrm{Ext}_{X_2(p_n)}(\gamma)}|^2 \to \infty$$

Lemma 4.7.2. *Suppose that for a sequence $p_n \in \Delta$ with $p_n \to p_0 \in \partial\Delta$ we have that $\mathrm{Ext}_{X_1(p_n)}(\gamma) \to \infty$ and $\mathrm{Ext}_{X_2(p_n)}(\gamma) \to \infty$. Suppose furthermore that γ is a cycle with an endpoint on an edge which degenerates geometrically to 0 as $n \to \infty$ in $X_1(p_n)$. Then*

$$|e^{\mathrm{Ext}_{X_1(p_n)}(\gamma)} - e^{\mathrm{Ext}_{X_2(p_n)}(\gamma)}|^2 \to \infty$$

Proof. We first prove lemma 4.7.1.

Consider the conformal polygons corresponding to the pair of orthodisks. Normalize the punctures by Möbius transformations so that

$$P_1 = -\infty, P_2 = 0, Q_1 = \epsilon, Q_2 = 1$$

for X_1 and

$$P_1 = -\infty, P_2 = 0, Q_1 = \epsilon', Q_2 = 1$$

for X_2. By the assumption of lemma 4.7.1, we know that $\epsilon, \epsilon' \to 0$ as $n \to \infty$. We now apply the monodromy corollary 4.7.5 below to the curve $\epsilon_0 e^{it}$ and conclude that either

$$\frac{|\operatorname{Per}\beta(X_1)|}{|\operatorname{Per}\gamma(X_1)|} + \frac{1}{\pi}\log\epsilon \tag{4.7.1a}$$

is single-valued in ϵ while

$$\frac{|\operatorname{Per}\beta(X_2)|}{|\operatorname{Per}\gamma(X_2)|} - \frac{1}{\pi}\log\epsilon' \tag{4.7.1b}$$

is single-valued in ϵ', or the same stament holds for analogous quantities with opposite signs. Without loss we can treat the first case.

Now suppose that ϵ' is real analytic (and hence single-valued) in ϵ near $\epsilon = 0$. Then using that X_1 and X_2 are conjugate implies that the absolute lengths of β in X_1 and X_2 are equal, as are those of γ; hence

$$\frac{|\operatorname{Per}\beta(X_1)|}{|\operatorname{Per}\gamma(X_1)|} = \frac{|\operatorname{Per}\beta(X_2)|}{|\operatorname{Per}\gamma(X_2)|}$$

after taking differences of formulae 4.7. Thus we see that, after subtracting 4.7.1b from 4.7.1a,

$$\log(\epsilon\epsilon'(\epsilon))$$

is single-valued in ϵ near $\epsilon = 0$ which contradicts that $\epsilon, \epsilon' \to 0$.

Now Ohtsuka's extremal length formula states that for the current normalization of $X_1(p_n)$ we have

$$\operatorname{Ext}(\gamma) = O\left(|\log\epsilon|^{-1}\right)$$

(see Lemma 4.5.3 in [WW] and [Oht]). We conclude that

$$|e^{1/\operatorname{Ext}_{X_1(p_n)}(\gamma)} - e^{1/\operatorname{Ext}_{X_2(p_n)}(\gamma)}| = O\left(\frac{1}{\epsilon} - \frac{1}{\epsilon'}\right)$$

which goes to infinity, since we have shown that ϵ and ϵ' tend to zero at different rates. This proves lemma 4.7.1.

The proof of lemma 4.7.2 is very similar: For convenience, we normalize the points of the punctured disks such that

$$P_1 = -\infty, P_2 = 0, Q_1 = 1, Q_2 = 1 + \epsilon$$

for X_1 and

$$P_1 = -\infty, P_2 = 0, Q_1 = 1, Q_2 = 1 + \epsilon'$$

for X_2.

By the assumption of lemma 4.7.2, we know that $\epsilon, \epsilon' \to 0$ as $n \to \infty$. We now apply the monodromy corollary 4.7.5 below to the curve $1 + \epsilon_0 e^{it}$ and conclude that

$$\frac{\operatorname{Per}\gamma(X_1)}{\operatorname{Per}\beta(X_1)} + \frac{1}{\pi}\log\epsilon$$

is single-valued in ϵ while

$$\frac{\operatorname{Per}\gamma(X_2)}{\operatorname{Per}\beta(X_2)} - \frac{1}{\pi}\log\epsilon'$$

is single-valued in ϵ'. The rest of the proof is identical to the proof of lemma 4.7.1. □

To prove the needed corollary 4.7.5, we need asymptotic expansions of the extremal length in terms of the geometric coordinates of the orthodisks. Though not much is known explicitly about extremal lengths in general, for the chosen cycles we can reduce this problem to an asymptotic control of Schwarz-Christoffel integrals. Their monodromy properties allow us to distinguish their asymptotic behavior by the sign of logarithmic terms.

We introduce some notation: Suppose we have an orthodisk such that the angles at the vertices alternate between $\pi/2$ and $-\pi/2$ modulo 2π. Consider the Schwarz-Christoffel map

$$F : z \mapsto \int_i^z (t - t_1)^{a_1/2} \cdot \ldots \cdot (t - t_n)^{a_n/2}$$

(see §3.2) from a conformal polygon with vertices at t_i to this orthodisk. Choose 4 distinct vertices $t_i, t_{i+1}, t_j, t_{j+1}$ so that $j \equiv i \pmod 2$, ensuring that the edges $t_i t_{i+1}$ and $t_j t_{j+1}$ are parallel in the orthodisk geometry. (See figure below.) Introduce a cycle γ in the upper half plane connecting edge (t_i, t_{i+1}) with edge (t_j, t_{j+1}) and denote by $\bar\gamma$ the closed cycle obtained from γ and its mirror image across the real axis. Similarly, denote by β the cycle connecting $(t_{j-1}t_j)$ with $(t_{j+1}t_{j+2})$ and by $\bar\beta$ the cycle together with its mirror image.

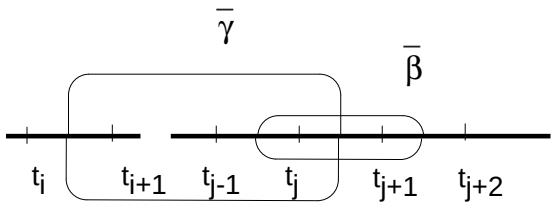

What are the a_n here? Also, there are too many uses of n in the paragraph above

Now consider the Schwarz-Christoffel period integrals

$$F(\gamma) = \frac{1}{2}\int_\gamma (t-t_1)^{a_1/2}\cdot\ldots\cdot(t-t_n)^{a_n/2}$$
$$F(\beta) = \frac{1}{2}\int_\beta (t-t_1)^{a_1/2}\cdot\ldots\cdot(t-t_n)^{a_n/2}$$

as multivalued functions depending on the *now complex* parameters t_i.

Lemma 4.7.3. *Under analytic continuation of t_{j+1} around t_j the periods change their values like*

$$F(\gamma) \to F(\gamma) + 2F(\beta)$$
$$F(\beta) \to F(\beta)$$

Proof. The proof is the same as of [WW], lemma 4.4.1: the path of analytic continuation of t_{j+1} around t_j gives rise to an isotopy of $\mathbb{C}$ which moves t_{j+1} along this path. This isotopy drags β and γ to new cycles β' and γ'.

Because the curve β is defined to surround t_j and t_{j+1}, the analytic continuation merely returns β to β'. Thus, because β' equals β, their periods are also equal. On the other hand, the curve γ is not equal to the new 'dragged' curve γ'. To see this, note that the period of γ' is obtained by developing the flat structure of the doubled orthodisk along γ'. To compute this flat structure, observe the crucial fact that the angles at the orthodisk vertices are either $\pi/2$ or $-\pi/2$, modulo 2π; thus the angles of the doubled orthodisk equal π, modulo 2π. Thus the arc γ' develops into the union of the arc γ with the arcs β and $\overline{\beta}$; in particular, we see that the period of γ' equals the period of γ plus twice the period of β. $\square$

Now denote by $\delta := t_{j+1} - t_j$ and fix all t_i other than t_{j+1}: we regard t_{j+1} as the independent variable.

Corollary 4.7.4. *The function $F(\gamma) - \frac{\log\delta}{\pi i}F(\beta)$ is single-valued and holomorphic near $\delta = 0$.*

Proof. By definition, the function is locally holomorphic near $\delta = 0$. By Lemma 4.7.3 it is single valued. $\square$

Now for the properness argument, we are interested in the geometric coordinates — these are the absolute values of the the periods. More precisely we are interested in

$$\|F(\gamma)\| := |\operatorname{Re} F(\gamma)| + |\operatorname{Im} F(\gamma)|$$

We translate the above statement about periods into a statement about their respective absolute values.

We consider two conjugate orthodisks parameterized by Schwarz-Christoffel maps F_1 and F_2 defined on the same conformal polygon. Recall that we have constructed β and γ to be purely horizontal or vertical.

Corollary 4.7.5. *Either* $\|F_1(\gamma)\| - \frac{\log\delta}{\pi}\|F_1(\beta)\|$ *or* $\|F_1(\gamma)\| + \frac{\log\delta}{\pi}\|F_1(\beta)\|$ *is real analytic in* δ *for* $\delta = 0$. *In the first case,* $\|F_2(\gamma)\| + \frac{\log\delta}{\pi}\|F_2(\beta)\|$ *is real analytic in* δ, *in the second* $\|F_2(\gamma)\| - \frac{\log\delta}{\pi}\|F_1(\beta)\|$.

Proof. Recall from the tedious section 4.1 that the above periods are linear combinations of the geometric coordinates where the coefficients are just signs, in the sense of being elements of $\{1, -1, i, -i\}$. Now by construction, $F_j(\beta)$ is purely real or purely imaginary; moreover, the direction of $F_j(\beta)$ is $\pm i$ times the direction of $F_j(\gamma)$. This, together with Corollary 4.7.4, implies the first claim. Next, note that (see for example the table in §3.4) if we turn left at a vertex in X_1, we will turn right at the corresponding vertex in the conjugate orthodisk X_2, and vice versa. Thus, if the directions of the corresponding edges for γ in corresponding orthodisks differ by $+i$, then the directions of the corresponding edges for β will differ by a $-i$, and vice versa. This implies the second claim.

§5. The Gradient Flow.

5.1 Overall Strategy.

5.1.1. In this section we continue the proof of the existence portions of the main theorems, Theorem A and Theorem B(i). In the previous sections, we assigned to a configuration $\mathcal{C}$ (the ones $\mathcal{C} = (UD)^k U$ and $\mathcal{C} = DH_{m,n}$ were of principal interest) a moduli space $\Delta = \Delta_{\mathcal{C}}$ of pairs of conformal structures $\{\Omega_{Gdh}, \Omega_{G^{-1}dh}\}$ equipped with geometric coordinates $\vec{\mathbf{t}} = (t_i, ..., t_l)$.

In the last section, we defined a height function $\mathcal{H}$ on the moduli space $\mathcal{M}$ and proved that it was a proper function: as a result, there is a critical point for the height function in Δ, and our overall goal in the next pair of sections is a proof that one of these critical points represents a reflexive orthodisk system in Δ, and hence, by Theorem 3.3.5, a minimal surface of the configuration $\mathcal{C}$. Our goal in the present section is a description of the tangent space to the moduli space Δ: we wish to display how infinitesimal changes in the geometric coordinates $\vec{\mathbf{t}}$ affect the height function. In particular, it would certainly be sufficient for our purposes to prove the statement

Model 5.1.1. *If* $\vec{\mathbf{t}_0}$ *is not a reflexive orthodisk system, then there is an element* V *of the tangent space* $T_{\vec{\mathbf{t}_0}}\Delta$ *for which* $D_V\,\mathcal{H} \neq 0$.

This would then have the effect of proving that our critical point for the height function is reflexive, concluding the existence parts of the proofs of the main theorem.

We do not know how to prove or disprove this model statement in its full generality. On the other hand, it is not necessary for the proofs of the main theorems that we do so. Instead we will replace this theorem by a pair of lemmas. The lemmas each have two cases, with the division into cases depending on whether, in the configuration $\mathcal{C} = DH_{m,n}$, we have $n = m$ or $m < n$.

Lemma 5.1.2. *Consider a configuration $\mathcal{C} = DH_{m,n}$. (i) Suppose $n = m$ and $\mathcal{Y} \subset \Delta$ is a real two-dimensional subspace of Δ which is defined by the equations $\mathcal{H}(t_i) = 0$ for all coordinates t_i with only two exceptions (say t_1 and t_2). Suppose also that the coordinates t_1 and t_2 refer to cycles which encircle neighboring edges, at most one of which is a finite edge. Then there is a sublocus $\mathcal{Y}^*$ along which $\mathcal{H}(t_{i_1}) = 0$, and along that one-dimensional sublocus, Then if $\vec{\mathbf{t}_0} \in \mathcal{Y}^*$ has positive height (i.e. $\mathcal{H}(\vec{\mathbf{t}_0}) > 0$), then there is an element $V \in T_{\vec{\mathbf{t}_0}}\mathcal{Y}^*$ of the tangent space $T_{\vec{\mathbf{t}_0}}\mathcal{Y}^*$ for which $D_V\,\mathcal{H} \neq 0$.*

(ii) If $m < n$ and if $\mathcal{Y} \subset \Delta$ is a real one-dimensional subspace of Δ which is defined by the equations $\mathcal{H}(t_i) = 0$ for all coordinates t_i with only one exception (say t_1), and that exception refers to a cycle which is not a finite edge bully. Then if $\vec{\mathbf{t}_0} \in \mathcal{Y}$ has positive height, then there is an element $V \in T_{\vec{\mathbf{t}_0}}\mathcal{Y}$ of the tangent space $T_{\vec{\mathbf{t}_0}}\mathcal{Y}$ for which $D_V\,\mathcal{H} \neq 0$.

Lemma 5.1.3. *Consider a configuration $\mathcal{C} = DH_{m,n}$.(i) If $n = m$, then for every configuration $\mathcal{C} = DH_{m,n}$, there is a non-singular analytic subspace $\mathcal{Y} \subset \Delta = \Delta_{\mathcal{C}}$, for which $\mathcal{Y} = \{\mathcal{H}(t_i) = 0 | i \neq i_1, i_2\}$, for some choice of i_1, i_2, where t_{i_1} and t_{i_2} refer to cycles encircling neighboring edges, of which at most one is a finite edge.*

(ii) If $m < n$, then for every configuration $\mathcal{C} = DH_{m,n}$, there is a non-singular analytic subspace $\mathcal{Y} \subset \Delta = \Delta_{\mathcal{C}}$, for which $\mathcal{Y} = \{\mathcal{H}(t_i) = 0 | i \neq i_1\}$, for some choice of i_1 and the cycle referred to by t_{i_1} is not a finite edge bully.

A cycle Γ is a *finite edge bully* for the previous lemma if each finite edge E of one of the orthodisks has a neighbor E' so that Γ foots on E but not E' or vice versa.

We introduce this concept because when $m + n$ is small, the technical requirements of the proof (see Lemma 5.3.1 and Definition 5.3.0) contrast with a shortage of sides; when $m + n \geq 5$ in case (ii) and $m + n \geq 11$ in case (i), no cycle is a finite edge bully, and these hypotheses are vacuous. In our proof of Lemma 5.1.3, we will produce a cycle that is not a finite edge bully.

think the above through carefully

Given these lemmas, the proofs of Theorems A and B(i) are straightforward.

Proofs of Theorem A and Theorem B(i). Consider the locus $\mathcal{Y}$ (or the sublocus $\mathcal{Y}^*$) guaranteed by Lemma 5.1.3. By Theorem 4.5, the height function $\mathcal{H}$ is proper on $\mathcal{Y}$ (resp. $\mathcal{Y}^*$), so the height function $\mathcal{H}$ has a critical point on $\mathcal{Y}$. By Lemma 5.1.2, this critical point represents a point where $\mathcal{H} = 0$, i.e a reflexive orthodisk by Lemma 4.5.5.

The proof of Lemma 5.1.2 occupies the current section while the proof of Lemma 5.1.3 is given in the following section.

rewrite this stuff below

5.1.2. Let us discuss informally the proof of Lemma 5.1.2. Because angles of corresponding vertices in the $\Omega_{Gdh} \leftrightarrow \Omega_{G^{-1}dh}$ correspondence sum to 0 mod 2π, the orthodisks locally topologically fit together along corresponding edges, so conjugacy of orthodisks requires corresponding edges to move in different directions: if the edge E on Ω_{Gdh} moves "out," the corresponding edge E^* on $\Omega_{G^{-1}dh}$ edge moves "in", and vice versa (see the figures below). Thus we expect that if γ has an endpoint on E, then one of the extremal lengths of γ decreases, while the other extremal length of γ on the other orthodisk would increase:

this will force the change of the height $\mathcal{H}(\gamma)$ of γ to have a definite sign, as desired. This is the intuition behind Lemma 5.2.1; a rigorous argument requires us to actually compute derivatives of relevant extremal lengths using the formula (2.2) and we will need to avoid some technical difficulties involving singularities of the holomorphic quadratic differentials arising in (2.2). We do this by displaying, fairly explicitly, the deformations of the orthodisks (in local coordinates on $\Omega_{Gdh}/\Omega_{G^{-1}dh}$) as well as the differentials of extremal lengths, also in coordinates. After some preliminary notational description in §5.2, we do most of the computing in §5.3. Also in section §5.3 is the key technical lemma, which relates the formalism of formula (2.2), together with the local coordinate descriptions of its terms, to the intuition we just described.

5.2 Deformations of $DH_{1,1}$.

We will prove Lemma 5.1.2 by first considering the special case of $\mathcal{C} = DH_{1,1}$. We will then note that this case, as it is defined in terms of precisely two curve systems and involves all the types of geometric situations encountered in all of the configurations $\mathcal{C}$, is only slightly different from the most general case: the arguments we give here extend immediately to prove the lemma in general, even though the exposition, in this specific low-dimensional case, can be much more concrete.

In the current section, we will describe the notation and results for this special case of $\mathcal{C} = DH_{1,1}$.

We begin by recalling the notation of section 4.2: there the geometric coordinates were labeled $\Delta = (y, b, g)$ corresponding to the curve systems labeled yellow, blue, and green (see the figures in §4.2). We introduced a fourth curve system, mauve, which we used with blue to define the height function.

Theorem 5.2.1. *There exists a reflexive orthodisk system for the configuration $DH_{1,1}$.*

Proof: In this case, the statement of Lemma 5.1.3(i) is vacuous as the moduli space $\Delta = \Delta_{1,1}$ is already two-dimensional. So we are left to prove Lemma 5.1.2 in this case. The plan is simple, as we consider a path $\Gamma \subset \Delta$ which has two limits: towards one end E, the size of the period $H_1H_2 - C_1P_1$ (and $H_3H_2 - P_3C_2$) decays to zero, and towards the other end E', the period $P_1P_2 - H_1C_1$ (and $P_2P_3 - C_2H_3$) decays to zero. We

Claim 5.2.2. $\operatorname{sgn}(\operatorname{Ext}_{\Omega_{Gdh}}(\text{blue}) - \operatorname{Ext}_{\Omega_{G^{-1}dh}}(\text{blue})) \neq \operatorname{sgn}(\operatorname{Ext}_{\Omega_{Gdh}}(\text{blue}) - \operatorname{Ext}_{\Omega_{G^{-1}dh}}(\text{blue}))$. ∎

Assuming the claim, we continue with the proof of Theorem 5.2.1. As the sign of $\operatorname{Ext}_{\Omega_{Gdh}}(\text{blue}) - \operatorname{Ext}_{\Omega_{G^{-1}dh}}(\text{blue}))$ changes along the arc $\Gamma = \{\Gamma(s)\}$, we know that there is a point $\Gamma(s_0)$ at which $\operatorname{Ext}_{\Omega_{Gdh}}(\text{blue}) - \operatorname{Ext}_{\Omega_{G^{-1}dh}}(\text{blue}))$ changes sign. Of course, this function $\operatorname{Ext}_{\Omega_{Gdh}}(\text{blue}) - \operatorname{Ext}_{\Omega_{G^{-1}dh}}(\text{blue}))$ is the difference of real analytic regular functions of the coordinates on *Delta* (see expanded discussion of the analyticity of the curve at the end of the proof of Lemma 6.2), and so there is an analytic path through $\Gamma(s_0)$ along which $\operatorname{Ext}_{\Omega_{Gdh}}(\text{blue}) = \operatorname{Ext}_{\Omega_{G^{-1}dh}}(\text{blue}))$. In keeping with the notations of Lemma 5.1.2 and 5.1.3, we denote that analytic path by $\mathcal{Y}^*$.

Our next task is to find a point on $\mathcal{Y}^*$ for which $\mathcal{H}(\text{mauve}) = 0$: at such a point, we would have $\mathcal{H}(\text{mauve}) = 0 = \mathcal{H}(\text{blue})$. As $\mathcal{Y}^*$ is one-dimesional, and mauve is not a finite-edge bully, we in effect prove Lemma 5.1.2. The idea is to make an "infinitesimal

push" along the edges H_1H_2 (and H_2H_3); we push H_1H_2 (and H_2H_3) "into" Ω_{Gdh} and then the requirement that Ω_{Gdh} and $\Omega_{G^{-1}dh}$ should remain conjugate then forces us to make an equal push of H_1H_2 (and H_2H_3) "out of" $\Omega_{G^{-1}dh}$. By the principle of domain monotonicity of extremal length, we expect the change in Ω_{Gdh} to increase the extremal length $\mathrm{Ext}_{\Omega_{Gdh}}(\text{mauve})$ and we expect the change in $\Omega_{G^{-1}dh}$ to decrease the extremal length $\mathrm{Ext}_{\Omega_{G^{-1}dh}}(\text{mauve})$. The rigorously defined formulae and the technical Lemma 5.3.1 will support this intuition (indeed, will show that it is true to first order), and we find that if $\mathcal{H}(mauve) \neq 0$ at a point $\vec{\mathbf{t}_0} \in \mathcal{Y}^*$, then there is an element $V \in T_{\vec{\mathbf{t}_0}}\mathcal{Y}^*$ of the tangent space $T_{\vec{\mathbf{t}_0}}\mathcal{Y}^*$ for which $D_V\,\mathcal{H} \neq 0$. This ocmpletes the proof of Lemma 5.1.2 in this case, as well as Theorem 5.1.2, up to the proof of the claim.

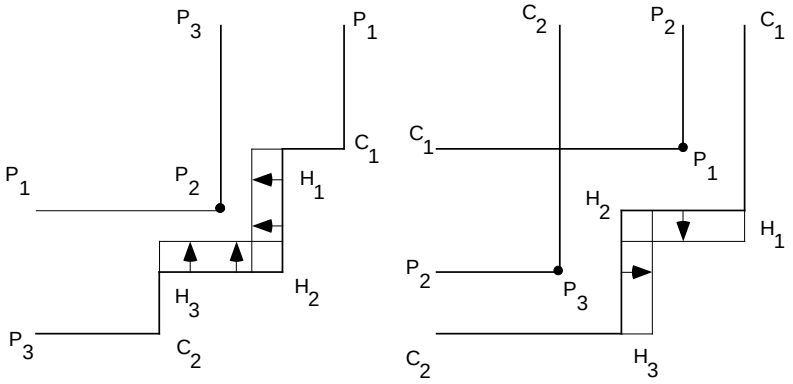

Pushing edges along the locus $\mathcal{Y}^*$

Proof of the Claim 5.2.2. It is evident that as the period $P_1P_2 - H_1C_1$ tends to zero (with the period $H_1H_2 - C_1P_1$ remaining bounded from below), the extremal length $\mathrm{Ext}_{\Omega_{Gdh}}(\text{blue})$ tends to a non-zero finite number, while the extremal length $\mathrm{Ext}_{\Omega_{G^{-1}dh}}(\text{blue})$ tends to infinity.

On the other hand, if we first send the period $P_2P_3 - H_1H_2$ to zero and then allow the period $H_1H_2 - P_1C_1$ to tend to zero, we see that $\mathrm{Ext}_{\Omega_{Gdh}}(\text{blue})$ is equal to the extremal length of blue on the quadrilateral component $P_1 - P_2 = H_2 - H_1 - C_1 - P_1$ of a noded surface, while $\mathrm{Ext}_{\Omega_{G^{-1}dh}}(\text{blue})$ is given in terms of the extremal length of blue on the pentagonal surface $P - 2 - H_2 - H_1 - C_1 - P_1 - P_2$. Yet the asymptotics of these extremal lengths of these explicit shapes are readily (if tediously) computable, and we find that $\mathrm{Ext}_{\Omega_{Gdh}}(\text{blue})$ decays to zero at a slower rate than $\mathrm{Ext}_{\Omega_{G^{-1}dh}}(\text{blue})$ as we send the period $H_1H_2 - P_1C_1$ to zero. Thus by allowing Γ to have ends near these two degenerate loci, we obtain the claim.

5.3 Infinitesimal pushes.

We need to formalize the previous discussion. As always we are concerned with relating the Euclidean geometry of the orthodisks (which corresponds directly with the periods of the Weierstraß data) to the conformal data of the domains Ω_{Gdh} and $\Omega_{G^{-1}dh}$. From the discussion above, it is clear that the allowable infinitesimal motions in Δ, which is parame-

terized in terms of the Euclidean geometry of Ω_{Gdh} and $\Omega_{G^{-1}dh}$, are given by infinitesimal changes in lengths of finite sides or in distances between sheets, with the changes being done simultaneously on Ω_{Gdh} and $\Omega_{G^{-1}dh}$ to preserve conjugacy. The link to the conformal geometry is the formula (2.2): a motion which infinitesimally transforms Ω_{Gdh}, say, will produce an infinitesimal change in the conformal structure. Tensorially, this tangent vector to the moduli space of conformal structures is represented by a Beltrami differential. Later, formula (2.2) will be used, together with knowledge of the cotangent vectors $d\,\mathrm{Ext}_{\Omega_{Gdh}}(\cdot)$ and $d\,\mathrm{Ext}_{\Omega_{G^{-1}dh}}(\cdot)$, to determine the derivatives of the relevant extremal lengths, hence the derivative of the height.

5.3.1 Infinitesimal Pushes. Here we explicitly compute the effect of infinitesimal pushes of certain edges on the extremal lengths of relevant cycles. This is done by explicitly displaying the infinitesimal deformation and then using this formula to compute the sign of the derivative of the extremal lengths, using formula (2.2). There will be four different cases to consider, all of which are apparent in the $DH_{1,1}$ orthodisks. This is why we can, without loss of generality, confine the computations to this case. To be concrete, we will choose for each case either the orthodisk Ω_{Gdh} or the orthodisk $\Omega_{G^{-1}dh}$.

The three sides H_1C_1, C_1P_1 and H_2H_1 are geometrically different and require separate treatments. Thus we break our discussion up into cases.

Case A. Finite *non-central* edges (see also [WW]) Example: H_1C_1 in Ω_{Gdh}.
Case B. Infinite edge whose finite vertex is unbranched. Example: H_1C_1 in $\Omega_{G^{-1}dh}$.
Case C. Infinite edge whose finite vertex is a branch point off the symmetry line. Example: C_1P_1 on $\Omega_{G^{-1}dh}$.
Case D. An edge (finite or infinite) and its symmetric side meet in a corner. Example: H_3H_2 and H_2H_1.

For each case there are two subcases, which we can describe as depending on whether the given sides are horizontal or vertical. The distinction is, surprisingly, a bit important, as together with the fact that we do our deformations in pairs, it provides for an important cancelation of (possibly) singular terms affecting the formulation of Lemma 5.3.1. We defer this point for later (see Remark 5.3.3), while here we begin to calculate the relevant Beltrami differentials in the cases.

Also, each infinitesimal motion might require two different types of cases, depending on whether the edge we are deforming on Ω_{Gdh} corresponds on $\Omega_{G^{-1}dh}$ to an edge of the same type or a different type. We will thus compute the Beltrami differentials only for a single domain, either Ω_{Gdh} or $\Omega_{G^{-1}dh}$.

Case A. Here the computations are quite analogous to those that we found in [WW]; they differ only in orientation of the boundary of the orthodisk.

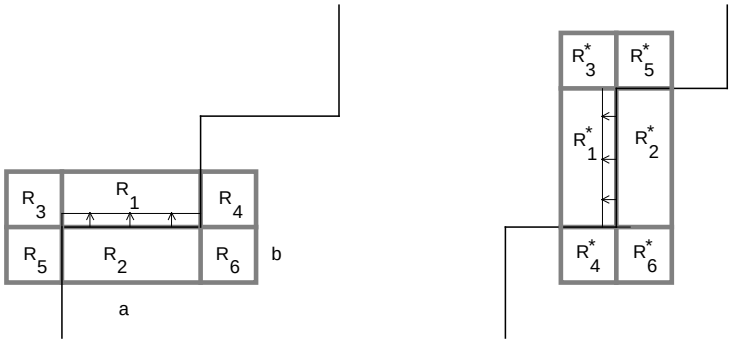

Beltrami differential computation — case A

We first consider the case of a horizontal finite side; as in the figure above, we see that the neighborhood of the horizontal side of the orthodisk in the plane naturally divides into six regions which we label R_1,...,R_6. Our deformation $f_\epsilon = f_{\epsilon,b,\delta}$ differs from the identity only in such a neighborhood, and in each of the six regions, the map is affine. In fact we have a two-parameter family of these deformations, all of which have the same infinitesimal effect, with the parameters b and δ depending on the dimensions of the supporting neighborhood.

(5.1a)

$$f_\epsilon(x,y) = \begin{cases} \left(x, \epsilon + \frac{b-\epsilon}{b} y\right), & \{-a \le x \le a, 0 \le y \le b\} = R_1 \\ \left(x, \epsilon + \frac{b+\epsilon}{b} y\right), & \{-a \le x \le a, -b \le y \le 0\} = R_2 \\ \left(x, y + \frac{\epsilon + \frac{b-\epsilon}{b} y - y}{\delta}(x + \delta + a)\right), & \{-a-\delta \le x \le -a, 0 \le y \le b\} = R_3 \\ \left(x, y - \frac{\epsilon + \frac{b-\epsilon}{b} y - y}{\delta}(x - \delta - a)\right), & \{a \le x \le a+\delta, 0 \le y \le b\} = R_4 \\ \left(x, y + \frac{\epsilon + \frac{b+\epsilon}{b} y - y}{\delta}(x + \delta + a)\right), & \{-a-\delta \le x \le -a, -b \le y \le 0\} = R_5 \\ \left(x, y - \frac{\epsilon + \frac{b+\epsilon}{b} y - y}{\delta}(x - \delta - a)\right), & \{a \le x \le a+\delta, -b \le y \le 0\} = R_6 \\ (x,y) & \text{otherwise} \end{cases}$$

where we have defined the regions $R_1, \ldots, R_6$ within the definition of f_ϵ. Also note that here the orthodisk contains the arc $\{(-a,y) \mid 0 \le y \le b\} \cup \{(x,0) \mid -a \le x \le a\} \cup \{(a,y) \mid -b \le y \le 0\}$. Let E denote the edge being pushed, defined above as $[-a,a] \times \{0\}$.

Of course f_ϵ differs from the identity only on a neighborhood of the edge E, so that f_ϵ takes the symmetric orthodisk to an asymmetric orthodisk. We next modify f_ϵ in a neighborhood of the reflected (across the $y = -x$ line) segment E^* in an analogous way with a map f_ϵ^* so that $f_\epsilon^* \circ f_\epsilon$ will preserve the symmetry of the orthodisk.

Our present conventions are that the edge E is horizontal; this forces E^* to be vertical and we now write down f_ϵ^* for such a vertical segment; this is a straightforward extension of the description of f_ϵ for a horizontal side, but we present the definition of f_ϵ^* anyway,

as we are crucially interested in the signs of the terms. So set

$$f_\epsilon^* = \begin{cases} \left(-\epsilon + \frac{b-\epsilon}{b}x, y\right), & \{-b \le x \le 0, -a \le y \le a\} = R_1^* \\ \left(-\epsilon + \frac{b+\epsilon}{b}x, y\right), & \{0 \le x \le b, -a \le y \le a\} = R_2^* \\ \left(x - \frac{-\epsilon+\frac{b-\epsilon}{b}x-x}{\delta}(y-\delta-a), y\right), & \{-b \le x \le 0, a \le y \le a+\delta\} = R_3^* \\ \left(x + \frac{-\epsilon+\frac{b-\epsilon}{b}x-x}{\delta}(y+\delta+a), y\right), & \{-b \le x \le 0, -a-\delta \le y \le -a\} = R_4^* \\ \left(x - \frac{-\epsilon+\frac{b+\epsilon}{b}x-x}{\delta}(y-\delta-a), y\right), & \{0 \le x \le b, a \le y \le a+\delta\} = R_5^* \\ \left(x + \frac{-\epsilon+\frac{b+\epsilon}{b}x-x}{\delta}(y+\delta+a), y\right), & \{0 \le x \le b, -a-\delta \le y \le -a\} = R_6^* \\ (x,y) & \text{otherwise} \end{cases} \tag{5.1b}$$

Note that under the reflection across the line $\{y = -x\}$, the region R_i gets taken to the region R_i^*.

Let $\nu_\epsilon = \frac{(f_\epsilon)_{\bar{z}}}{(f_\epsilon)_z}$ denote the Beltrami differential of f_ϵ, and set $\dot{\nu} = \frac{d}{d\epsilon}\Big|_{\epsilon=0} \nu_\epsilon$. Similarly, let ν_ϵ^* denote the Beltrami differential of f_ϵ^*, and set $\dot{\nu}^* = \frac{d}{d\epsilon}\Big|_{\epsilon=0} \nu_\epsilon^*$. Let $\dot{\mu} = \dot{\nu} + \dot{\nu}^*$. Now $\dot{\mu}$ is a Beltrami differential supported in a bounded domain in one of the domains Ω_{Gdh} or $\Omega_{G^{-1}dh}$. We begin by observing that it is easy to compute that $\dot{\nu} = [\frac{d}{d\epsilon}\Big|_{\epsilon=0} (f_\epsilon)]_{\bar{z}}$ evaluates near E to

$$\dot{\nu} = \begin{cases} \frac{1}{2b}, & z \in R_1 \\ -\frac{1}{2b}, & z \in R_2 \\ \frac{1}{2b}[x+\delta+a]/\delta + i\,(1-y/b)\,\frac{1}{2\delta} = \frac{1}{2b\delta}(\bar{z}+\delta+a+ib), & z \in R_3 \\ -\frac{1}{2b}[x-\delta-a]/\delta - i\,(1-y/b)\,\frac{1}{2\delta} = \frac{1}{2b\delta}(-\bar{z}+\delta+a-ib), & z \in R_4 \\ -\frac{1}{2b}[x+\delta+a]/\delta + i\,(1+y/b)\,\frac{1}{2\delta} = \frac{1}{2b\delta}(-\bar{z}-\delta-a+ib), & z \in R_5 \\ \frac{1}{2b}[x-\delta-a]/\delta - i\,(1+y/b)\,\frac{1}{2\delta} = \frac{1}{2b\delta}(\bar{z}-\delta-a-ib), & z \in R_6 \\ 0 & z \notin \operatorname{supp}(f_\epsilon - \mathrm{id}) \end{cases} \tag{5.2a}$$

We further compute

$$\dot{\nu}^* = \begin{cases} -\frac{1}{2b}, & R_1^* \\ \frac{1}{2b}, & R_2^* \\ \frac{1}{2b\delta}(i\bar{z}-\delta-a+bi) & R_3^* \\ \frac{1}{2b\delta}(-i\bar{z}-\delta-a-bi) & R_4^* \\ \frac{1}{2b\delta}(-i\bar{z}+\delta+a+bi) & R_5^* \\ \frac{1}{2b\delta}(i\bar{z}+\delta+a-bi) & R_6^* \end{cases} \tag{5.2b}$$

Cases B, C. For both infinite sides the deformations are the same, here represented in the horizontal case. (Here we have deferred the case of infinite sides that meet along the symmetry line $\{y = -x\}$ until we treat Case D, where it will fit more naturally.)

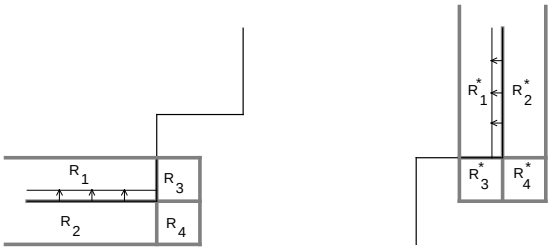

Beltrami differential computation — cases B and C

$$f_{\epsilon;b,\delta}(x,y) = \begin{cases} \left(x, \epsilon + \frac{b-\epsilon}{b} y\right), & R_1 = \{x \le 0, 0 \le y \le b\} \\ \left(x, \epsilon + \frac{b+\epsilon}{b} y\right), & R_2 = \{x \le 0, -b \le y \le 0\} \\ \left(x, y - \frac{\epsilon + \frac{b-\epsilon}{b} y - y}{\delta}(x-\delta)\right), & R_3 = \{0 \le x \le \delta, 0 \le y \le b\} \\ \left(x, y - \frac{\epsilon + \frac{b+\epsilon}{b} y - y}{\delta}(x-\delta)\right), & R_4 = \{0 \le x \le \delta, -b \le y \le 0\} \\ (x,y) & \text{otherwise} \end{cases}$$

Thus our infinitesimal Beltrami differential is given by

$$\dot\nu_{b,\delta} = \begin{cases} \frac{1}{2b}, & z \in R_1 \\ -\frac{1}{2b}, & z \in R_2 \\ \frac{1}{2b\delta}(-\bar z + \delta - ib), & z \in R_3 \\ \frac{1}{2b\delta}(\bar z - \delta - ib), & z \in R_4 \\ 0 & z \notin \operatorname{supp}(F_{\epsilon;b,\delta} - \mathrm{id}) \end{cases}$$

The formulas for a push of a vertical edge are analogous.

Case D. We have separated this case out for purely expositional reasons. We can imagine that the infinitesimal push that moves the pair of consecutive sides along the symmetry line $\{y = -x\}$ is the result of a composition of a pair of pushes from Case A or from Case C: i.e. our diffeomorphism $F_{\epsilon;b,\delta}$ can be written $F_{\epsilon;b,\delta} = f_\epsilon \circ f_\epsilon^*$, where the maps differ from the identity in the *union* of the supports of $\dot\nu_{b,\delta}$ and $\dot\nu^*_{b,\delta}$.

It is an easy consequence of the chain rule applied to this formula for $F_{\epsilon;b,\delta}$ that the infinitesimal Beltrami differential for this deformation is the sum $\dot\nu_{b,\delta} + \dot\nu^*_{b,\delta}$ of the infinitesimal Beltrami differentials $\dot\nu_{b,\delta}$ and $\dot\nu^*_{b,\delta}$ defined in formula (5.2) for Case A (even in a neighborhood of the vertex along the diagonal where the supports of the differentials $\dot\nu_{b,\delta}$ and $\dot\nu^*_{b,\delta}$ coincide).

5.3.2. Derivatives of Extremal Lengths.

In this section, we combine the computations of $\dot\nu_{b,\delta}$ with formula (2.2) (and its background in §2) and some easy observations on the nature of the quadratic differentials $\Phi_\mu = \frac{1}{2} d\,\mathrm{Ext}_{(\cdot)}(\mu)\,\big|_\cdot$ to compute the derivatives of extremal lengths under our infinitesimal deformations of edge lengths.

We begin by recalling some background from §2. If we are given a curve γ, the extremal length of that curve on an orthodisk, say Ω_{Gdh}, is a real-valued C^1 function on the moduli space of that orthodisk. Its differential is then a holomorphic quadratic differential $\Phi_\gamma = \frac{1}{2} d\,\mathrm{Ext}_{(\cdot)}(\gamma)\,\big|_{\Omega_{Gdh}}$ on that orthodisk; the horizontal foliation of Φ_γ consists of curves which connect the same edges in Ω_{Gdh} as γ, since Φ_γ is obtained as the pullback of the quadratic differential dz^2 from a rectangle where the image of γ connects the opposite vertical sides. We compute the derivative of the extremal length function using formula (2.2), i.e.

$$\left(d\,\mathrm{Ext.}(\gamma)\,\big|_{\Omega_{Gdh}}\right)[\nu] = 4\,\mathrm{Re}\int_{\Omega_{Gdh}} \Phi_\gamma \nu$$

It is here where we find that we can actually compute the sign of the derivative of the extremal lengths, hence the height function, but also encounter a subtle technical problem. The point is that we will discover that, in suitable circumstances, just the topology of the curve γ on Ω_{Gdh} will determine the sign of the derivative on an edge E, so we will be able to evaluate the sign of the integral above, if we shrink the support of the Beltrami differential $\dot\nu_{b,\delta}$ to the edge by sending b, δ to zero. (In particular, the sign of Φ_γ depends precisely on whether the foliation of $\Phi = \Phi_\gamma$ is parallel or perpendicular to E, and on whether E is horizontal or vertical.) We then need to know two things: 1) that this limit exists, and 2) that we may know its sign via examination of the sign of $\dot\nu_{b,\delta}$ and Φ_γ on the edge E. We phrase this as

Definition 5.3.0. Φ is admissable on an edge E iff at a vertex v of E and in a conformal parameter z centered at v, we have $|z|\Phi(z) = o(1)$.

Lemma 5.3.1. *Let Φ be admissable for the edge E.* (1) $\lim_{b\to 0,\delta\to 0} \mathrm{Re}\int \Phi\dot\nu$ *exists, is finite and non-zero.* (2) *The foliation of Φ is either parallel or orthogonal to the interior of the segment which is* $\lim_{b\to 0,\delta\to 0}(\mathrm{supp}\,\dot\nu)$*, and* (3) *The expression $\Psi\dot\nu$ has a constant sign on that segment E, and the integral (2.2) also has that (same) sign.*

In the statement of the lemma, the foliation refers to the horizontal foliation of the holomorphic quadratic differential $\Phi = \Phi_\gamma$, whose core curve is γ.

This lemma provides the rigorous foundation for the intuition described in the paragraph of strategy §5.1.2.

5.3.3 Proof of the Technical Lemma and a Remark on its Limitations.

Proof of Lemma 5.3.1.

The foliation of Φ, on say Ω_{Gdh}, lifts to a foliation on the punctured sphere (which we'll denote by S_{Gdh}), symmetric about the reflection about the equator. This proves thr second statement. The third statement follows from the first (and from the above discussion of the topology of the vertical foliation of Φ_γ, once we prove that there is no infinitude coming from either the neighborhood of infinity of the infinite edges or the regions R_3 and R_4 for the finite vertices. This finiteness will follow from the proof of the first statement. Thus, we are left to prove the first statement.

In the case of an edge with a finite vertex, we estimate the contribution to $\operatorname{Re}\int \Phi\dot{\nu}$ of a neighborhood N of a vertex from regions R_1 and R_2 (and R_1^* and R_2^*) as

$$\begin{aligned} |\operatorname{Re}\int \Phi\dot{\nu}| &\leq \int_0^b \int_N \frac{1}{2b}\cdot|\Phi|dxdy \\ &= \frac{1}{2b}\int_0^b \int_N o(x^2+y^2)^{-1/2}dxdy \end{aligned}$$

which converges by the dominated convergence theorem. The other regions are analogous.

In the case of an edge with an infinite vertex, the argument is somewhat easier, as the possible growth of $|\Phi|$ as we tend towards the vertex has an a priori bound of rapid decay. We compute this decay by observing that in the coordinate w of the plane, the quadratic differential Φ has expansion $\Phi = c_1/w + \{h.o.t.\}dw$, and the Schwarz-Christoffel map from the half-plane to the orthodisk has integrand $\omega = \{c_0 z^{-3/2} + h.o.t.\}dz$. It is then straightforward that in the coordinate z of the orthodisk, the quadratic differential Φ decays faster than $|z|^{-2}$. $\square$

Computations like those in the final paragraph of the above proof prove the

Proposition 5.3.2. *The holomorphic quadratic differential Φ is admissable on an edge E if Φ relates to the vertices v_1 and v_2 of E in one of the following ways*

(i) *The orthodisk has an angle of $\pi/2$ of v_i*
(ii) *The vertex v_i is at infinity*
(iii) *The orthodisk has an angle of $3\pi/2$ at v_i, and the foliations of Φ are either both parallel to the edges incident to v_i or both orthogonal for those edges.*
(iv) *The vertex v_i is a branch point where the orthodisk makes an angle of $5\pi/2$, and the holomorphic quadratic differential has a singularity at v_i.*

In the last case (iv), a singularity arises if and only if the foliation is parallel to the edges incident to v_i and a leaf emanates from v_i, or the foliation is orthogonal to those edges and at least two leaves emanate from v_i.

Proof. As an example, we discuss (iii). Here, an appropriate branch of the map $z \mapsto z^{2/3} = w$ takes a neighborhood of v_i in the orthodisk to a neighborhood of the origin in the upper half plane. The condition on the foliation on the proposition allow us to conclude [Str] that the holomorphic quadratic differential Φ has the expansion in the upper half plane as $(c_0 + c_1 z + h.o.t.)dz^2$, from which the statement follows.

Remark 5.3.3. In light of the previous proposition, we see that it is quite common to have an edge which is not admissable for a holomorphic quadratic differential: for instance we need only consider the differential of extremal length for a cycle which has feet on an isolated edge with a vertex where the orthodisk has angle at least $3\pi/2$. Thus, it is a significant problem to find extremal lengths so that Lemma 5.3.1 may be invoked.

Moreover, in the cases where an edge E is not admissable for a given holomorphic quadratic differential, we cannot — in general — expect to have control over $\operatorname{Re}\int_E \Phi\dot{\nu}$. This follows from an analysis similar to that in the proof of the previous proposition or

in the final paragraph of the proof of Lemma 5.3.1: by choosing a branch of the map from a neighborhood of a vertex to the upper half plane, it is easy to see that there is no guarantee that $\lim_{b,\delta\to 0} \operatorname{Re} \int \Phi \dot{\nu}_{b,\delta}$ exists. However, a choice of consistent branches of those maps from a neighborhood $N(\nu)$ of a vertex ν and from the reflection $N(\nu^*)$ of $N(\nu)$ across the central diagonal show that $\operatorname{Re}\left[\int_{N(\nu)} \Phi \dot{\nu}_{b,\delta} + \int_{N(\nu^*)} \Phi \dot{\nu}^*_{b,\delta}\right] = O(1)$ as b, $\delta \to 0$, i.e. the contributions from the terms in the expansions of Φ of order $z^{-\alpha}$ from $\alpha \geq 1$ cancel in pairs. Thus, while we then find that $\lim_{b,\delta\to 0} \operatorname{Re} \int \Phi \dot{\nu}_{b,\delta}$ exists — which we expect from $\dot{\nu}_{b,\delta}$ always representing a unique tangent vector to Δ — we also find that the contributions of the terms $z^{-\alpha}(\alpha \geq 1)$ to the sign of Φ on nearby edges muust be ignored in evaluating $\lim_{b,\delta\to 0} \operatorname{Re} \int \Phi \dot{\nu}_{b,\delta}$.

Conclusion of the proof of Theorem 5.2.1. Conjugacy of the domains Ω_{Gdh} and and $\Omega_{G^{-1}dh}$ requires that if we push an edge $E \subset \partial\overline{\Omega_{Gdh}}$ into the domain Ω_{Gdh}, we will change the Euclidean geometry of that domain in ways that will force us to push the corresponding edge $E^* \subset \partial\overline{\Omega_{G^{-1}dh}}$ out of the domain $\Omega_{G^{-1}dh}$. To see this, observe that for finite length edges, the fact that the angles add to multiples of 2π (see the table in §3.4) means that there is a pair of homeomorphisms of Ω_{Gdh} and $\Omega_{G^{-1}dh}$, respectively, which preserves the verticality or horizontality of the bounding edges, but allows the two image domains ${\Omega_{Gdh}}^*$ and ${\Omega_{G^{-1}dh}}^*$, respectively, to fit together to form a locally Euclidean space. (We can also require the homeomorphisms to preserve the lengths of finite boundary edges; the domains will continue to fit together as above.) We first discuss the situation of pushes of finite boundary edges. Conjugacy requires that Ω_{Gdh} and $\Omega_{G^{-1}dh}$ have the same Euclidean lengths, and for finite edges, this length is but a single measurement in the Euclidean complex ${\Omega_{Gdh}}^* \cup {\Omega_{G^{-1}dh}}^*$. But in this complex ${\Omega_{Gdh}}^* \cup {\Omega_{G^{-1}dh}}^*$, a push out of a finite edge of ${\Omega_{Gdh}}^*$ is simultaneously a pushing in of the corresponding edge of ${\Omega_{G^{-1}dh}}^*$, and vice versa. Thus, because our homeomorphisms could be taken to preserve a neighborhood of the boundary of the domains Ω_{Gdh} and and $\Omega_{G^{-1}dh}$, we see that a push out of a finite edge of Ω_{Gdh} is simultaneously a pushing in of the corresponding edge of $\Omega_{G^{-1}dh}$, and vice versa. The corresponding statement for infinite edges is argued for analogously, once we remark that in the above argument about finite edges, (i) we never made use of the lengths of the (finite) edges being pushed, so this quantity is irrelevant to the discussion, and (ii) we also never made formal use of the cone angles being at finite points in the plane – the arguments applied equally well to boundaries of Ω_{Gdh} and $\Omega_{G^{-1}dh}$ fitting together at ∞.

We apply this general reasoning to the case of $\mathcal{C} = DH_{1,1}$. Our only pushing is along the locus $\mathcal{Y}^* = \{\mathcal{H}(\text{blue}) = 0\}$, and we seek to push H_1H_2 and H_2H_3. Here the measured foliations for the holomorphic quadratic differentials $\Phi_{\text{mauve}} = \frac{1}{2} dExt_{\Omega_\cdot}(\text{mauve})$ are parallel to the sides being pushed and to the neighboring sides. Proposition 5.3.2(i),(iii) then assert that the quadratic differentials are admissable for those edges; Lemma 5.3.1 then implies that since the Beltrami differentials $\dot{\nu}_{\Omega_\cdot}$ have opposite signs on corresponding edges, so do $\Phi_{\text{mauve}} \dot{\nu}_{\Omega_\cdot}$; thus

$$\operatorname{sgn} dExt_{\Omega_{Gdh}}(\text{mauve})[\dot{\nu}_{\Omega_{Gdh}}] = -\operatorname{sgn} dExt_{\Omega_{G^{-1}dh}}(\text{mauve})[\dot{\nu}_{\Omega_{G^{-1}dh}}].$$

This concludes the proofof Lemma 5.1.2 in this case, and hence also the proof of Theorem 5.2.1.

Conclusion of the proof of Lemma 5.1.2. We begin with statement (i). The general case of this statement is precisely analogous to the case of Theorem 5.2.1; indeed, we can regard the locus $\mathcal{Y}$ from Lemma 5.1.2 as being a version of the moduli space Δ we studied in Theorem 5.2.1. The coordinates t_{i_1} and t_{i_2} from the lemma are given by periods $H_1C_1 - P_1P_2$ exactly as in the treatment of $\Delta_{1,1}$. In particular, the asymptotic estimates calculated in the proofof Claim 5.2.2 continue to hold exactly as before, as the setting for those estimates has changed in only insubstantial ways. (To see this, note that the only changes are the we do not necessarily have that P_2 tends to H_2 on Ω_{Gdh} (which does not affect the estimates since we continue to have $|H_1C_1 - P_1P_2|$ bounded away from zero), and the angle at P_2 on Ω_{Gdh} has changed (also immaterially as P_2 is at some bounded distance from where the degeneracy is occurring).)

Moreover, because the rest of the terms of $\mathcal{H}_{\mathcal{C}}$ vanish along the locus $\mathcal{Y}$ to second order in the deformation variable, we see that any deformation of the orthodisk will not alter the contribution of these terms to $\mathcal{H}_{\mathcal{C}}$. Thus the only effect of an infinitesimal deformation of an orthodisk system on $\mathcal{Y}$ to the height function $\mathcal{H}_{\mathcal{C}}$ is to the terms $\mathcal{H}(t_{i_1})$ and $\mathcal{H}(t_{i_2})$, which we control as in Theorem 5.2.1.

For statement(ii) of the lemma, we deform as we did along the locus $\mathcal{Y}^* \subset \mathcal{Y}$, here pushing on a finite edge which is parallel to the foliation for Φ_{t_i} (in the obvious notation) if and only its neighbors are. (It is worth remarking that in the case of $DH_{1,2}$, we will not be able to find an edge which is finite on both Ω_{Gdh} and $\Omega_{G^{-1}dh}$; in this case we will push on H_1C_1, which, relative to the cycle $H_2H_3 - P_1P_2$ is admissable by Proposition 5.3.2(i),(ii). Thus the proof above for the case $m = n$ also extends to this case.)

This concludes the proof of the lemma.

§6. Regeneration.

rewrite this with our curve systems in mind

In the previous section we showed how we might reduce the height function $\mathcal{H}_{\mathcal{C}}$ at a critical point of a smooth locus $\mathcal{Y}$, where the locus $\mathcal{Y}$ was defined as the null locus of all but two of the heights, say $\mathcal{H}(t_{i_1})$ and $\mathcal{H}(t_{i_2})$. In this section, we prove Lemma 5.1.3, which guarantees the existence of such a locus $\mathcal{Y}$.

We will continue with the rather concrete exposition we used in §5, i.e. we will prove the existence of the genus five Costa tower, $DH_{2,2}$ by using Theorem 5.2.1 (the existence of the genus three Costa tower, $DH_{1,1}$) to imply the existence of a locus $\mathcal{Y} \subset \Delta = \Delta_{2,2}$ – the Lemma 5.1.2 and the properness Theorem 4.5.1 then prove the existence. The arguments we give will immediately generalize to prove the existence of a genus $2n + 1$ Costa tower $DH_{n,n}$, given the existence of a genus $g = 2n - 1$ Costa tower $DH_{n-1,n-1}$.

Indeed, our proof of Theorem A is by induction: we make the

Inductive Assumption A: There exists a genus $2n - 1$ Costa tower, $DH_{n-1,n-1}$.

Thus, all of our surfaces are produced from only slightly less complicated surfaces; this is the general principle of 'handle addition' referred to in the title.

For concreteness, our present goal is the proof of

Theorem 6.1. *There is a reflexive orthodisk system for the configuration $DH_{2,2}$.*

Start of proof. Let us use the given height $\mathcal{H}_{2,2}$ for $DH_{2,2}$ and consider how the height

$\mathcal{H}_{1,1}$ for $DH_{1,1}$ relates to it, near a solution X_1 for the $DH_{1,1}$ problem. (As we observed, the situation extends to general $DH_{n,n}$ and $DH_{n-1,n-1}$ with simply added notation.)

Our notation is given in §4.4 and is recorded in the diagrams below: for instance, the curve system δ_1 connects the edges P_1P_2 and H_2H_3.

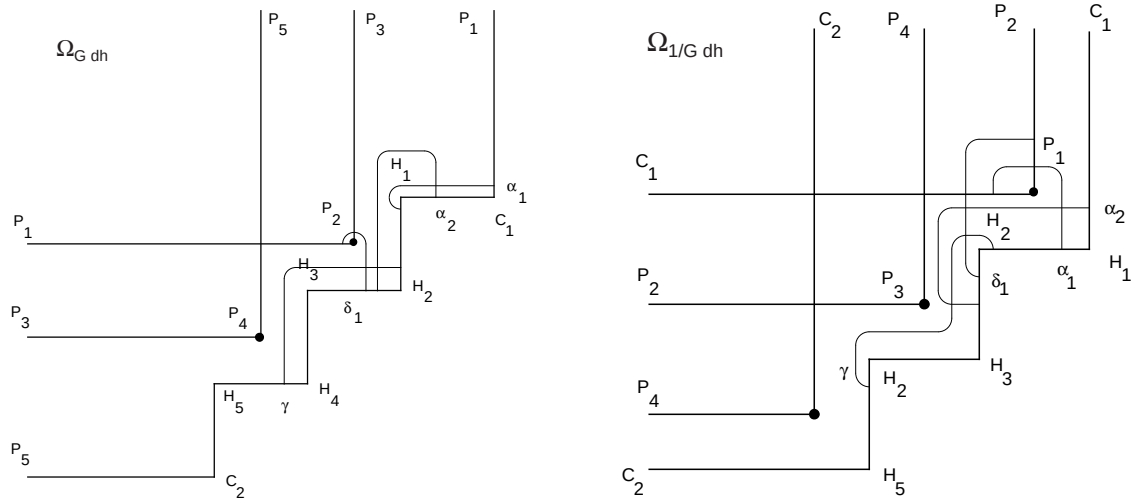

Curve system used for regeneration

We are very interested in how an orthodisk system might degenerate. One such degeneration is shown in the next figure, where the branch point P_1 has collided with the vertex H_1 on the orthodisk $\Omega_{G^{-1}dh}$. This has the effect, on the orthodisk Ω_{Gdh} of causing H_1C_1 to collapse and forcing the line P_1P_2 (respectively, P_4P_5) to lie directly across from (resp., over) the point $H_1 = C_1$ (resp., $C_2 = H_5$). The point is that the degenerating family of (pairs of) Riemann surfaces in $\Delta_{\mathcal{C}}$ limits on (a pair of) surfaces with nodes. (We recall that a surface with nodes is a complex space where every point has a neighborhood complex isomorphic to either the disk $\{|z| < 1\}$ or a pair of disks $\{(z, w) \in \mathbb{C}^2 | zw = 0\}$.) In the case of the surface corresponding to $\Omega_{G^{-1}dh}$, the components of the noded surface (i.e. the regular components of the noded surface in the complement of the nodes) are difficult to observe, as the flat structures on the thrice-punctured sphere components are simply single points; on the other hand, in the case of the surface corresponding to Ω_{Gdh}, the nodes are quite visible, as coming from a pair of sheets on the orthodisk, with one infinite point and one finite point (drawn in dotted lines on the figure below on the right).

Remark. In all of this, it is important to keep in mind that our flat structures represent a Riemann surface with a meromorphic one-form. Thus while there are no non-trivial holomorphic one-forms on a sphere (so that the flat structure is given by the trivial form $0 \cdot dz$, and is hence a point), there are non-trivial *mero*morphic forms on a thrice-punctured sphere with poles only at the punctures. The flat structures for those that occur in our present situation are represented by our method by a bigon, with one finite and one infinite vertex, connected by one horizontal and one vertical side.

An important issue in this section is that some of our curves cross the pinching locus on the surface, i.e. the curve on the surface which is being collapsed to form the node. In particular, in the diagram, the curves α_1 and α_2 are such curves, so their depiction in the degenerated figure is, well, degenerate: the curves either surround a point, or connect a point and an edge, or connect a pair of edges on opposite sides of a node.

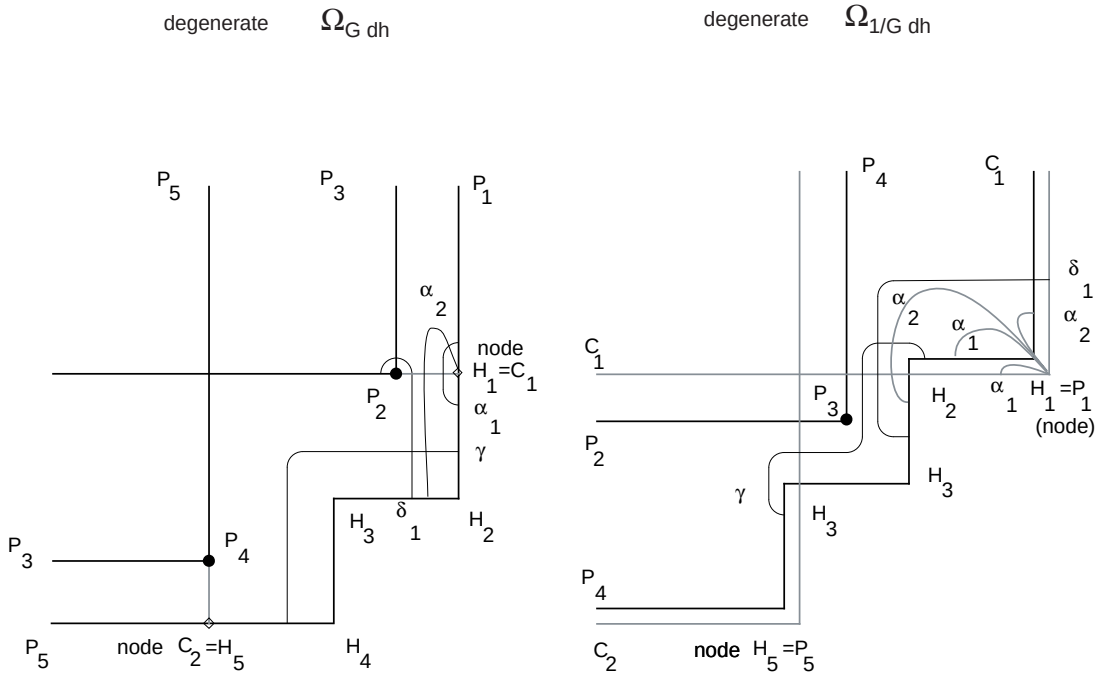

Degenerated orthodisks for the Costa towers

When we remove the thrice-punctured sphere components, we observe (compare with the figures in §5.2 and §3.6) that we are left with an orthodisk system for the lower genus configuration $\mathcal{C}_{DH_{1,1}}$, up to possibly relabeling Ω_{Gdh} as $\Omega_{G^{-1}dh}$ and vice versa.

Our basic approach is to work backwards from this understanding of degeneration – we aim to "regenerate" the locus $\mathcal{Y}$ in $\Delta_{DH_{2,2}}$ from the solution $X_1 \in \Delta_{DH_{1,1}}$.

We focus on the curves δ_1 and γ, ignoring the degenerate curves α_1 and α_2. Let Δ_2 be the geometric coordinate simplex for $DH_{2,2}$.

(In the general case for $\Delta_{DH_{n,n}}$, there are $2n-2$ non-degenerate curves (say, for notational convenience $\{b_1, ..., b_{2n-2}\}$), and two degenerate curves, α_1 and α_2. The case of $DH_{m,n\neq m}$ requires a separate but parallel treatment.)

We restate Lemma 5.1.3 in terms of the present (simpler) notation.

Lemma 6.2 (Regeneration). *: There is a smooth two-dimensional analytic closed locus $\mathcal{Y} \subset \overline{\Delta_n}$ so that $\mathrm{Ext}_{\Omega_{Gdh}}(b_i) = \mathrm{Ext}_{\Omega_{G^{-1}dh}}(b_i)$ on $\mathcal{Y}$, and $\mathcal{Y}$ is proper in Δ_n.*

Proof. We again continue with the notation for $n = 2$, as the general situation follows with just added notation.

As putatively defined in the statement of the lemma, the locus $\mathcal{Y}$ would be clearly

closed, and would have non-empty intersection with $\overline{\Delta_2}$ as $\overline{\Delta_2}$ contains the solution X_1 to the genus 3 problem.

We parameterize $\overline{\Delta_2}$ near X_1 as $\Delta_1 \times [(0,\epsilon) \times (0,\epsilon)]$ and consider the map

$$\Phi : (X, (t_1, t_2)) : \Delta_1 \times [(0,\epsilon) \times (0,\epsilon)] \longrightarrow \mathbb{R}^2$$

given by

$$(X, (t_1, t_2)) \mapsto (\mathrm{Ext}_{\Omega_{Gdh}}(\delta_1) - \mathrm{Ext}_{\Omega_{G^{-1}dh}}(\delta_1), \mathrm{Ext}_{\Omega_{Gdh}}(\gamma) - \mathrm{Ext}_{\Omega_{G^{-1}dh}}(\gamma)).$$

Here, coordinates t_1 and t_2 refer to a specific choice of normalized geometric coordinate, i.e. $t_1 = \mathrm{Im}(P_5C_2 \longrightarrow H_5H_4)$ and $t_2 = \mathrm{Re}(C_2H_5 \longrightarrow P_4P_5)$, where the periods $P_5C_2 \longrightarrow H_5H_4$ and $C_2H_5 \longrightarrow P_4P_5$ are measured on the domain Ω_{Gdh} (see the figure below). In terms of these coordinates, we note that whenever either $t_1 = 0$ or $t_2 = 0$, we are in a boundary stratum of $\overline{\Delta_2}$. The locus $\{t_1 > 0, t_2 > 0\} \subset \overline{\Delta_2}$ is a neighborhood in $Int(\Delta_2)$ with X_1 in its closure.

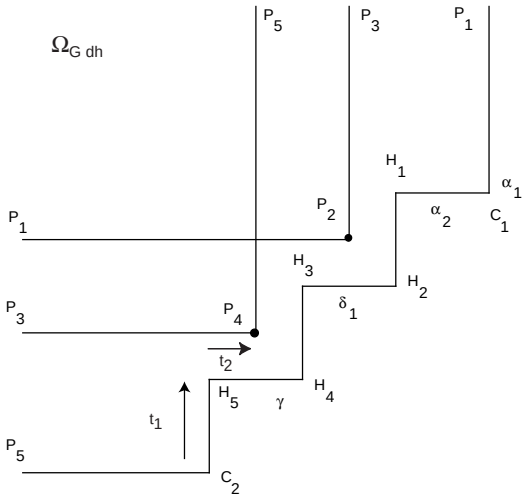

Geometric coordinates t_1 and t_2 for Δ_2

Note that $\Phi(X_1, (0,0)) = 0$ as X_1 is reflexive.

Now, to find the locus $\mathcal{Y}$, we apply the implicit function theorem. The implicit function theorem says that if

(i) the map Φ is differentiable, and

(ii) the differential $d\Phi \big|_{T_{X_1}\Delta_1}$ is an isomorphism onto $\mathbb{R}^2$,

then there exists a differentiable family $\mathcal{Y} \subset \overline{\Delta_2}$ for which $\Phi \big|_{\mathcal{Y}} \equiv 0$.

In order to show the differentiability condition (i), we require a clarification as to the meaning of the curve system γ, for points in $\Delta_1 \subset \partial\overline{\Delta_2}$. Here on X_1 we consider the distinguished points x and x' on the $\Omega_{G^{-1}dh}$ orthodisk, as shown below.

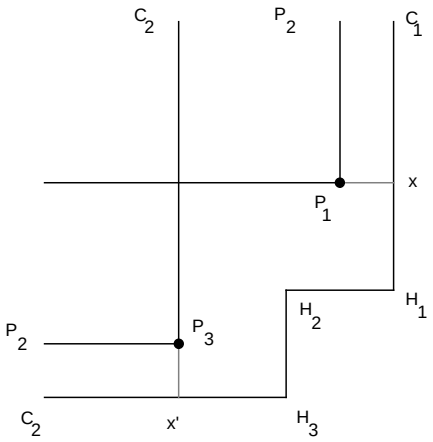

Definitions of the points x and x'

By definition, these points x and x' on $\Omega_{G^{-1}dh}$ of the solution X_1 are determined from continuing the levels C_1P_1 and P_3C_2 until they meet the axis at H_1C_1 and C_2H_3, respectively. Then γ is defined on $\Delta_1 \subset \partial\overline{\Delta_2}$ as the curve family connecting H_1x and H_3x'. We extend the notion of the points x and x' to the interior of Δ_2 by declaring there that $x = H_1$ and $x' = H_5$, respectively. The definition of γ then extends continuously to $\overline{\Delta_2}$.

We now prove the differentiability (condition (i)) of Φ: as the locus of $\overline{\Delta_2} \in \widehat{\overline{\mathcal{M}}_5} \times \widehat{\overline{\mathcal{M}}_5}$ is differentiable (here $\widehat{\overline{\mathcal{M}}_5}$ refers to a smooth cover of the relevant neighborhood of $X_1 \subset \overline{\mathcal{M}}_5$, where $\overline{\mathcal{M}}_5$ is the Deligne-Mostow compactification of the moduli space of curves of genus five) the theorem of Gardiner-Masur [GM] implies that Φ is differentiable, as we have been very careful to choose curves $\{\delta_1, \gamma\}$ which are non-degenerate in a neighborhood of $\overline{\Delta_2}$ near the genus three solution X_1, with both staying in a single regular component of the noded surface.

We are left to treat (ii), the invertibility of the differential $d\Phi \mid_{T_{X_1}\Delta_1}$. To show that $d\Phi \mid_{T_{X_1}\Delta_1}$ is an isomorphism, we simply prove that it has no kernel. To see this, choose a tangent direction in $T_{X_1}\Delta_1$; as we may regard $\Delta_1 \subset T_{0,8} \times T_{0,8}$ as a subspace of the product of two Teichmüller spaces of 8-times punctured spheres, we may regard a tangent direction as a pair $(\nu_{Gdh}, \nu_{G^{-1}dh})$ of Beltrami differentials, each representing a tangent direction to the points $[\Omega_{Gdh}] \in T_{0,8}$ and $[\Omega_{G^{-1}dh}] \in T_{0,8}$, respectively. Yet at X_1, the points $[\Omega_{Gdh}]$ and $[\Omega_{G^{-1}dh}]$ represent the identical point in $T_{0,8}$, so we begin by computing how the Beltrami differentials ν_{Gdh} and $\nu_{G^{-1}dh}$ relate to one another. To this end, consider how an infinitesimal push in the sense of §5.3 on an edge E defines Beltrami differentials ν_{Gdh} and $\nu_{G^{-1}dh}$. Of course the conjugacy of Ω_{Gdh} and $\Omega_{G^{-1}dh}$ provides, via the formulas of §5.3 the basic defining relation that if ν_{Gdh} has local expansion $\nu_{Gdh}(z) = \frac{1}{2b}\frac{d\bar{z}}{dz}$ near an interior point of an edge E, then $\nu_{G^{-1}dh}(\zeta) = \frac{1}{2b}\frac{d\bar{\zeta}}{d\zeta}$. However, since X_1 is reflexive, we may also assume, in this particular case, the existence of a conformal map $\zeta : \Omega_{Gdh} \longrightarrow \Omega_{G^{-1}dh}$ which preserves the vertices. Such a map takes vertical sides to horizontal sides

by construction and this has the local expansion $\zeta = \pm i|c|z + 0(|z|^2)$ near an interior point of an edge. We therefore compute the pullback of $\nu_{G^{-1}dh}$ to Ω_{Gdh} as

$$\begin{aligned}\nu_{G^{-1}dh}(\zeta)\frac{d\bar{\zeta}}{d\zeta} &= \nu_{G^{-1}dh}(\zeta)\bar{\zeta}'/\zeta'\frac{d\bar{z}}{dz} \\ &= (-\nu_{G^{-1}dh}(\zeta) + h.o.t.)d\bar{z}/dz \\ &= -\frac{1}{2b}\frac{d\bar{z}}{dz}\end{aligned}$$

along the edge E. Thus $\zeta^*\nu_{G^{-1}dh} = -\nu_{Gdh}$, and since any deformation of X_1 is given by a linear combination of such infinitesimal pushes, we conclude that $[\nu_{Gdh}] = -[\nu_{G^{-1}dh}]$ as elements of the tangent space $T_{\Omega_{Gdh}}T_{0,8} = T_{\Omega_{G^{-1}dh}}T_{0,8}$. Thus, any conjugacy preserving deformation of X_1 destroys the conformal equivalence of Ω_{Gdh} and $\Omega_{G^{-1}dh}$ to the order of the deformation, a statement which implies that $\ker(d\Phi) = \{0\}$, as required.

To finish the proof of the lemma, we need to show that $\mathcal{Y}\big|_{\Delta_2}$ is an analytic submanifold of $T_5 \times T_5$, where T_5 is the Teichmüller space of genus five curves: this follows *on the interior of* Δ_2 from the fact that Ohtsuka's formulas for extremal length are analytic and the map from Δ_2 to extremal lengths has non-vanishing derivative.

This concludes the proof of Lemma 6.2 for the case $n = 2$ and hence also the proof of Theorem 6.1. We have already noted that the argument is completely general, despite our having presented it in the concrete case of $DH_{2,2}$; thus, by adding more notation, we have proven Lemma 6.2 in full generality.

check this stuff in the next paragraph, too
rewrite this with new curve footing on central edge and branched edge

Conclusion of the proof of Lemma 5.1.3. All that is left in the proof of lemma 5.1.3 is the remaining case (Case (ii)) of $m < n$. In this case, the degeneration of the genus $g+1$ case to the genus g case is given by a much simpler operation than that of the degeneration described earlier in this section: here the degeneration consists of collapsing the two central finite edges of the outer sheet of both Ω_{Gdh} and $\Omega_{G^{-1}dh}$ (see the figures below). Thus, the corresponding regeneration consists of removing a neighborhood of the central finite edges of the outer sheet of both Ω_{Gdh} and $\Omega_{G^{-1}dh}$, and reconnecting the boundary with a pair of short edges (see the figures below and compare to the identical operation in [WW]).

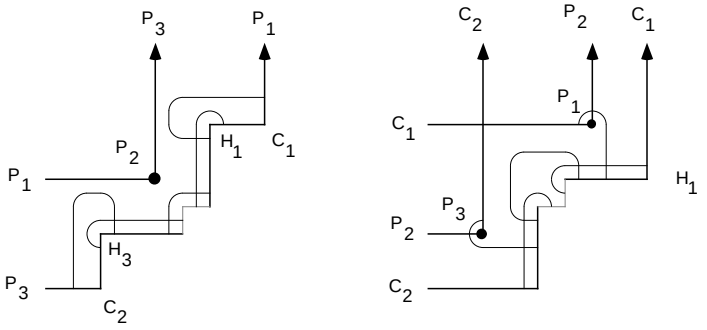

rethink this

(Recall that in the special case of $(m, n) = (1, 2)$ (pictured above), we made a special choice of the curve γ.) The effect of this surgery is to replace the central vertex with a triple of vertices which lie close to each other, as well as changing the cone angle of the central vertex. The proof of Lemma 5.1.3 is then virtually identical to that of the case of $m = n$: the only change is that instead of there being two curves α_1 and α_2 that degenerate under the degeneration, there is, in the present case, just a single degenerate curve α_n. Then with that change, the implicit function theorem argument given above goes through unchanged, up to substituting α_n for α_1 and α_2, and obtaining a locus $\mathcal{Y}$ which is one-dimensional, rather than the two-dimensional locus $\mathcal{Y}$ we obtained in the previous case $m = n$. To satisfy the requirement that the cycle corresponding to the t_i not be a finite edge bully, we choose our new cycle to foot on the central finite edge and on an infinite edge. Once we do this, the furthest finite edge $E = H_1C_1$ (and, unless $(m, n) = (1, 2)$, its immediate neighbors) will have neighbors which are parallel to the foliation for Φ_{t_i} if and only if that foliation is parallel to E. This concludes the proof of Lemma 5.1.3, and hence of the Main Theorems A and B(i) (see the discussion after Lemmas 5.1.2 and 5.1.3), up to the proof that $DH_{m,n}$ is embedded outside a compact set, which we treat in §9.

§7. Non-existence of $DH_{m,n}$ for $m > n$.

In the previous sections, we have seen that it is possible to add inductively a handle or a plane together with a handle to the minimal surfaces of type $DH_{m,n}$, starting at $DH_{1,1}$. This raises the question whether one can just add planar ends. If we would be able to do this with a single surface $DH_{n,n}$, this would (assuming its embeddedness) provide a counterexample to the Hoffman-Meeks conjecture. In this section, we will show that this is not the case, at least not in our setting of symmetry assumptions and chosen module sequences.

More precisely, we show that there are no surfaces of type $DH_{m,n}$ for $m > n$. This proves the second statement of Theorem B. Recall that the class of surfaces excluded by this statement consists only of those construed from module sequences of type $DH_{m,n}$ which were characterized among other possible module sequences as follows: The intersection of the surface with the vertical symmetry planes has one connected component joining all points with vertical normal on the z-axes; all other components join just two consecutive ends.

Before proving the general statement, we give the basic example:

Example 7.1: There is no $DH_{1,0}$. If there were an example of such a surface, then we could compute, as in §3, that the corresponding domains Ω_{Gdh} and $\Omega_{G^{-1}dh}$ would have the following shapes:

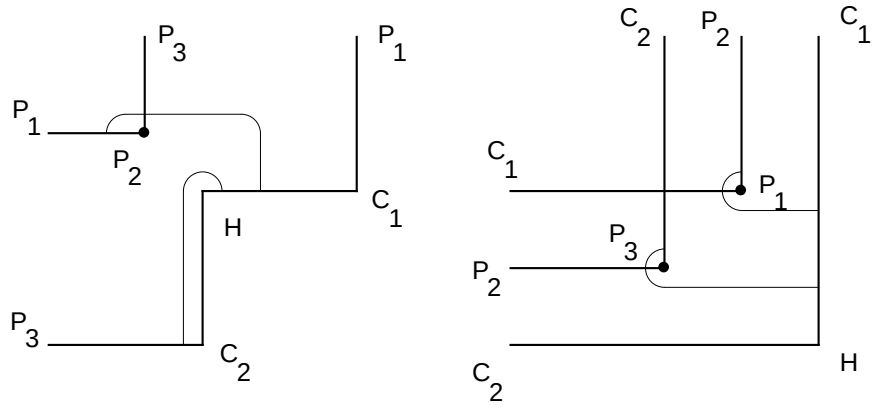

Non-existence of $DH_{1,0}$

For these domains to be conjugate, we require that the corresponding periods from Ω_{Gdh} and $\Omega_{G^{-1}dh}$ sum to lie on one line – in all of our examples so far, this line has been the 45-degree line $\{y = x\}$. In the present case, we first determine this conjugation line by looking at the periods of the cycle $P_3C_2 \to HC_1$. In Ω_{Gdh}, the period points upwards while in $\Omega_{G^{-1}dh}$, it points to the right. So the conjugation line is necessarily the $\{y = x\}$ diagonal. Now look at the cycle $HC_1 \to P_1P_2$. By symmetry, its period must point upwards in Ω_{Gdh}. By conjugacy, its period in $\Omega_{G^{-1}dh}$ must point to the right . This is impossible, since the branch point P_1 cannot lie outside the outer sheet.

Theorem 7.2. *There is no minimal surface of type $DH_{m,n}$ with $m > n$.*

Proof. Assume that we have a pair of reflexive orthodisks with $m > n$. Depending on the parities of m and n, there are 4 cases to distinguish, but the argument is the same in all cases. For the sake of concreteness, let's look at the case m even and n odd. As in the example above, the conjugation line is necessarily the $y = x$ axis. Now (in this parity case) the orthodisks have the form, near the symmetry axis, as in the diagrams below:

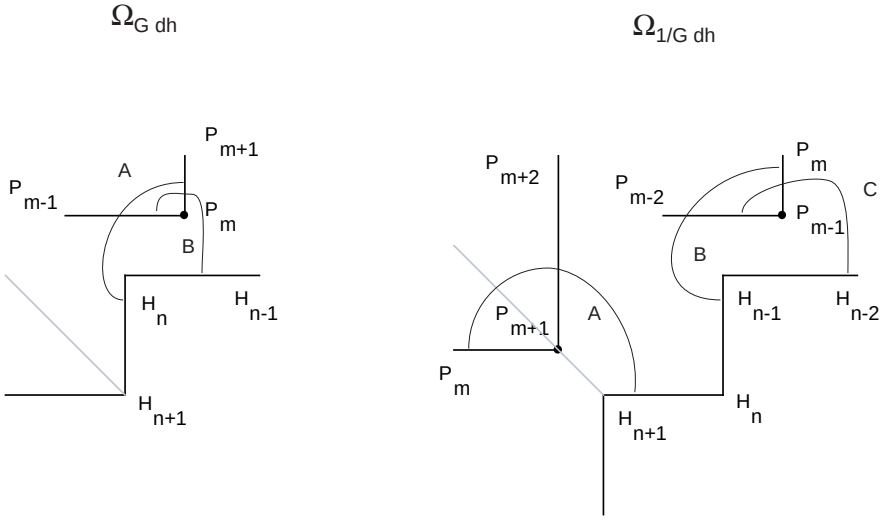

General nonexistence by induction

By symmetry, the cycle $A : H_{n+1}H_n \to P_mP_{m+1}$ has in $\Omega_{G^{-1}dh}$ a period pointing upwards, so in Ω_{Gdh} a period pointing to the right. To keep the branch point P_m within the outer sheet, this forces the period of the cycle $B : H_nH_{n-1} \to P_{m-1}P_m$ to point upwards in Ω_{Gdh} and hence to the right in $\Omega_{G^{-1}dh}$. This in turn forces the period of the cycle $C : H_{n-1}H_{n-2} \to P_{m-2}P_{m-1}$ to point upwards in $\Omega_{G^{-1}dh}$. Proceeding inductively like this, we will reach at some point the conclusion that the cycle $H_1C_1 \to P_{m-n}P_{m-n+1}$ (which exists because of $m > n$) points upwards in Ω_{Gdh} and hence to the right in $\Omega_{G^{-1}dh}$. However, this clearly forces the branch point P_{m-n} to lie outside the outer sheet. The other cases are completely analogous, starting always at the symmetry diagonal on the orthodisk with a central inner sheet.

§8. Extensions and Generalizations.

8.1 Higher dihedral symmetry.

It is a well known phenomenon that a surface like our $DH_{m,n}$ with 4-fold dihedral symmetry has companions with higher symmetry. In the framework of our approach, this is quite easy to achieve — we only have to change the setup in §3 while the rest of the arguments in §§4-6 remain valid. The orthodisks which reflect, in their orthogonal geometry, the 4-fold dihedral symmetry have to be replaced by *skewdisks* whose interior or exterior angles are $2\pi/d$ where d is the order of the dihedral symmetry group.

Recall that our orthodisks represent a piece of the surface obtained by cutting the surface by its two vertical symmetry planes with the metric induced by a meromorphic 1-form. In the same way, a surface with $2d$-fold dihedral symmetry and an additional rotational symmetry around (say) the x-axis is cut into $2d$ pieces, which we represent by skewdisks.

Vice versa, given such a skewdisk, one can take its double to obtain a skewsphere and then take a d-fold cyclic branched cover branched over the vertices. This covering should be chosen so that every second edge of the original orthodisk becomes a branch cut, and that each of the d copies of the skewspheres is glued to two other spheres along these cuts. This is needed to guarantee that the lifted cone metrics indeed define meromorphic 1-forms, i.e. have no linear holonomy.

Here is an example of two such skewdisks for $d = 4$ which represent Weierstraß candidate data for the $DH_{1,1}$ surface with 8-fold dihedral symmetry:

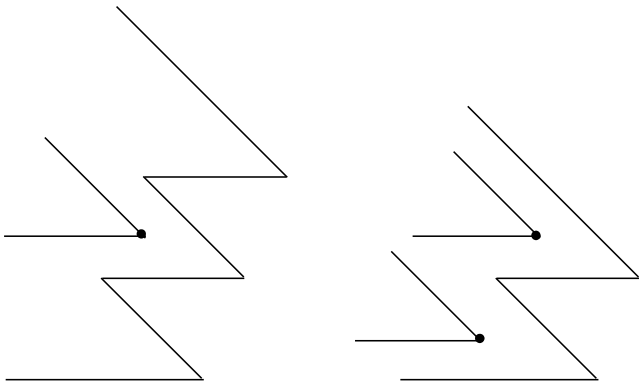

Skewdisk for surfaces with 8-fold dihedral symmetry

All of the definitions and claims from section 3 apply to this situation, with but a few modifications. The vertex data become odd integers $a_i \equiv \pm 1 \pmod{2d}$ where a_i represents a vertex with angle $\pi(a_i+2)/d$. Under the construction of the Riemann surface, this becomes a cone angle $2\pi(a_i+2)$ which corresponds to a zero of order a_i+1 of the corresponding meromorphic 1-form. The sufficient condition in lemma 3.3.4 becomes $a_i + b_i \equiv 0 \pmod{d}$, with similar straightforward changes in the other affected results in §3. Also note that by definition of the skewdisks and the associated Riemann surfaces, the divisors of G and dh balance so that we obtain the Weierstraß representation of a complete regular minimal surface.

In section 4, the construction of the height function is completely unchanged, and for the proof of its properness only section 4.7 needs to be changed slightly: in corollary 4.7.4 we get a different phase factor due to the fact that the angles under consideration are no longer right angles. But all we need in this section is is that

(1) the angles are $\equiv \pm\pi/d \pmod{2\pi}$
(2) corresponding angles of Ω_{Gdh} and $\Omega_{G^{-1}dh}$ always add to $0 \pmod{2\pi}$

For sections 5 and 6 we note that the skewdisks are just affinely distorted orthodisks; this gives complete and explicit control over the behavior of all extremal lengths, so that the tedious computations of §5 do not need to be repeated.

Thus we arrive at

Theorem 8.1.1. *For every triple of integers (d, m, n) with $d \geq 2$, $1 \leq m \leq n$ there exists a complete minimal surface $DH_{d,m,n} \subset \mathbb{E}^3$ of genus $(m+n+1)(d-1)$ which is embedded outside a compact set with the following properties: it has $2n+1$ vertical normals at flat points of order d, $2m+1$ planar ends, and two catenoid ends. The symmetry group is generated by a dihedral group of order $2d$ and a rotational symmetry around a horizontal axis.*

8.2 Deformations with more catenoidal ends.

The surfaces of type $DH_{m,n}$ described in Theorem B had two catenoid ends and $2m+1$ planar ends. Planar ends can be viewed as catenoid ends with a vanishing coefficient of growth (compare [Kap]), so it is natural to conjecture that the surfaces described in Theorem B are each elements of a family of surfaces obtained by deforming some of the planar ends into catenoid ends of varying growth rates, at least for growth rates near zero. In this section, we prove a theorem that confirms that conjecture within the context of the surfaces we study in this paper, i.e. those surfaces with exactly eight symmetries.

We begin with some notation. We define the *growth rate* α_i of a catenoidal or planar end E_i to be the residue of the form dh at that end. The surfaces we will create in this section will have a symmetry about a central line: thus the growth rate α_i of the i^{th} end E_i will be the negative of the growth rate α_{2m+4-i} of the symmetric end E_{2m+4-i}.

For a minimal surface with catenoidal or planar ends, let p denote the number of planar ends and k denote the number of catenoidal ends.

Theorem 8.2.1. *Choose growth rates $\alpha_1, \ldots, \alpha_m \in \mathbb{R}$ near zero. Then there is a complete minimal surface $DH_{m,n}(\alpha_1, \ldots, \alpha_m)$ in $\mathbb{E}^3$ with $2n+1$ vertical normals, k catenoidal*

ends and $p \geq 1$ planar ends, where $k + p = 2m + 3$. The ends have growth rates 1, $\alpha_1, \ldots, \alpha_m, 0, -\alpha_m, \ldots, -\alpha_1$, -1.

The proof follows the outline of the previous work, but involves a new type of special point of the type R described in the table in §.4. Space considerations require us to defer the complete proof to [WW2]. There we also discuss how to combine the constructions of Theorems 8.1.1 and 8.2.1.

§8.3. Embeddedness Aspects of $DH_{m,n}$.

In this section we collect some information about how embedded our minimal surfaces $DH_{m,n}$ are. First, for a complete minimal surface of finite total curvature to be embedded, the ends must be planar or catenoidal, all parallel and at different height. For different catenoidal ends which open up in the up direction, the growth rate of the higher end must be larger than the growth rate of the lower end so that they do not intersect. A similar statement holds for catenoidal ends opening in the down direction.

These conditions are necessary but not sufficient for embeddedness.

Definition 9.1. We call a complete minimal surface of finite total curvature satisfying the above condition *eventually embedded*.

In the next result, we state that all of the surfaces $DH_{m,n}$ (with two catenoidal ends) are eventually embedded, completing the proof of Theorem B. In fact, we prove a slightly more general statement:

Theorem 9.2. *Suppose there is a complete minimal surface of finite total curvature given by Ω_{Gdh} and $\Omega_{G^{-1}dh}$ orthodisks such that the formal Weierstraß data a_i and b_i satisfy*

(1) $a_i, b_i \in \{-3, -1, 1, 3\}$
(2) $2 + a_i + b_i \leq |a_i - b_i|$
(3) $\alpha_i + b_i \equiv 0 \pmod 2$

Suppose that there are only two catenoidal ends, one necessarily pointing up and the other down. Finally we assume that all planar ends occur in only one component of the orthodisk boundaries from which the two catenoidal vertices have been removed. Then the minimal surface is eventually embedded.

Proof. The first condition ensures that we only have catenoidal ends or planar ends, the second is equivalent to completeness. Because we only have two catenoidal ends, we do not have to consider growth rates. The only thing which remains to be checked is that the ends are at different heights. Using the third condition and applying Lemma 3.3.4, we see that dh has only imaginary periods. Clearly the two catenoidal ends represent the only infinite vertices of the dh orthodisk. By assumption, all other ends are on one component of the orthodisk boundary without the catenoidal vertices removed, so they have to arrange themselves in order. But the dh integrates to the height coordinate, so the ends are all at different height.

There is some further evidence that our surfaces are embedded: The Costa surface is embedded, moreover, there is a periodic surface, due to Callahan, Hoffman and Meeks (see

example 3.5.6.), which is also embedded, and which is, at least in a weak sense, a limit of the Costa towers $DH_{m,m} = CT_{2m+1}$.

Theorem 9.2 shows that the surfaces $DH_{m,n}$ are embedded outside of a compact set. We do not yet have a proof that these surfaces, in general, are embedded, yet we state next that any lack of embeddedness is somewhat inessential. Again space considerations require us to defer the argument to [WW2], where we give two proofs, one exploiting the algebraic aspects (in particular we use the Arf invariant – see [KS, Pin, HH]) of our construction, and one exploiting the geometric aspects of our construction.

Proposition 9.3. *The surface $DH_{m,n}$ is regularly homotopic in $\mathbb{E}^3$ to an embedding via a compactly supported regular homotopy that fixes neighborhoods of the critical points of dh.*

References

[Blo] D. Bloß, *Elliptische Funktionen und vollständige Minimalflächen*, PH.D. Thesis, Freie Universität, Berlin, 1989.

[Bo] E. Boix, *Thesis*, École Polytechnique, 1994.

[CHM] M. Callahan, D. Hoffman, W.H. Meeks III, *Embedded Minimal Surfaces with an infinite number of ends*, Inventiones Math. **96** (1989), 459–505.

[Cos] C. Costa, *Example of a complete minimal immersion in $\mathbb{R}^3$ of genus one and three embedded ends*, Bull. Soc. Bras. Mat. **15** (1984), 47–54.

[EL] J. Eells and L. Lemaire, *Deformations of Metrics and Associated Harmonic Maps*, Patodi Memorial Vol. Geometry and Analysis (Tata Inst., 1981), 33–45.

[FLP] A. Fathi, F. Laudenbach, V. Poenaru, *Traveaux de Thurston sur les Surfaces*, Astérisque, vol. 66-67, Société Mathématique de France.

[Gar] F. Gardiner, *Teichmuller Theory and Quadratic Differentials*, Wiley Interscience, New York, 1987.

[GM] F.P. Gardiner and H. Masur, *Extremal length Geometry of Teichmüller Space*, Complex Analysis and its Applications **16** (1991), 209–237.

[HH] Hass, J., and Hughes, J., *Immersions of Surfaces in* 3*-Manifolds*, Topology **24** (1985), 97–112.

[HM] J. Hubbard and H. Masur, *Quadratic Differentials and Foliations*, Acta Math. **142** (1979), 221–274.

[Ho-Ka] D. Hoffman, H. Karcher, *Complete embedded minimal surfaces of finite total curvature*, Geometry V (R. Osserman, ed.), Encyclopaedia of Mathmatical Sciences, vol. 90, Springer, Berlin, Heidelberg, New York, 1997.

[Ho-Me] D. Hoffman and W.H. Meeks III, *Embedded Minimal Surfaces of Finite Topology*, Ann. of Math. **131** (1990), 1–34.

[J] J.A. Jenkins, *On the Existence of certain general Extremal Metrics*, Ann. of Math. **66** (1957), 440–453.

[J-M] L. Jorge, W.H. Meeks III, *The topology of complete minimal surfaces of finite total Gaussian curvature*, Topology **22(2)** (1983), 203–221.

[Kap] N. Kapouleas, *Complete Embedded Minimal Surfaces of Finite Total Curvature*, J. Differential Geom. **47** (1997), 95-169.

[Kar] H. Karcher, *Construction of minimal surfaces*, Surveys in Geometry, University of Tokyo, 1989, pp. 1–96.

[Ke] S. Kerckhoff, *The asymptotic geometry of Teichmüller Space*, Topology **19** (1980), 23–41.

[K-S] R. Kusner and N. Schmitt, *The Spinor Representation of Surfaces in Space*, University of Massachusetts preprint.

[Laws] H.B. Lawson, Jr., *Lectures on Minimal Submanifolds*, Publish or Perish Press, Berkeley, 1971.

[Lop] F.J. Lopez, *The classification of complete minimal surfaces with total curvature greater than* -12π, Trans. Amer. Math. Soc. **334(1)** (1992), 49–74.

[MW] F. Martín and M. Weber, *On Properly Embedded Minimal Surfaces with Three Ends*, Duke Math. Journal **107(3)** (2001), 533–559.

[Oht] M. Ohtsuka, *Dirichlet Problem, Extremal Length, and Prime Ends*, Van Nostrand Reinhold, New York, 1970.

[Oss1] R. Osserman, *Global properties of minimal surfaces in* E^3 *and* E^n, Annals of Math. **80(2)** (1964), 340–364.

[Oss2] R. Osserman, *A Survey on Minimal Surfaces*, 2nd edition, Dover Publications, New York, 1986.

[Pin] U. Pinkall, *Regular Homotopy Classes of Immersed Surfaces*, Topology **24** (1985), 421–434.

[Sch] R. Schoen, *Uniqueness, Symmetry and Embeddedness of Minimal Surfaces*, J. Diff. Geometry **18** (1983), 791–809.

[Str] K. Strebel, *Quadratic Differentials*, Springer, Berlin, 1984.

[W] M. Weber, *On the Horgan Minimal Non-Surface*, Calc. of Variations and Partial Diff. Eqns. **7** (1998), 373–379.

[WW] M. Weber and M. Wolf, *Minimal Surfaces of Least Total Curvature and Moduli of Plane Polygonal Arcs*, Geom. and Funct. Anal., **8** (1998), 1129-1170.

[WW2] ———, *Minimal Surfaces, Flat Structures and Teichmüller Theory*, in preparation.

[Woh1] M. Wohlgemuth, *Higher genus minimal surfaces by growing handles out of a catenoid*, Manuscripta Math. **70** (1991), 397–428.

[Woh2] M. Wohlgemuth, *Minimal Surfaces of Higher Genus with Finite Total Curvature*, Arch. Rational Mech. Anal. **137** (1997), 1–25.

[Wo] M. Wolf, *On Realizing Measured Foliations via Quadratic Differentials of Harmonic Maps to* $\mathbb{R}$*-Trees*, J. D'Analyse Math **68** (1996), 107–120.